CARBON NANOTUBE BASED TARGETED DRUG DELIVERY SYSTEMS FOR BREAST CANCER AND OTHER DRUG DELIVERY APPLICATIONS

Wei Shao

Biomedical Technology and Cell Therapy Research Laboratory
Department of Biomedical Engineering
Faculty of Medicine
McGill University
Montreal, Quebec, Canada

Oct. 2014

A thesis submitted to McGill University in partial fulfillment of the requirements of the degree of Doctor of Philosophy

To my family

ABSTRACT

Breast cancer is the most commonly diagnosed cancer in women and the second leading cause of death among all cancers. Surgical removal of breast tumour tissues is the primary treatment for breast cancer. However, this does not rule out relapse at local or distant sites, so, chemotherapy is widely used as an adjuvant therapy. Although effective, chemotherapy drugs often cause severe side effects due to their non-specificity to cancer cells. Nanotechnology for drug delivery is an emerging field focused on targeting drugs to the desirable sites, such as tumour tissues, while minimizing the unwanted side effects of chemotherapy drugs on other tissues. Discovery of a new type of nanomaterial opens more opportunities for drug delivery. The carbon nanotube (CNT) is a novel type of synthetic material that has shown great potential for targeted delivery of anti-cancer agents. The initial hurdle for biomedical applications of CNT has been its hydrophobicity. Proper surface modification of CNT, or CNT functionalization, so as to prepare well-dispersed and biocompatible CNT in biologically compatible solutions, is a primary step for its biomedical application. In this thesis, noncovalent functionalization of CNT using various polymers is first explored to make well-dispersed CNT. By identifying the problems of the existing CNT-based drug delivery systems, three novel schemes for CNT-based, targeted drug delivery systems are designed and developed for delivery of a potent breast cancer chemotherapy drug paclitaxel (PTX). The three CNT-PTX delivery systems are characterized and evaluated for their toxicity, drug-loading capacity, cell penetration and cancer cell growth inhibition *in vitro*. Of the three schemes, the CNT-drug carrier developed through a lipid-drug approach is the best delivery system in terms of drug loading capacity, targeted drug delivery features and potential multifunctional drug delivery. Hence, the CNT-lipid-drug delivery system has been selected for further evaluation for its *in vivo* tumour growth inhibition, safety and toxicity using a breast cancer xenograft mice model. The CNT-lipid-drug approach has shown good results in a breast cancer animal model. Overall, this thesis explores a new type of nanomaterial as a drug carrier to overcome major limitations of chemotherapy drugs. As a newly discovered nanomaterial, research on CNT as a drug carrier is still in its infancy. Each of these schemes offers a new route of drug loading on CNT, which contributes to our present knowledge on construction of CNT-based drug delivery systems.

RESUME

Le cancer du sein est le cancer le plus communément diagnostiqué chez les femmes et la seconde cause de mort de tous les cancers. L'ablation chirurgicale du tissu cancéreux constitue à ce jour le premier traitement. Mais, il n'empêche pas les récidives à des sites locaux ou distants. De fait, la chimiothérapie est largement utilisée comme traitement adjuvant. Bien qu'elle soit efficace, la plupart des chimiothérapies causent des effets secondaires importants, dus a leurs non-spécificités aux cellules cancéreuses. Les nanotechnologies ont été testées pour la livraison ciblée de médicaments aux tumeurs. La découverte d'un nouveau type de nanomatériel ouvre de nombreuses opportunités pour la livraison de médicaments. Les nanotubes de carbone (NTC) constituent un nouveau type de matériel synthétique qui a montré un potentiel important pour la livraison ciblée d'agents anticancéreux. Malheureusement, le premier obstacle aux applications biomédicales des NTC est leur réduite. Cependant, la modification de surface des NTC, aussi nommée la fonctionnalisation des NTC, les rend biocompatibles et favorise leur dispersion et stabilité dans des solutions biocompatibles. Dans cette thèse, dans un premier temps, la fonctionnalisation non-covalente de NTC à partir de polymères est explorée pour préparer des NTC solubles dans l'eau et biocompatibles. A partir de l'analyse des problèmes et limitations des systèmes de livraison ciblée de médicaments composés de NTC déjà existants, trois nouveaux schémas de système de livraison de médicaments composés de NTC sont développés pour la livraison d'une medicament chimiotherapeutique paclitaxel (PTX) potentielle. Ces trois schémas ont été caractérisés et évalués pour leur stabilité, capacité de charge médicamenteuse, de pénétration dans les cellules et d'inhibition de la croissance des cellules cancéreuses. Le NTC-PTX développé par une approche de système de livraison lipides/médicament a montré d'excellentes propriétés pour la délivrance multifonctionnelle de médicaments. Ainsi, le NTC-lipides/médicament fut sélectionné pour une évaluation approfondie pour sa capacité à inhiber in vivo la croissance des tumeurs et pour sa sécurité et toxicité dans un modèle de cancer du sein xénogreffe. L'approche de NTC-lipides/médicament a montré des bons résultats dans le modèle animal de cancer du sein. De manière générale, cette thèse explore un nouveau type de nanomatériel utilisé comme un moyen de chargement de

médicaments afin de surmonter les limitations majeures des chimiothérapies médicamenteuses. Chacun de ces schémas offre une nouvelle approche de chargement de médicaments sur des NTC. Cela contribue au savoir pour la fabrication de système de délivrance de médicaments à partir de NTC.

ACKNOWLEGEMENTS

I would like to express my deep gratitude to my supervisor Dr. Satya Prakash who has provided me the opportunity to work in his lab. I am impressed with his enthusiasm for pursuing new science, which inspired me to explore various unfamiliar areas in my research. I am very grateful for his guidance, advice, encouragement and constant support in my project. On the other hand, I found it very invaluable that Dr. Prakash has given me enough freedom in terms of project design, trying new types of materials, and finding potential collaborators, which greatly boosted my interest in my research subjects. Because of his open-minded supervision, my PhD study has been enjoyable and rewarding. I believe that his training has helped me to grow as an independent researcher.

I am very grateful for the advice, guidance and criticism provided by my committee members, Dr. Robert Kearney and Dr. David Juncker from the Department of Biomedical Engineering, Dr. Amine Kamen from the Department of Bioengineering and Dr. Moulay Alaoui-Jamali from the Department of Oncology and Cancer Centre.

This work was supported by the Canadian Institutes of Health Research (CIHR). I also acknowledge the Excellence Awards that I obtained from the Department of Biomedical Engineering, and Graduate Awards from the Fonds de Recherche en Santé du Québec (FRSQ). These scholarships not only gave me confidence on the importance of the research that I was doing, but also allowed me to complete my studies without worry about my finances.

I would like to thank my fellow colleagues in the Biomedical Technology and Cell Therapy Laboratory, particularly, Arghya, Sana, Laetitia and Afshan for their laboratory support, discussion and proof-reading for the manuscripts presented in the thesis. I also thank my collaborators Bing Zhao and Zeng Huiying from the Department of Chemistry, Crystal Lee from the Department of Microbiology and Immunology, McGill University, and Rana Imani from the Department of Biomedical Engineering, Amirkabir University of Technology, Tehran, Iran. I would earnestly thank for Prof. Maryam Tabrizian and lab members in the Biomat'X laboratory, McGill University for allowing and assisting me to use their

facilities. I would like to extend my thanks to the technicians at the McGill University Animal Resources Centre, especially Anna Jimenez, Rosalie Michaud, Geneviève Bérubé, for their assistance with animal handling and sampling. I would like to thank Dr. David Liu from the Department of Physics for his help with Electron Transmission Microscopy (TEM); Mr. Petr Fiursak at FEMR facility in the Department of Chemistry, McGill for training on UV-NIR, TGA, FITR, and GPC facilites; Dr. Frederick Morin for the help with training and test of NMR samples; Dr. Jo-Ann Bader at the Goodman Cancer Research Centre for histological analysis on mice tissue samples.

Last but the not least, I am very grateful to my family for their love and support for my PhD studies. Their support and love help me to cope with all kinds of difficulties that I encounter in my life.

Wei Shao

PREFACE

In accordance with *McGill University Thesis Preparation Guidelines*, as an alternative to the traditional thesis format, I have taken the option of presenting my thesis as manuscript-based form. The thesis includes articles already published or in the process of review for publication. These manuscripts comprise Chapter 3-6 of the thesis, and are written in sections of an abstract, introduction, materials and methods, results and discussion, and conclusion. A common abstract, general introduction, literature review, general discussion, summary of observations and claimed original contributions, and recommendations are included in this thesis in accordance with the guidelines.

TABLE OF CONTENTS

LIST OF TABLES

LIST OF FIGURES

LIST OF ABBREVIATIONS AND TERMINOLOGY

5-FU	5-Fluorouracil
CBP	Carboplatin
CdS	Cadmium selenide
CHI	Chitosan
CNT	Carbon nanotube
CPT	Camptothecin
CSP	Cisplatin
CYC	Cyclophosphamide
DIPC	Diisopropylcarbodiimide
DMAP	4-N, N-dimethylaminopyridine
DMEM	Dulbecco's modified Eagle's medium
DMF	Dimethylformamide
DMSO	Dimethyl sulfoxide
DNA	Deoxyribonucleic acid
DTX	Docetaxel
EDC	1-ethyl-3-(3-dimethylamino-propyl) carbodiimide
EGF	Epidermal growth factor
EPR	Enhanced permeability and retention
ER	Estrogen receptor
f-CNT	Functionalized CNT made by cycloaddition
FA	Folic acid
FBS	Fetal bovine serum
FDA	Food and Drug Administration
FITC	Fluorescein isothiocyanate
GI	Gastrointestinal
H&E	Haematoxylin and eosin
HER-2	Human epidermal growth factor receptor 2
HPMA	N-(2-Hydroxypropyl) methacrylamide
HSA	Human serum albumin

MDR	Multidrug resistance
MPS	Mononuclear phagocytic systems
MRI	Magnetic resonance imaging
MTX	Methotrexate
MWNT	Multi-walled carbon nanotube
MX	Mitoxantrone
NGR	Peptide of asparagine-glycine-arginine
NIR	Near infrared
NMR	Nuclear magnetic resonance
PAA	Poly(acrylic acid)
PAMAM	Poly(amidoamine)
PBS	Phosphate buffered saline
PEG	Polyethylene glycol
PEI	Polyethylenimine
PGA	Polyglutamic acid
Pgp	P-glycoprotein
PR	Progesterone receptor
PS	Polystyrene
Pt	Platinum
PTT	Photothermal therapy
PTX	Paclitaxel
QD	Quantum dot
RBC	Red blood cell count
RES	Reticuloendothelial system
RGD	Peptide of arginine-glycine-aspartate
ROS	Reactive oxygen species
RT	Room temperature
SERS	Surface-enhanced Raman scattering
Sgc8c	An aptamer bound to PTK7
siRNA	Small interfering RNA
SWNT	Single-walled carbon nanotube
TEM	Transmission electron microscopy

TGA	Thermogravimetric analysis
TLC	Thin layer chromatography
TNBC	Triple-negative breast cancer
UV–NIR	Ultraviolet–Near Infrared
VCS	Vincristine
VDS	Vindesine
VRL	Vinorelbine
WBC	White blood cell count

CHAPTER 1 GENERAL INTRODUCTION, RESEARCH HYPOTHESIS AND THESIS OBJECTIVES

1.1 General introduction

Breast cancer is the most commonly diagnosed cancer in women and the second leading cause of death in all cancers [1, 2]. For treatment of breast cancer, one of the most successful approaches is surgical removal of primary breast tumours. But, this does not rule out the relapse at local or distant sites because of the presence of micrometastases at the time of the diagnosis. Chemotherapy is widely used as adjuvant therapy in women with tumours that are >1 cm in size. Widespread use of adjuvant therapy for breast cancer has led to an improvement in survival.

Although effective, most chemotherapy drugs cause severe side effects due to their non-specificity to cancer cells. In addition, most cancer drugs are hydrophobic, the use of surfactants for delivery results in additional severe side effects [3, 4]. Nanotechnology has been applied to solve the problems of chemotherapy drug delivery [5]. The properties of nanoparticles are beneficial in cancer drug delivery. Firstly, the size of nanoparticles is preferable for accumulation in tumour tissues. Secondly, the nanoparticles have a high surface area-to-volume ratio, which afford large amounts of payloads, including one type or multiple types therapeutics, for potential multifunctional delivery. Thirdly, nanoparticles can be designed to contain both hydrophilic and hydrophobic environments for loading hydrophobic drugs. Lastly, some nanoparticles are cell permeable that can carry drugs into cell cytoplasm to take effects inside of cells. Currently, several nanoparticle formulated chemotherapy drugs have been approved for the market or are in advance phases of clinical trials. This includes liposomal doxorubicin (DOX), albumin nanoparticle encapsulated paclitaxel (PTX) and polymer micelle encapsulated PTX, etc [5-7]. These formulations showed reduced side effects. However, they still have limitations, *e.g.* burst drug release in liposomes or polymer micelles encapsulated drugs [8]. There is a need for development of new types of chemotherapy drug delivery systems.

Carbon nanotube (CNT) is a type of synthetic nanomaterial that is made of carbon atoms. The discovery of CNT is largely attributed to Sumio Iijima in 1991 [9], although CNT has been produced and observed under a variety of conditions prior to 1991 [10]. In the last decade, CNT has been investigated for biomedical applications, including targeted drug delivery for treatment of cancer, nanoscaffold for tissue engineering and others [11]. Among many features of CNT, the high aspect ratio offers CNT with the advantage of effectively crossing biological barriers, which would allow its use in the delivery of therapeutically active molecules, including drugs, genes and targeting molecules, into one cell to exert multi-valence effect [12]. Furthermore, owing to the distinct optical properties of CNT, such as, high absorption in the near-infrared (NIR) range, photoluminescence, and strong Raman shift [13], CNT is an excellent agent for biology detection and imaging. Combined with high surface area of CNT for attaching molecular recognition molecules, CNT-based, targeted delivery systems can be developed for selective targeting, imaging and treatment.

1.2 Rationale

Development of a tumour-targeted drug delivery system by applying both passive and active targeting strategies would provide solutions for chemotherapy drugs. The unique structural and optical properties of CNT allow the development of multifunctional drug delivery. With high surface area, the CNT is able to simultaneously carry therapeutic agents and targeting molecules for efficient tumour targeting, monitoring and killing.

1.3 Research hypothesis and objectives

Novel polymer-functionalized, CNT-based drug delivery systems can be designed for delivery of chemotherapy agents so as to improve their efficacy, overall safety and toxicity profile.

Main objective

To design a novel CNT-based targeted drug delivery system for treatment of breast cancer

The specific objectives of this thesis are:

I. To examine functionalization of CNT using appropriate polymers, and to characterize the properties of functionalized CNT as a drug carrier, including its size, morphology, surface property, stability and the cell internalization capacity, etc.

II. To design new schemes for CNT-based chemotherapy drug delivery systems using PTX as a model drug.

III. To characterize the novel CNT-based PTX delivery systems *in vitro*

IV. To investigate the CNT-drug formulation in terms of *in vivo* drug efficacy, safety and toxicity in an experimental breast cancer animal model.

CHAPTER 2 LITERATURE REVIEW

2.1 A brief introduction to breast cancer

Breast cancer is the most common cancer in women worldwide and the second leading cause of death in women [1, 2]. The incidence of breast cancer is roughly 1/8. Despite advances in early detection and intervention have increased overall survival, the mortality of breast cancer remains high. One major way of defining the types of breast cancer is based on the specific receptors that are overexpressed in breast cancer cells. Three types of receptors are important in breast cancer: estrogen receptor (ER), progesterone receptor (PR) and human epidermal growth factor receptor 2 (HER-2). Tumours that express ER or PR are responsive to hormone suppression treatment and have a positive prognostic outcome; tumours that overexpress *HER-2* oncogene or other growth factor related genes usually show poor prognosis; tumours that lack expression of all the above three receptors are known as "triple negative" (ER, PR, and HER-2 negative), which have a very poor prognosis [14].

2.2 Available treatment modalities for breast cancer and their limitations

As reproductive hormones play a critical role in initiation and promotion of breast cancer, endocrine therapies are important for breast cancer [15, 16]. For ER/PR positive breast cancer patients, the use of ER antagonists (*e.g.* tamoxifen) or the inhibitors of estrogen biosynthesis (*e.g.* aromatase) could significantly enhance response rate [17-19]. However, up to 50% breast cancer patients are not responsive to this therapy since they lack ER or PR receptors in their breast tumours. There is also a renewed interest in ovariectomy and ovarian suppression therapy in the adjuvant treatment of premenopausal women with breast cancer [20]. However, this is associated with side effects like premature menopause, infertility, vaginal dryness, and osteoporosis, etc [21].

Note: Parts of this chapter have been published in the following journals/books:

1. Shao W, Paul A, Prakash S (2013) "Carbon nanotubes for cancer and stem cell therapeutics", Chapter 21 in *Selected Topics in Nanomedicine*, World Scientific Publishing, ISBN: 978-981-4472-85-2
2. Shao W, Paul A, Mai Y.Y, Rodes L, and Prakash S (2012) "Carbon nanotubes for use in medicine: potentials and limitations" chapter in *Recent Progress in Carbon Nanotube Research / Book 1*, InTech
3. Prakash S, Malhotra M, Shao W, Tomaro-Duchesneau C, Abbasi S (2011) "Polymeric nanohybrids and functionalized carbon nanotubes as drug delivery carriers for cancer therapy" Adv Drug Deliv Rev. 63(14-15): 1340-51.

One of the most successful approaches involves surgical removal of primary breast tumour. However, tumours could relapse at local or distant sites because of the presence of micrometastases at the time of the diagnosis. Chemotherapy is a necessary after-surgery treatment for breast cancer. Depending on the sub-groups of breast tumours, more specific treatments may be applied in combination with chemotherapy. For HER-2 positive breast cancer, HER-2 antibodies (*e.g.* Trastuzumab) adjuvant to chemotherapy drugs demonstrate improved drug efficacy [22]. However, for triple-negative breast cancer (TNBC), which accounts for 10–20% of all breast cancer, no specific therapy is available [23, 24], so these patients have to rely on chemotherapy.

2.3 Chemotherapy for breast cancer

All the chemotherapy drugs are small molecules that act to inhibit cell proliferation by interruption of critical cellular functions. In general, chemotherapy drugs are classified by the following mechanisms of actions: 1) DNA damage by intercalating the base pairs of nucleic acids, 2) DNA damage by adding alkyl groups in DNA, 3) inhibition of DNA synthesis by incorporation of analogs of the bases to DNA molecules, 4) interruption of mitosis by disturbing the microtubule dynamics (depolymerization and polymerization of microtubules) [25]. The actions of the commonly used chemotherapy drugs for breast cancer are summarized in table 2.1 and described below.

Table 2.1 Conventional chemotherapy drugs for breast cancer

Anthracyclines		**Alkylating agents**	
Doxorubicin	(DOX)	Cyclophosphamide	(CYC)
Daunorubicin	(DAU)	Carboplatin	(CBP)
Epirubicin	(EPI)	Cisplatin	(CSP)
Anti-metabolites		**Topoisomerase II inhibitors**	
5-Fluorouracil	(5-FU)	Mitoxantrone	(MX)
Methotrexate	(MTX)		
Taxane		**Mitotic inhibitors**	
Paclitaxel	(PTX)	Vindesine	(VDS)
Docetaxel	(DTX)	Vinorelbine	(VRL)
		Vincristine	(VCS)

2.3.1 Chemotherapy drugs

DNA-damage is the major mechanism for cancer chemotherapy since DNA integrity is critical for normal cellular functions as well as cell proliferation. High level of DNA damage often induces cell cycle arrest. If damaged DNA cannot be repaired, cell death may result. Since cancer cells normally undergo rapid replication, they are more susceptible to DNA-damaging agents than normal cells. Anthracycline family drugs are among the most potent DNA-damage drugs. They act by intercalating DNA, thus inducing apoptosis. Clinically applied anthracycline drugs include doxorubicin, daunorubicin and epirubicin. Except for DNA damage, anthracycline drugs have also been shown to inhibit topoisomerase II (an key enzyme for DNA synthesis) function and to generate free radicals, etc [26]. However, anthracycline drugs cause severe cardiotoxicity, which become a dose-limiting factor for these drugs.

The alkylating agents damage DNA by adding alkyl groups in DNA. Alkylation of DNA prevents DNA strands from uncoiling, which is necessary in DNA replication. Examples of alkylating agents include nitrogen mustards and cyclophosphamide. The platinum-based agents, *e.g.* carboplatin and cisplatin, act the similar way as the alkylating agents. Instead of cross-linking of DNA by adding alkyl groups, the platinum-based drugs permanently coordinate to the bases of DNA so as to prevent DNA uncoiling [27]. Because of this similarity, the platinum-based drugs are also called alkylating-like drugs and usually classified to alkylating subgroups agents.

Antimetabolites are types of chemotherapeutic agents that affect DNA function by blocking DNA biosynthesis. Most antimetabolites are analogs of DNA building blocks (purine or pyrimidine). The incorporation of these analogs into DNA would lead to failure of DNA replication [28]. For example, 5-Fluorouracil is an analog of pyrimidine, which is often used in combination with other chemotherapy drugs for the treatment of breast cancer. Other antimetabolites, such as methotrexate, act as inhibitors of key enzymes responsible for nucleotide biosynthesis [28].

Apart from DNA synthesis, another effective target for the treatment of breast tumours is microtubule [29]. The process of microtubule assembly is highly dynamic, in that the microtubules extend and shorten continually within the cellular milieu. The dynamic property of the microtubules is critical for their cellular functions. Especially, the accurate chromosome segregation during mitosis requires an exquisite regulation of spindle microtubule dynamics, even minor alteration of microtubule dynamics could halt mitotic progression, which is probably the primary basis for the use of microtubule-interfering agents in cancer chemotherapy [30, 31]. Some drugs inhibit polymerization of microtubules, *e.g.* vinca alkaloids; whereas, others affect depolymerization of microtubules, *e.g.* taxane drug family. Taxane drugs bind to the microtubules so as to block their disassembly, which leads to cell cycle arrest and apoptosis. Within this drug family, paclitaxel (PTX) and docetaxel are among the most important drugs for treatment of hormone-refractory breast tumours.

2.3.2 Limitations of available conventional chemotherapies for breast cancer

Although chemotherapy is one of the most important treatments for breast cancer and other cancers, the conventional chemotherapy drugs exist some limitations. First of all, chemotherapy drugs are not specific to tumour cells. They affect all the cells that undergo rapid multiplying, *e.g.* bone marrow, hair follicles and GI tract, thus, causing severe side effects, such as, neutropenia, anemia, alopecia, diarrheal, nausea and vomiting [32]. In addition, most cancer drugs are hydrophobic, so it is necessary to use surfactants for delivery, which often cause additional side effects [3, 4]. For example, the clinical PTX formulation, Taxol® (formulated with Cremophor EL), could cause hypersensitivity reactions in patients [33, 34], which limits its clinical uses. On the other hand, being small molecules, chemotherapy drugs are easily removed by renal clearance following intravenous drug administration. Because of insufficient blood circulation time, the drug molecules are not able to reach biological targets at therapeutic concentration. Taking together, the severe side effects and poor biodistribution of the chemotherapy drugs severely affect the efficacy of chemotherapy drugs.

Multidrug resistance (MDR) is another major obstacle for the efficacy of chemotherapy. One of the mechanisms of MDR is caused by up-regulation of P-glycoprotein (P-gp), an efflux molecular "pump" in tumour cell membrane that is responsible for transporting a wide variety of drug molecules out of cells [35]. Usually, the P-gp induced by exposure to one type of chemotherapy drug could cause the resistance to the treatment with other types drugs, thus leading to the failure of chemotherapy.

2.4 Introduction to nanoparticles and their potentials & limitations in cancer drug delivery

Nanoparticles could provide solutions for chemotherapy. With the nanoscopic dimension, nanoparticles could directly interact with biology systems at molecular level. It has been found that the nanoparticles with optimal size and surface characteristics display longer blood circulation, and therefore facilitate their tumour accumulation [5]. Motivated by this important finding, the application of nanotechnology in the field of cancer therapies becomes a rapidly developed research area [5]. The rationales of using nanoparticles for cancer treatment, as well as the types of clinical applied nanoparticles are discussed in more detail in the following subsections.

2.4.1 Rationales for use of nanoparticles for delivery of anti-cancer agents

As fast growing tissues, tumours display enhanced vascular permeability due to high demand for nutrients and oxygen. The poorly aligned, defective endothelial layer is one of the most important features of tumour vasculature. Such a feature can be utilized for delivery of anti-cancer agents. Small molecule drugs do not distinguish normal tissues from tumour tissue, as they pass through all type of tissues by free diffusion. In contrast, the nanoparticles or some macromolecules, *e.g.* liposomes, polymer micelles, and lipoproteins, etc, cannot pass through endothelial barrier in normal tissues, however, they tend to enter the defective tumour tissues (Fig. 2.1). On the other hand, tumour tissues lack drainage system, so the clearance of these nanoparticles and macromolecules from tumours is impaired, thus resulting their retention in tumour tissues for a long time. The phenomenon is termed as tumour-selective *Enhanced Permeability and Retention* (EPR)

effect [36] (Fig. 2.1). The EPR effect has been observed in large proteins (larger than 50 kDa), liposomes (50 – 400 nm) and some lipids in a variety of experimental and human solid tumours [36]. The EPR effect has been applied as passive tumour-targeting strategy (Fig. 2.1) [37]. The targeting efficacy mainly depends on the properties of the nanoparticles, such as the size and surface properties of the nanoparticles. Since many physiological barriers are present in the route of drug delivery, including renal clearance, uptake of foreign particles by macrophages in reticuloendothelial systems (RES), and other barriers in tumour tissues, usually, very small particles (with diameters of less than 10 nm) are rapidly removed by the renal clearance; whereas, large particles (with diameters larger than 400 nm) are easily captured by immune cells in reticuloendothelial systems (RES) [38]. Even for the particles with the diameters within 400 nm, although they can escape from clearance by RES, they may have limited diffusion in the interstitial space within the tumour tissues. So, the diameter of spherical nanoparticles in the range of 10 -100 nm is thought to be appropriate for accessing cancer cells [5].

Surface properties, such as surface charge and surface hydrophobicity, are also important factors that influence blood circulation time of nanoparticles. The fate of nanoparticles is determined by interaction of the nanoparticles with their local environment. Nanoparticles with more hydrophobic surface easily absorb proteins through hydrophobic interactions, which could tag these nanoparticles to be sent to RES system for degradation [39]. Coating nanoparticles with hydrophilic polymers is a common strategy to minimize the nonspecific interactions with proteins, and therefore improves tumour accumulation [40]. One of the most effective coating methods involves PEGylation − a technique using polymer polyethylene glycol (PEG) for coating of nanoparticles. PEGylation has been shown to increase circulation half-life and to reduce toxicity and immunogenicity of nanoparticle drugs [41-44]. PEG is among the few polymers that are approved by Food and Drug Administration (FDA) for clinical applications. Many PEG-modif ed drugs have been approved for drug market [5].

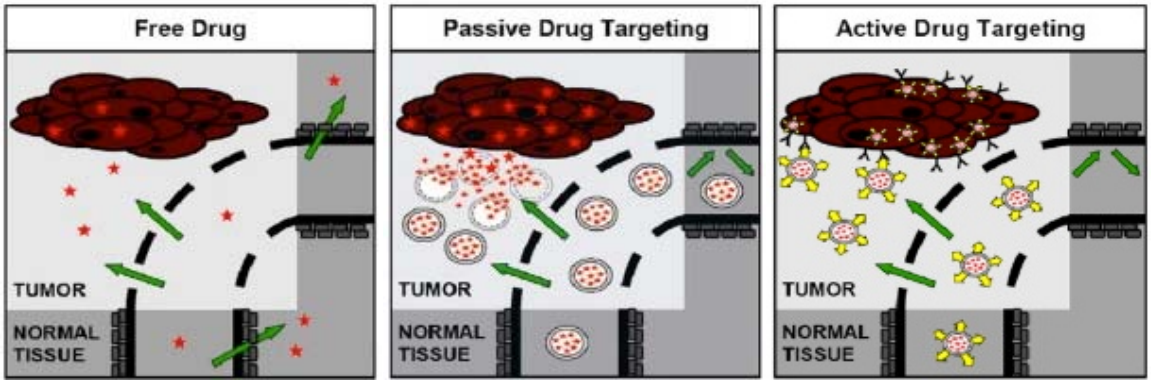

Figure 2.1 Schematic presentation of passive tumour targeting *via* EPR effect and active tumour targeting *via* receptor mediated internalization of nanoparticles [37]

2.4.2 Active tumour-targeting strategy

Active targeting strategy involves conjugation of tumour-recognizing molecules to nanoparticles. These targeting molecules are usually the ligands for specific surface biomarkers (antigens or receptors) on cancer cells. Conjugation of the targeting ligands could further enhance targeting efficacy of the nanoparticles towards tumour tissues. In some cases, upon binding of these ligands to the receptors, the internalization of these ligand-conjugated nanoparticles occur *via* receptor-mediated endocytosis (Fig. 2.1) [5]. A range of cancer-targeting molecules have been discovered, which can be broadly classified as antibodies, peptides and others (*e.g.* vitamins and carbohydrate). Examples of the commonly applied targeting molecules for cancer therapy include antibody Trastuzumab, peptide RGD, and folic acid, etc. Trastuzumab, which recognizes HER-2 receptor in breast cancer cells, has therapeutic effect by its own, and also serves as tumour recognition moities for drug delivery systems [45]. RGD is a group of peptides that contain Arginine-Glycine-Aspartate (RGD) triad, which has strong affinity to the alpha (V) beta (3) receptors overexpressed on many types of tumours. RGD has been widely applied for targeted delivery of imaging agents and nanoparticle drugs for treatment of many types of cancers [46]. Folic acid is a small molecule vitamin that binds to folate receptors overexpressed in a variety of cancer cells, including breast, colon, renal and lung tumours [47]. Currently, the folic acid conjugated anti-microtubule drug desacetylvinblastinemonohydrazide (EC145) has entered phase III of clinical trials [48].

2.4.3 Major types of nanoparticles used in breast cancer therapy

There are two major types of nanoparticles that are applied for cancer therapies [49]: 1) nanoparticles assembled by the components made by organic materials, *e.g.* lipids, polymers, and proteins; 2) nanoparticles made of inorganic materials, *e.g.* quantum dots, iron and gold. Currently, several nanoparticle formulations have been approved for the treatment of breast cancer. For examples, the liposomal DOX formulations have been approved for market for breast cancer since the mid-1990s [6]; the albumin nanoparticle encapsulated PTX formulation, Abraxane®, has been approved in 2005 [7].

The above-mentioned two types of nanoparticles are discussed in more detail in the following subsections.

2.4.3.1 Organic nanoparticles

The most studied organic nanoparticles include liposomes, polymeric micelles, and polymer-drug conjugates. These nanoparticles are summarized in table 2.2 and discussed separately below.

Liposomes are made of amphiphilic phospholipids. Structurally, liposomes are vesicles that contain one or more bilayers that are assembled with phospholipids. Their sizes range from 50 nanometer to several hundred nanometer in diameter. Because the liposomes contain both hydrophilic (interior of liposomes) and hydrophobic (lipid bilayers) compartments, they are able to entrap both hydrophilic and hydrophobic drugs. Although the liposomal carriers are versatile, they face several challenges, such as, burst release of encapsulated drugs before reaching their targets, and non-specific uptake by RES, etc. To avoid opsonization (a process of particles that are ingested by immune cells) by the RES, and to extend drug circulation time in blood, the liposomal carriers are modified by conjugation with PEG, which greatly increased their blood circulation time. For example, the circulation half-life of doxorubicin is only 0.8 hr, when the drug molecules are encapsulated into PEGylated liposomes (Doxil®), the circulation half-life reach 84 hrs, which facilitates uptake of drugs by EPR effect [5]. As a result, the

liposomal doxorubicin has shown improved efficacy and much decreased cardiotoxicity compared to free DOX. However, liposomal Doxil® may cause side effect of hand-foot syndrome, which is caused by extravasation of the drugs to the skin [50]. Currently, the targeted liposomal formulations are under development aiming to reduce this side effect [51].

Polymeric micelles are assembled by synthetic amphiphilic block polymers. Micelles are generated by association of the hydrophobic portions of amphiphilic block polymers due to hydrophobic interactions while hydrophilic portions facing towards outside. Since polymeric micelles contain hydrophobic cores, they are suitable for encapsulation of hydrophobic drugs. Polymeric micelles usually have smaller size (sub-100 nm) compared with liposomes, and therefore accumulate more readily in tumours than the liposomes [6]. Several polymer micelle formulations are under clinical evaluations, *e.g.* NK911 (encasing doxorubicin), NK105 (encasing PTX) and Genexol-PM® (encasing PTX). Among them, Genexol-PM® has been approved for market in South Korea [5].

Polymer-drug conjugates are made by covalently linked drug molecules to polymers. In the conjugates, a homing moiety could be attached to the same polymers for targeted delivery [52]. Usually, drug molecules are covalently conjugated to polymers *via* cleavable chemical bonds because the release of drugs from the conjugates is necessary for their actions. Specific linkers can be designed to allow controlled drug release from the polymers. For example, drug PTX was attached to polymer N-(2-Hydroxypropyl) methacrylamide (HPMA) *via* a specific linker that is stable under physiological condition (pH 7.4) but can be hydrolyzed at pH ~ 5 (endosomal pH) so as to release the drugs to cytosol following endocytosis of polymer-drug conjugates. To date, a dozen polymer-drug conjugates are under evaluation in clinical trials [53], among them, polyglutamic acid (PGA)-conjugated PTX (XYOTAX) has entered clinical trial phase III and is expected to be the first polymer-drug conjugate that will be approved for the market [53].

Table 2.2 Examples of clinically applied nanoparticles

Types	Structures	Drugs	Formulation trade names	Ref
Liposomes	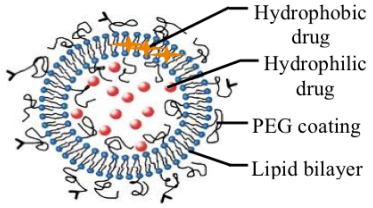	Daunorubicin Doxorubicin	DaunoXome® Doxil®	[54]
Polymeric micelles	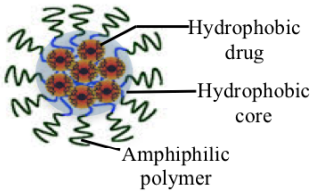	Doxorubicin Paclitaxel Paclitaxel	NK911 NK105 Genexol®	[6]
Polymer-drug conjugates	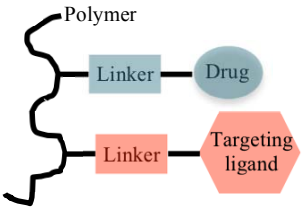	Paclitaxel Camptothecin Camptothecin	XYOTAX CT-2106 IT-101	[53]

2.4.3.2 Inorganic nanoparticles

Inorganic nanoparticles are usually made from metallic materials. These metallic materials contain fluorescent, magnetic, or optical properties that can be potentially used for detection and imaging. The common structure for inorganic nanoparticles could be depicted as a central core made of metals, and a coating layer made of hydrophilic molecules/polymers (Fig. 2.2). The hydrophilic outer layer acts to increase the dispersity of the inorganic nanoparticles and to protect the core from degradation in a physiologically aggressive environment. The outer layers could be modified to attach drugs, antibodies and tumour-targeting ligands for multifunctional delivery [55-57] (Fig. 2.2).

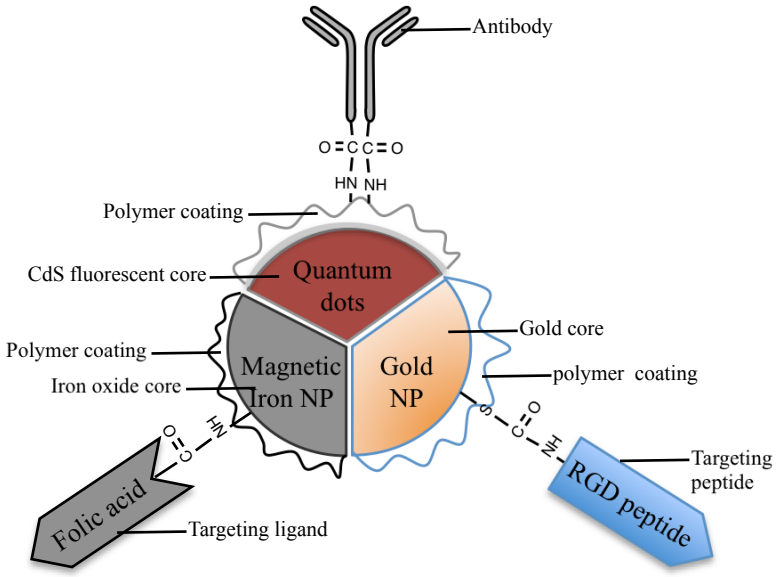

Figure 2.2 Schematic presentation of basic structure of inorganic nanoparticles

Quantum dots are semi-conductive fluorescent nano crystals with the sizes ranged from 2 – 10 nm in diameter. A quantum dot contains a cadmium selenide (CdS) core and a polymer out layer (Fig. 2.2). Quantum dots emit powerful fluorescence, which is superior to many organic dyes. The quantum dots have been conjugated to HER-2 antibodies for simultaneous labeling and quantification of HER-2 expression in breast cancer [49]. Although very sensitive, the clinical applications of quantum dots are limited by the toxic effects of the heavy metals.

A magnetic iron nanoparticle (usually 3 – 10 nm in diameter) contains a core made of iron oxide. Because of the magnetic property, the iron nanoparticles have been widely used as contrast enhancement agents to improve sensitivity of magnetic resonance imaging (MRI) [58]. Iron nanoparticles also display toxicity, which is mainly due to their hydrophobicity, so surface functionalization of iron nanoparticles is important for improving their biocompatibility. Surface functionalized magnetic iron nanoparticles do not show much toxicity and have been widely explored for *in vivo* tumour-targeting, detection and drug delivery [59].

Gold nanoparticles are synthesized by the reduction of Au [III] derivatives, *e.g.* aurochloric acid. Similar to iron nanoparticles, gold nanoparticles can also be applied as MRI contrast agents. In addition, gold nanoparticles exhibit unique surface-enhanced Raman scattering (SERS) properties [60], which can potentially be used for detection using Raman spectroscopy (reviewed in [61]).

Apart from the advantage of metallic nanoparticles in tumour detection and imaging, some nanoparticles, *e.g.* magnetic iron oxide and gold nanoparticles, are able to generate heat by absorbing energy through near-infrared (NIR) light excitation. Usually, the small sized iron or gold nanoparticles are able to enter cells, by conjugation of tumour-targeting moities, these nanoparticles afford specifically targeting tumour tissues followed by killing of cancer cells by heating upon NIR exposure [62].

In summary, inorganic nanoparticles possess intrinsic, distinct optical and thermal properties, in combination of conjugation of targeting molecules, and/or chemotherapy drugs, these nanoparticles afford simultaneous tumour detection, imaging, hyperthermia and chemotherapy. Although promising, current available metallic nanoparticle carriers have some limitations, such as low payloads, and the toxicity of heavy metals, etc.

2.5 General introduction to carbon nanotube, and its potentials & limitations in delivery of anti-cancer agents

Carbon nanotube (CNT) is a synthetic nanomaterial made of carbon atoms. Structurally, CNT can be viewed as a hollow tube wrapped from graphitic sheets. Each of graphic sheets is one-atom thick, in which carbon atoms are arranged in an sp^2-bonded hexagonal pattern similar to polycyclic aromatic rings. Based on the numbers of layers of the graphitic sheets, the CNT can be classified into two categories: single-walled carbon nanotube (SWNT) and multi-walled carbon nanotube (MWNT) [63]. CNT has a diameter of less than one nm to several nm and a length ranged from hundreds to a thousand nm (Fig. 2.3). The well-ordered molecular structure brings CNT many remarkable physical properties, such as, excellent mechanic strength, high surface area, distinct optical properties [64], and excellent electrical and thermal conductivity [65], etc.

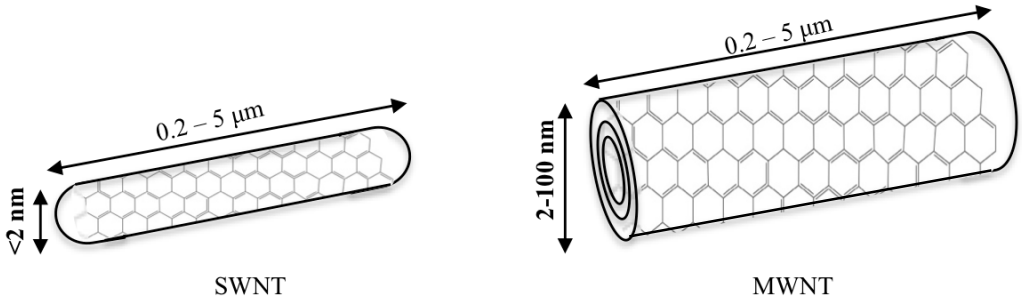

Figure 2.3 Schematic presentation of typical carbon nanotube structures

The discovery of CNT offers up new opportunities for cancer drug delivery. Inspired by an important finding that CNT can penetrate cells by themselves without apparent cytotoxic effect to cells [12], CNT is widely explored for *in vitro* and *in vivo* delivery of therapeutics. The high aspect ratio makes CNT outstanding from spherical nanoparticles in that the long and thin nanotube facilites cell internalization without constraint of loading large amounts of payloads. Furthermore, owing to the distinct optical properties of CNT, such as, high absorption in the near-infrared (NIR) range, photoluminescence, and strong Raman shift [13]. Because of these optical properties, CNT is an excellent candidate for biology detection and imaging.

2.5.1 Preparation of carbon nanotube for use in medicine and other biomedical applications

Pristine CNT, possessing a metallic nature, cannot be well dispersed in water and most solvents. For its use in biomedical applications, the initial hurdle has been its poor solubility. Due to the hydrophobic nature, pristine CNT has strong tendency to aggregate into large bundles, which is responsible for the toxicity observed in many studies [66-68]. Surface modification of CNT, or CNT functionalization, so as to disperse them into aqueous solutions becomes a key step for their biomedical applications.

Two types of strategies are involved in CNT surface modification: non-covalent and covalent methods. The non-covalent modification utilizes the hydrophobic nature of CNT

for adsorption of amphiphilic molecules, such as surfactants [69], lipid-polymer conjugates [70], and some copolymers [71]; while, the covalent modifications generate chemical bonds on the backbone of CNT *via* chemical reactions, which are usually followed by further conjugation of hydrophilic molecules/polymers. Both covalent and noncovalent modification strategies could remarkably improve the dispersity of CNT in aqueous solutions; meanwhile, they provide functional moieties for further linkage of therapeutic agents, such as genes (DNA or siRNA), drugs and others. The covalent and noncovalent modification of CNT are discussed in more detail below:

2.5.1.1 Covalent surface modification of carbon nanotube

The covalent modification of CNT is an emerging area in materials science. Among the various strategies, the most common ones are: 1) oxidation of CNT followed by conjugation of hydrophilic molecules by esterification and amidation, 2) cycloaddition reactions to generate of functional groups on CNT sidewalls.

Oxidation of CNT is carried out by reflexing of pristine CNT in strong acidic media, *e.g.* HNO_3/H_2SO_4 (Fig. 2.4a). Under this condition, the caps at both ends of nanotube are opened, and carboxylic groups are formed at the ends and at some defect sites on nanotube sidewalls [72] (Fig. 2.4a). The carboxylic groups are usually used for further derivation of the CNT through esterification or amidation reactions. For example, organic molecules containing amine groups can be directly condensed with the carboxylic groups on CNT [73, 74]. Alternatively, the carboxyl moieties can be activated with thionyl chloride and subsequent react with amine groups-containing molecules [73, 74] (Fig. 2.4a). In most cases, the length of nanotubes is often shortened [72], but the electronic properties of such functionalized CNT remain intact. One limitation of this method is that oxidation reaction only generates limited numbers of carboxylic groups mainly on ends and defect spots of CNT, which limits the water dispersibility and stability of the oxidized CNT.

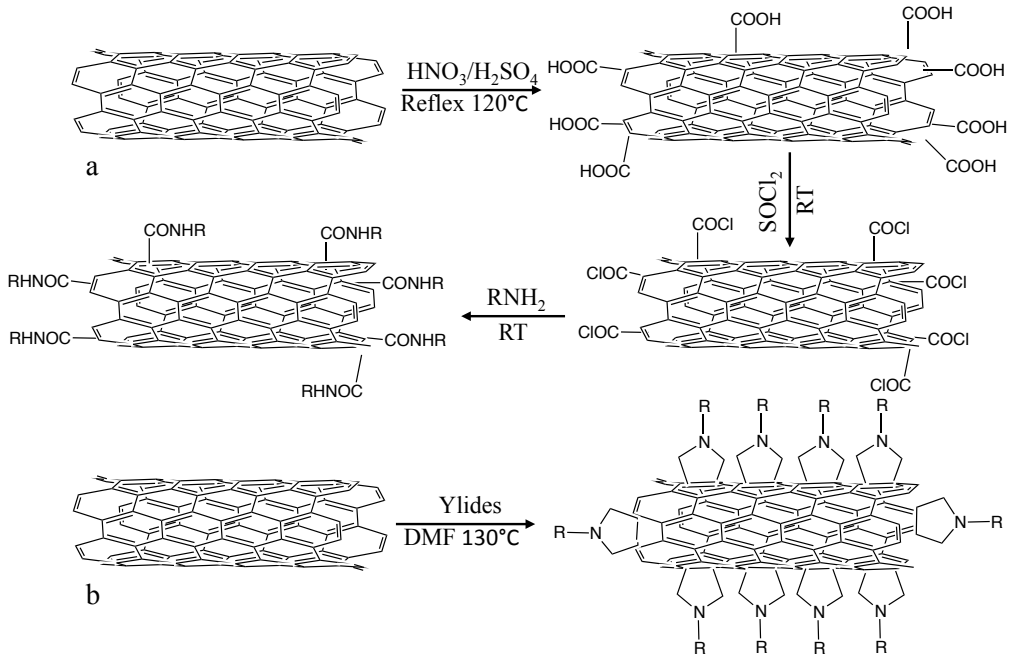

Figure 2.4 Schematic presentation of covalent modification of carbon nanotube

a) Oxidization of carbon nanotube followed by further attaching hydrophilic molecules *via* amidation reactions b) 1,3-dipolar cycloaddition reaction

Cycloaddition reaction is a very powerful methodology for covalent modification of CNT. Cycloaddition of CNT forms pyrrolidine-fused rings on nanotube surfaces by reacting with ylides [75]. In contrast to oxidation of CNT, cycloaddition generates a large number of pyrrolidine rings all around of CNT, including sidewalls and the ends of CNT (Fig. 2.4b). Thus, the resulting functionalized CNT can be well-dispersed in water [76]. It is also worth noting that the method greatly shortens the length of the CNT, which could improve its toxicological [77]. In addition, the pyrrolidine rings generated from cycloaddition can be substituted with many functional groups, which allows further linking therapeutic agents, including DNA, antibiotics and chemotherapy drugs through covalent conjugation [78, 79]. However, cycloaddition of CNT disrupts sp^2-conjugated polybenzene structure of CNT, which affects its electronic and optical performances [80].

2.5.1.2 Non-covalent surface modification of carbon nanotube

Noncovalent modification of CNT is realized by attaching coating materials *via* van der Waals force, π-stacking or hydrophobic interactions [80]. Compared with covalent

modifications, the noncovalent methods do not disturb CNT sp^2 hybridization, and therefore the optical or electronic properties of CNT are preserved, which are important for biomedical applications of CNT in imaging and detection.

Surfactants are very effective for noncovalent functionalization of CNT; however, usually high concentration of surfactant is needed, which is very toxic for the cells, so, they are not so useful in biological applications. Amphiphilic polymers are also applied for noncovalent functionalization of CNT. There are three types of polymers that have been shown effective in CNT dispersion: 1) aliphatic chain-containing polymers *e.g.* phospholipid conjugated polyethylene glycol (PL-PEG) [70, 81, 82]; 2) polyaromatic rings-containing amphiphilic block polymers, *e.g.* polystyrene-polyacrylic acid (PS-b-PAA) [71, 83-85]; 3) macromolecules that display helical structure, such as DNA and some polysaccharides (amylose, chitosan and alginate etc) [86-88] (Fig. 2.5), in which, the aliphatic chain wraps CNT through Van de Waal force and other hydrophobic interactions; the poly aromatic rings stick tightly to CNT through π-stacking; and the helical macromolecules wrap spontaneously around the tubular CNT surface *via* both favorable Van der Waals attraction and hydrophobic interactions, resulting in a compact, helical structure stabilized by an interlaced hydrogen-bond network [89, 90].

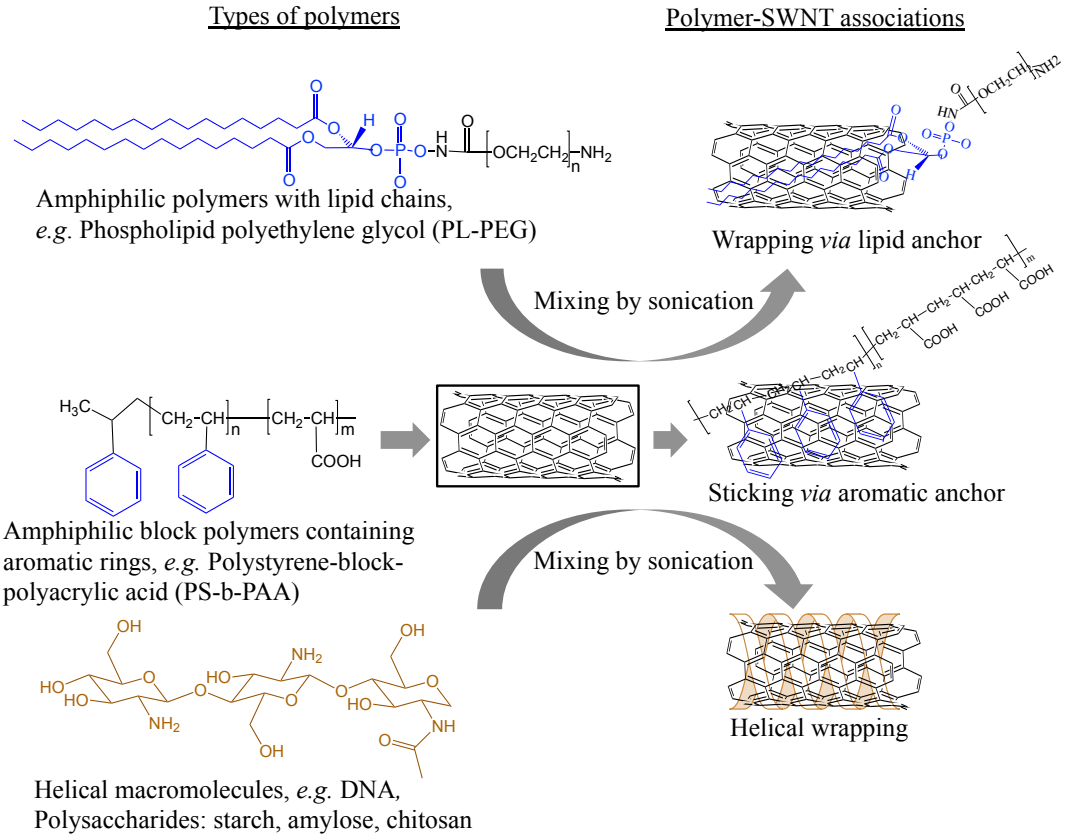

Figure 2.5 Schematic presentation of non-covalent functionalization of carbon nanotube with different types of polymers

2.5.2 Carbon nanotube based applications for cancer

In last decade, CNT has been widely explored for many biomedical applications, especially in the field of cancer therapies. Studies have shown that CNT coated with PEG generally obtain a prolonged blood circulation, which favours tumour specific targeting *via* EPR effects [91, 92]. The tumour targeting efficiency of CNT can be further enhanced by conjugation of tumour targeting molecules [93]. Moreover, the optical properties of CNT, such as NIR absorption, photoluminescence, and Raman shift etc., can be used for biological detection and imaging. In this section, the biomedical applications of CNT in the field of cancer related therapies are highlighted, including gene delivery, hyperthermia cancer therapy, tumour detection & imaging, and chemotherapy drug delivery (Fig. 2.6).

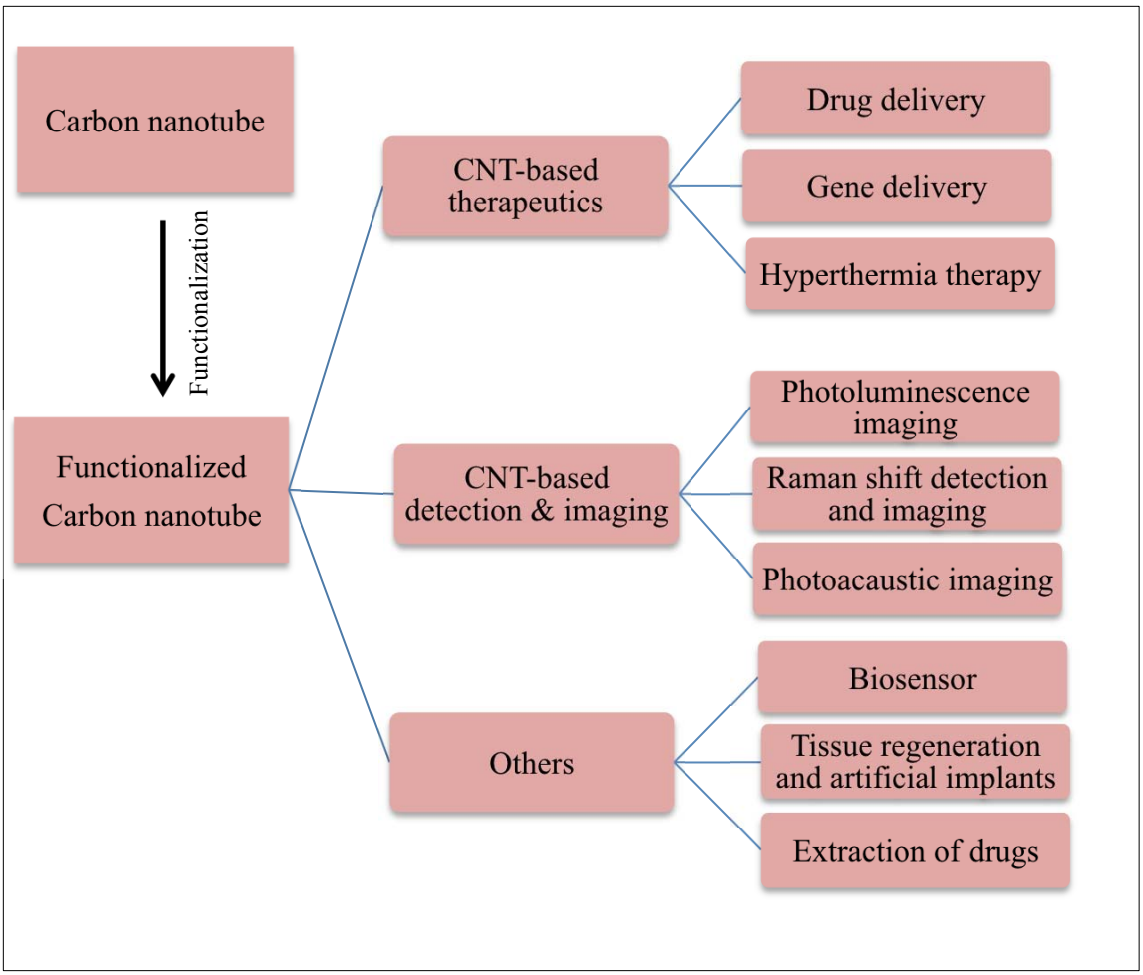

Figure 2.6 Biomedical applications of carbon nanotube

2.5.2.1 Carbon nanotube for imaging and detection of tumours

The well-ordered molecular structure attributes CNT with multiple remarkable optical properties, include strong NIR absorption, photoluminescence and Raman shift [94], which can be used for detection and imaging.

Semiconducting SWNT emits NIR photoluminescence upon photoexcitation [69]. One advantage of the photoluminescence of SWNT over organic fluorescence dyes is that SWNT has no apparent photo bleaching, which is important for tracking the changes in living systems. NIR photoluminescence has been successfully applied for tracking endocytosis and exocytosis of functionalized SWNT in NIH-3T3 cells in real time [95, 96]. *In vivo*, antibodies conjugated SWNT was successfully applied for deep tissue

penetration and high-resolution microscopy imaging of tumour vessels beneath thick skin [97, 98].

SWNT also exhibits specific resonance Raman scattering. The Raman spectrum of CNT has high sensitivity and requires only small quantity of samples. Consequently, Raman spectroscopy is one of most popular technique for detection and characterization of CNT. On the other hand, since Raman spectrum of CNT is distinguishable from autofluorescence of the tissue samples, Raman microspectroscopy of SWNT has been developed for imaging of tissue samples, live cells and small animal models [60, 99, 100].

CNT is a good candidate as a photoacoustic contrast agent owing to its strong light absorption feature [101]. In combination of targeting strategies, SWNT has been targeted delivered to tumour tissues for *in vivo* photoacoustic imaging. One study showed that RGD conjugated SWNT has been successfully delivered to tumour tissues *via* intravenous administration using a xenograft tumour mice model, in which RGD-SWNT has shown eight times stronger photoacoustic signal in the tumours than non-targeted SWNT [102].

2.5.2.2 Carbon nanotube for thermal destruction of tumours

Heat-based cancer treatment is an active research area. Tissues are known to be highly transparent to 700- to 1,100-nm NIR light, whereas, CNT strongly absorbs in this range, which generates significant amount of heat. Previous studies have shown that targeting molecules folic acid and antibodies conjugated SWNT effectively kill the cancer cells, but not the neighboring healthy cells by hyperthermia [103, 104]. Furthermore, the thermal ablation effect of CNT can be further enhanced by combination with chemotherapy drugs delivery by CNT [105].

2.5.2.3 Carbon nanotube for gene delivery

Gene therapy is an important treatment for cancer and other genetic diseases. As DNA and siRNA are macromolecules that cannot pass through cell membrane by themselves, carriers are needed to take them inside of cells to take effects. CNT is an excellent candidate for gene delivery since CNT is found to easily penetrate cells [12]. As discussed in section 2.5.1.2, DNA or siRNA can be used as CNT surface coating molecules to disperse CNT in water solution [90], by which, DNA or siRNA serves both CNT-dispersing agent and the cargo (Fig. 2.7a). It has been shown that the siRNA functionalized SWNT readily enters cells and exerts its biological activity in cultured cells [90]. *In vivo* studies with intratumoural injection of siRNA functionalized SWNT also showed significantly inhibition effect in cancer animal models [106]. Alternative to the direct wrapping method, negative charged DNA or siRNA can also be formulated with cationic polymer-coated CNT (Fig. 2.7b). It has also been found that the use of the cationic polymers, *e.g.* polyethylene imine (PEI), could protect encapsulated DNA or siRNA from degradation by nucleases [107-110].

In addition to the above-mentioned gene formulating methods, genes can also be covalently conjugated to CNT *via* cleavable chemical bonds [111, 112]. Thiol-modified siRNA has been covalently conjugated to polymer PL-PEG functionalized SWNT *via* disulfide bond [112]. The cleavage of disulfide bonds by cellular thiol digesting enzymes allows the release of the siRNA for its actions upon cellular internalization. The SWNT-mediated siRNA delivery showed much better gene transfection efficiency than liposome-based delivery system, especially in hard-to-transfect human T cells and primary cells lines [111].

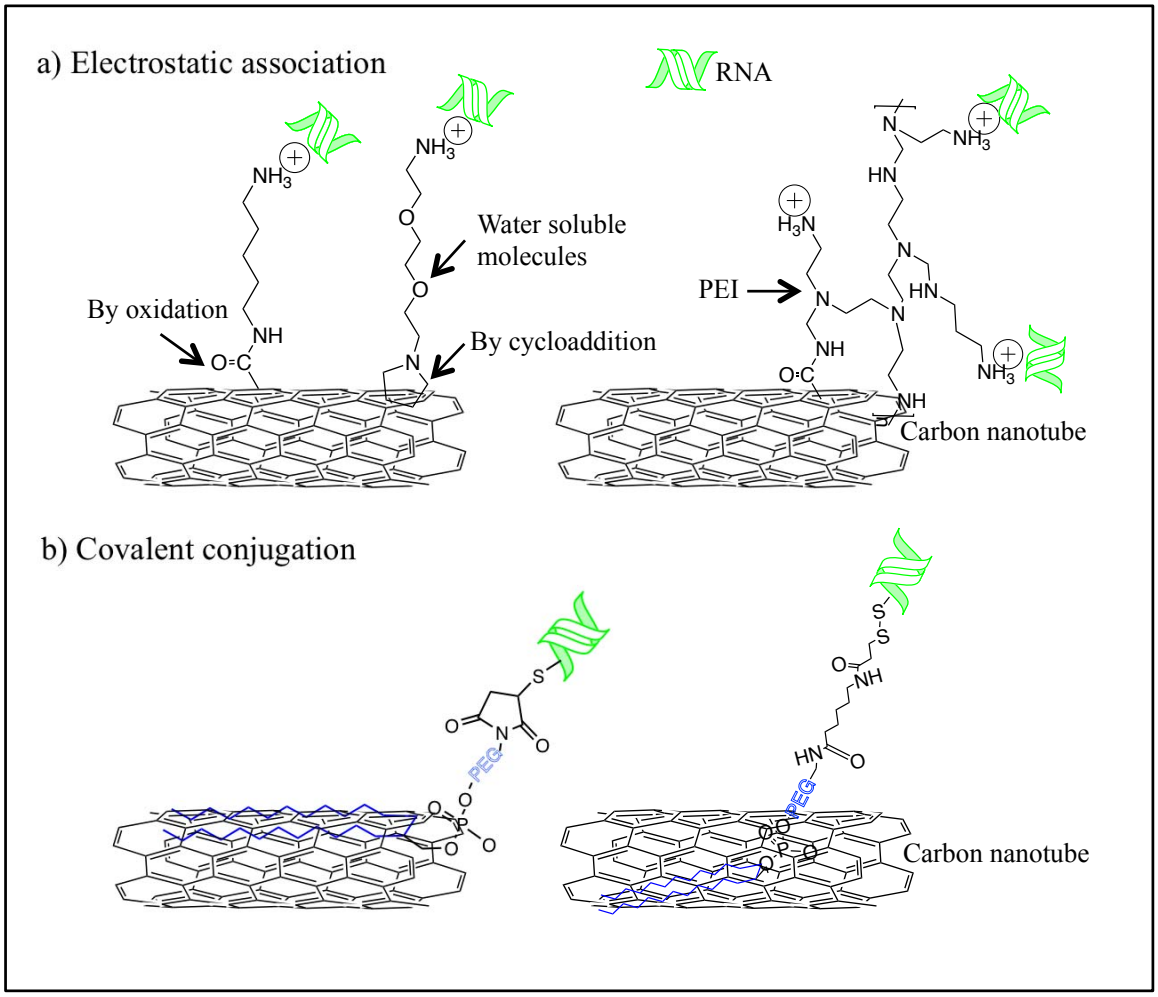

Figure 2.7 Strategies for DNA or siRNA delivery by carbon nanotube

a) Binding of genes to cationic CNT by electrostatic association b) Covalent conjugation of genes to the CNT-coating polymers *via* cleavable chemical bonds.

2.5.2.4 Carbon nanotube for chemotherapy drug delivery

Since CNT is a nanosized hollow tube, both the interior and the surface of the nanotubes can be utilized for loading of small molecule drugs. Up to date, many CNT-based drug delivery systems (DDS) have been developed for *in vitro* and in *vivo* delivery of chemotherapy drugs. For example, chemotherapy drug doxorubicin has been absorbed onto CNT by π-stacking [113, 114]. With conjugation of tumour-targeting molecules to the CNT-based DDS, the targeted SWNT-DOX have shown more effective inhibition of the of cancer cells *in vitro* and *in vivo* [105, 114-116]. Anticancer agent cisplatin was conjugated to oxidized SWNT *via* covalent bonding for delivery [117]. EGF tagged

SWNT-cisplatin has shown to specifically target and kill squamous cancer cells [117]. Alternatively, drug molecules can be covalently linked to polymer end of functionalized SWNT for delivery. For example, drug PTX was conjugated to PL-PEG functionalized SWNT for intravenous administration in murine breast cancer model, and the result showed higher tumour growth inhibition and decreased side effects than the free drug formulation [118]. The examples of CNT-based targeted delivery systems are listed in table 2.3.

Table 2.3 Examples of carbon nanotube based drug delivery systems

Therapeutics	Targeting Moieties	Drug-loading Methods	Ref.
Carboplatin	*N/A*	Filling	[119]
Cisplatin	EGF	Covalent conj.	[117]
Daunorubicin	Sgc8c aptamer	Adsorption	[115]
Docetaxel	NGR	Adsorption	[105]
Doxorubicin	Folate/Magnetic	Adsorption	[116]
Doxorubicin	RGD	Adsorption	[113]
Doxorubicin	Folate	Adsorption	[114, 120]
Doxorubicin /hyperthermia	NGR	Adsorption	[105]
Gemcitabine	Magnetic	Adsorption	[121]
Methotrexate	*N/A*	Covalent conj.	[122, 123]
Paclitaxel	*N/A*	Absoption	[105, 124]
Paclitaxel	*N/A*	Covalent conj.	[118]
Platinum (IV)	Folate	Covalent conj.	[125]

2.5.3 Limitations of existing carbon nanotube based chemotherapy drug delivery systems

CNT contains ultrahigh surface area, which can be theoretically loaded with a large amount of payloads. However, CNT is a pre-formed, covalent bonded supramolecular structure, challenges exist in attaching payloads to this pre-formed structure. To date, several schemes have been developed for CNT-based chemotherapy drug delivery utilizing passive and active targeting strategies. They can be categorized into five types of common schemes: I) filling drugs to the interior of CNT; II) adsorption of drugs to CNT

sidewall; III) covalent conjugation of drugs to the CNT backbone modified by oxidation reaction; IV) covalent conjugation of drugs to the CNT backbone modified by cycloaddition reaction; V) covalent conjugation of drugs to CNT-dispersing polymers. The strength and limitation of these schemes are discussed below and summarized in table 2.4.

I) Filling drugs to the interior of CNT

Because of unique hollow structure, CNT can be used as a nano-sized container to fill small molecule drugs [126-129]. Drug filling to the interior of CNT is facilitated by capillary driving force [119]. For filling drugs to CNT, MWNT is usually used, since MWNT has larger inner diameter than SWNT, which enables a higher filling capacity [119]. To fill drugs, the cap ends of the CNT need to be opened with treatment using nitric acid [119]. The drug-filling process is simple, however, the drug loading capacity is usually low.

II) Adsorption of drugs to CNT sidewall

Researchers have also found that pre-functionalized CNT still exists a large surface area that can be used for direct attachment of small molecule drugs. Because the carbon atoms in CNT surface form highly ordered benzene ring structure, the aromatic ring-containing drugs can be efficiently loaded on CNT *via* strong π-stacking force. Using this method, a large amount of DOX (~ 400%w/w) have been loaded onto the pre-functionalized SWNT for delivery [113, 114]. Binding to and the release of the drug molecules from the nanotube could be controlled by changing the pH. An *in vivo* study using this SWNT-based DOX formulation has demonstrated a significantly enhanced therapeutic efficacy in a murine breast cancer model compared with free drug [113]. By attaching additional tumour targeting molecules, *e.g.* FA or RGD, to the SWNT-drug, the targeted SWNT-based DOX showed more effective antitumour effects *in vitro* and *in vivo* compared with non-targeted SWNT-based DOX [105, 114-116]. Other structurally similar anthracycline drugs, *e.g.* epirubicin (EPI), and daunorubicin (DAU), can also be loaded onto CNT in a high capacity [105, 115, 124]. Although very effective, this drug-loading method is only suitable for the drugs that are flat and contain aromatic ring structure.

III) Covalent conjugation of drugs to that CNT backbone modified by oxidation reaction

Oxidized CNT contains carboxyl groups that can be used for drug conjugation. Usually, the drugs become inactive when linking to CNT, and the active drugs have to be released to exert effects, so the linkages between the drugs and CNT have to be cleavable. The common linkers used for drug delivery include ester, peptide, and disulfide bonds. These linkers could be cleaved by the enzymes present in the route of delivery. Previously, drug cisplatin has been conjugated to the oxidized SWNT *via* a peptide linker. With further conjugation of epidermal growth factor (EGF) to the SWNT-cisplatin conjugates, the targeted SWNT-cisplatin showed more efficient tumour inhibition than both free cisplatin and non-targeted SWNT-cisplatin [117]. However, oxidation reaction of CNT only generates a small number of carboxyl groups on CNT, which provides limited drug-loading capacity on CNT.

IV) Covalent conjugation of drugs to the CNT backbone modified by cycloaddition reaction

Cycloaddition reaction is a powerful tool that generates substantial amounts of functional groups on sidewall and ends of CNT [75], which affords much higher level of drug loading than oxidized CNT. Many types of therapeutics, including peptides, proteins, genes and drugs, have been examined by conjugation to functionalized CNT made by cycloaddition (denoted as *f*-CNT) for delivery [78]. For example, drug methotrexate, due to limited cellular permeability [130], was linked to *f*-CNT for intracellular drug delivery [122]. Owing to considerable amounts of functional groups that can be generated on *f*-CNT, both drug MTX and fluorescent dyes were conjugated to the same *f*-CNT for delivery, which allowed tracking intracellular localization of the CNT-drug [122]. One limitation of this method is that cycloaddition reaction disrupts sp^2-conjugated molecular structure of CNT, thus affects its optical properties [80], and therefore, is not useful for combined imaging and drug treatment applications.

V) Covalent conjugation of drugs to CNT-dispersing polymers

Alternative to direct drug-CNT conjugation, the drug molecules can also be linked to CNT-dispersing polymers for delivery. For example, PTX was conjugated to PL-PEG functionalized SWNT *via* reversible ester bond [118]. By this drug-loading method, the amounts of drugs loaded on CNT depend on the amounts of polymers that can be attached to CNT. In the case of PL-PEG functionalized CNT, only ~3 PL-PEG could be attached to each 10 nm of SWNT [113], so a large part of nanotube surface cannot be efficiently utilized. On the other hand, when drugs occupy the CNT-dispersing polymers, there is no space for linking targeting molecules, or other functionalities [118], thus targeted or multifunctional delivery is not possible.

Building upon the current literature on CNT-based drug delivery applications, we found that all current available CNT-based drug delivery systems have limitations. It is in part of the thesis to develop new schemes for construction of a more effective CNT-based drug delivery system for treatment of breast cancer.

Table 2.4 Current available schemes for CNT-based drug delivery systems

Drug loading schemes	Strengths	Limitations	Ref
Filling 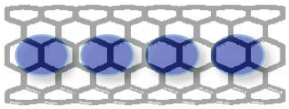	• convenient formulation • preserved intrinsic CNT electrical and optical properties	• low drug-loading capacity • limited to water-soluble drugs	[119]
Adsorption 	• convenient formulation • high loading capacity • preserved intrinsic CNT electrical and optical properties • both CNT surface and its dispersing polymer can be used for different functionalities, e.g. drugs, targeting molecules, etc.	• only effective for molecules that are flat and contain aromatic rings structure	[113]
Covalent conjugation to CNT modified by oxidization reactions 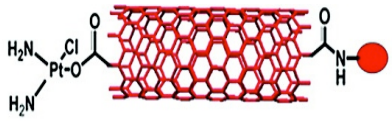	• suitable for all types of drugs that contain reactive functional groups	• low drug-loading capacity due to low level of -COOH groups formed on CNT surface	[117]
Covalent conjugation to CNT modified by cycloaddition reaction 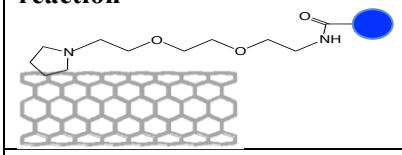	• suitable for all type of drugs that contain reactive functional groups • high drug-loading capacity due to high level of functional groups generated on CNT	• disruption of electrical and optical properties of CNT by cycloaddition reaction	[122]
Covalent conjugation to CNT-dispersing polymers 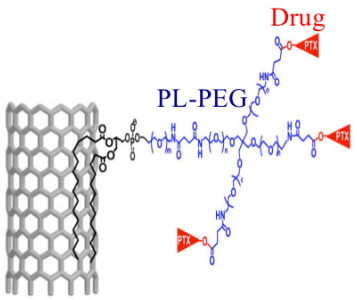	• suitable for all type of drugs that contain reactive functional groups • preserved intrinsic CNT electrical and optical properties	• in the cases of low level of polymer-coating on CNT – low drug-loading capacity – not space for linking targeting molecules or other functionalities	[118]

2.5.4 Potentials and limitations of carbon nanotube

The unique structural and optical properties offer CNT many advantages over other nanoparticles in terms of drug delivery applications: 1) both the interior and the surface of CNT can be employed to load therapeutics; 2) with all atoms exposed on the surface, the CNT affords large surface area for drug-loading; 3) the unique long and thin structure of CNT facilitates cell internalization, thus the intracellular delivery of therapeutics; 4) with the intrinsic optical properties, *e.g.* NIR absorption, Ramen shift, fluorescence, etc, CNT has potential for simultaneous tumour detection and drug delivery, as well as hyperthermia cancer therapy; 5) comparing with other metallic nanoparticles that also display intrinsic optical properties, CNT, being made of all carbon atoms, which is the chemical basis of all lives, in essence is non-toxic.

On the other hand, the toxicity of CNT has received much attention [67, 77, 131-133], although CNT, being made of all carbon atoms, is expected to be biocompatible. The concerns of CNT toxicology are due to its small size since, being the nano-sized material, the toxicological effects differ from those of the same composition but with larger particle sizes [133, 134]. Actually, toxicity evaluation faces many challenges for nanoparticles. This is because, under physiological condition, nanoparticles interact with biological entities, such as plasma proteins and electrolytes. Very often, these nanoparticles form aggregates due to hydrophobic interactions and electrostatic attractions, consequently resulting changes in size, surface area, and surface charge, etc, which cause differences in their toxicological behaviours.

In addition, due to the fibre-like structure of CNT, its toxicity might be associated with asbestos and other pathogenic fibres [135-140]. One important study reported that administration of long (>10 μm) and rigid pristine nanotubes *via* intraperitoneal injection led to mesothelioma (a cancer of the membranous lining that covers the outer surface of the chest and abdominal cavities) in mice, which resembled the length-dependent, pathogenic behaviour of asbestos [135]. This result has brought a hot debate on overall toxicological profile of the coated and uncoated nanotubes, as well as the effects of the CNT lengths to its toxicity [77]. Indeed, many studies on CNT toxicities published so far

are controversial and barely comparable due to multiple factors, including dispersion status, size and length of nanotubes, metal impurities, surface functionalization methods, and treatment dosages etc. With present knowledge, we do not have a comprehensive view of toxicological effect of CNT, however, there is an agreement that well dispersed CNT showed decreased or no toxicity *in vitro* and *in vivo* (reviewed in[67, 132, 141]).

Among the studies examining the well-dispersed CNT, two types of functionalized CNT, the PL-PEG coated SWNT (SWNT-PL-PEG) [93] and covalently functionalized CNT *via* cycloaddition reactions (*f*-CNT) [142], are carefully evaluated in terms of their tissue distribution, accumulation and excretion. It is evident for SWNT-PL-PEG that 1) it did not lead to acute or chronic toxicity in treated mice when administrated in high doses *via* intravenous injection; 2) it persisted within liver and spleen macrophages for 4 months in mice without apparent toxicity [143]; 3) it was excreted slowly from mice *via* the biliary and renal pathways [93]. The *f*-CNT is also shown not toxic both *in vitro* and *in vivo* [142], however, distinct from the SWNT-PL-PEG, the *f*-CNT showed predominant renal excretion following intravenously administration [142]. It has been suggested that urinary excretion and low tissue accumulation might be due to shortened and better-dispersed nanotubes due to cycloaddition reactions [77]. These data also suggested that the types of CNT surface modifications are important in dictating tissue accumulation and excretion.

In summary, CNT has great potential in drug delivery in many diseases including breast cancer. However, research on CNT as a drug carrier is still in its infancy. The purpose of this thesis is to develop CNT-based delivery systems vis-à-vis their design, suitability and effectiveness for breast cancer treatment using *in vitro* and *in vivo* experimental models.

PREFACE TO CHAPTERS 3-6

The initial hurdle of biomedical applications of CNT has been its poor solubility. To test the research hypothesis of construction of an SWNT-based drug carrier, I firstly examined noncovalent functionalization of SWNT so as to disperse and stabilize SWNT in aqueous solutions. **Chapter 3** describes noncovalent functionalization of SWNT using three different types of polymers: a lipid-conjugated polymer, an amphiphilic block polymer, and a polysaccharide. The three types of polymers attach to SWNT through different types of SWNT-polymer interactions. Although, these polymer-functionalized CNT were examined separately by different groups previously, it is the first time that, noncovalent functionalization of SWNT using these polymers were compared under same experimental conditions in terms of the SWNT dispersibility, stability, cytotoxicity, and the cell internalization.

Based on the result obtained in **Chapter 3,** I proposed three new schemes (denoted as SWNT-lipid-PTX, SWNT-HSA-PTX and SWNT-polymer-PTX respectively) for SWNT-based drug delivery systems using chemotherapy drug PTX as a model drug. The three SWNT-based PTX delivery systems were characterized and evaluated *in vitro* using cancer cell lines and other *in vitro* procedures. Among them, the SWNT-lipid-drug was chosen for further evaluation in an experimental animal model due to high drug-loading capacity and its potential for targeted/multifunctional drug delivery. Each of these schemes offers a new route of drug loading on CNT, which contributes to our present knowledge on construction of CNT-based drug delivery systems. The three SWNT-PTX schemes are presented respectively in chapter 4-6.

Chapter 4 describes a new scheme of SWNT based PTX drug delivery system using human serum albumin (HSA) nanoparticle conjugated SWNT (denoted as SWNT-HSA-PTX). The HSA is chosen due to its high binding affinity to PTX. In this study, cross-linked HSA nanoparticles were covalently conjugated to SWNT for PTX loading. The design strategy, preparation, characterization, and *in vitro* antitumour efficacy of SWNT-HSA-PTX were presented.

In **Chapter 5**, polymer-drug approach was applied to construct an SWNT-based drug delivery for PTX. In this study, PTX was firstly grafted to a polyacid-containing polymer and then used for SWNT coating. The chemical synthesis of the polymer-PTX, as well as the characterization and *in vitro* evaluation of SWNT-polymer-PTX were presented.

Chapter 6 introduces a novel drug-loading method on SWNT using lipid-drug approach. A proof-of-concept study was performed in breast cancer animal model using SWNT-lipid-PTX. The design strategies and advantages of the lipid-drug approach for construction of SWNT-based drug delivery system was firstly described and the construction, characterization and *in vitro* evaluation of SWNT-lipid-PTX were presented. Finally, the *in vivo* tumour growth inhibition, safety and toxicity of the SWNT-lipid-PTX were further evaluated in a breast cancer xenograft mice model.

Original research articles included in the thesis (accepted/submitted):

1. **Shao W,** Imani R and Prakash S, Comparison of carbon nanotube functionalization with various biocompatible polymers: dispersion, characterization, toxicity, and cell internalization (submitted to Journal of Nanoscience and Nanotechnology, 2014)
2. **Shao W,** Paul A, Zhao B, Lee C, Rodes L and Prakash S (2013) Carbon nanotube lipid drug approach for targeted delivery of a chemotherapy drug in a human breast cancer xenograft animal model, Biomaterials, 34 (38), 10109-10119
3. **Shao W**, Paul A, Rodes L and Prakash S, A novel human serum albumin nanoparticle conjugated carbon nanotube for intracellular delivery of paclitaxel: design, preparation and evaluation of *in vitro* antitumour activity (submitted to Cell Biochemistry and Biophysics, 2013, presently, the manuscript was tentatively accepted with minor revision)
4. **Shao W,** Zeng H.Y, Paul A and Prakash S, Design and construction of a new carbon nanotube-based paclitaxel delivery system using polymer-drug approach (submitted to Journal of Biomaterial Applications, 2014)

Original research articles not included in the thesis (published/submitted):

5. Aries A, Whitcomb J, **Shao W**, Komati H, Saleh M, Nemer M, Caspase-1 cleavage of transcription factor GATA4 and regulation of cardiac cell fate (submitted to Nature Communication, 2014)

6. Paul A, Abbasi S, **Shao W**, Khan A, Malhotra M, Satya Prakash, HIV-1 Tat peptide incorporated albumin nanocarriers for efficient siRNA delivery: *in vitro* analysis for breast cancer therapy (submitted to Therapeutic Delivery, 2013)

7. Rodes L, Tomaro-Duchesneau C, Saha S, Paul A, Malhotra M, Marinescu D, **Shao W**, Kahouli I and Prakash S, Enrichment of Bifidobacterium longum subsp. infantis ATCC 15697 within the human gut microbiota using alginate-poly-L-lysine-alginate microencapsulation oral delivery system: an *in vitro* analysis using a computer-controlled dynamic human gastrointestinal model, J Microencapsul 31 (3), 230 (2013)

8. Rodes L, Khan A, Paul A, Coussa-Charley A, Marinescu D, Tomaro-Duchesneau D, **Shao W**, Kahouli I and Prakash S, Effect of probiotics Lactobacillus and Bifidobacterium on gut-derived lipopolysaccharides and inflammatory cytokines: an *in vitro* study using a human colonic microbiota model, Journal of microbiology and biotechnology 23 (4), 518 (2013)

9. Paul A, **Shao W**, Shum-Tim D, Prakash S, The attenuation of restenosis following arterial gene transfer using carbon nanotube coated stent incorporating TAT/DNA (Ang1+Vegf) nanoparticles. Biomaterials 2012. Epub 2012/07/24.

10. Paul A, **Shao W**, Abbasi S, Shumtim D, Prakash S, PAMAM dendrimer-baculovirus nanocomplex for microencapsulated adipose stem cell-gene therapy: *in vitro* and *in vivo* functional assessment. Mol Pharm 2012. Epub 2012/07/24.

11. Abbasi S, Paul A, **Shao W**, Prakash S, Cationic albumin nanoparticles for enhanced drug delivery to treat breast cancer: preparation and *in vitro* assessment. Journal of Drug Delivery 2012; Epub 2011/12/22.

12. Yeretssian G, Doiron K, **Shao W**, Leavitt BR, Hayden MR, Nicholson DW, et al. Gender differences in expression of the human caspase-12 long variant determines susceptibility to Listeria monocytogenes infection. Proc Natl Acad Sci U S A. 2009;106(22):9016-20. Epub 2009/05/19.

13. Roy S, Sharom JR, Houde C, Loisel TP, Vaillancourt JP, **Shao W**, et al. Confinement of caspase-12 proteolytic activity to autoprocessing. Proc Natl Acad Sci U S A. 2008;105(11):4133-8. Epub 2008/03/12.

14. **Shao W**, Yeretssian G, Doiron K, Hussain SN, Saleh M. The caspase-1 digestome identifies the glycolysis pathway as a target during infection and septic shock. J Biol Chem. 2007;282(50):36321-9. Epub 2007/10/26.

Review & Book chapters

1. **Shao W**, Paul A, Mai Y, Laetitia R and Prakash S, in Synthesis and Applications of Carbon Nanotubes and Their Composites, S. Suzuki, Ed. InTech, Rijeka, Croatia, 2013

2. **Shao W**, Paul A and Prakash S, Selective Topics in Nanomedicine, T.M.S Chang, Ed., World Scientific, Singapore 2013

3. Paul A, **Shao W**, Burdon T, Shum-Tim D, Prakash S, Dendrimer Nanoparticles and Their Applications in Biomedicine. Chapter 10 (339-362) in Nanomaterials in Drug Delivery, Imaging and Tissue Engineering, A.Tiwari and A. Tiwari Ed. WILEY-Scrivener Publishing LLC 2012

4. Prakash S, Malhotra M, **Shao W**, Tomaro-Duchesneau C and Abbasi S, Polymeric nanohybrids and functionalized carbon nanotubes as drug delivery carriers for cancer therapy, Adv Drug Deliv Rev 63 (14-15), 1340, 2011

Poster presentations (presenting authors indicated with an asterisk *)

1. **Shao W***, Paul S, Rodes L, Tomaro-Duchesneau C, Saha S and Prakash S "Carbon nanotube toxicity: investigation of single-walled carbon nanotubes in experimental nude mice model." 16th Canadian Society for Pharmaceutical Sciences (CSPS) Annual Symposium, June 11-14, 2013, University of British Columbia, Vancouver, BC, Canada
2. Rodes L*, Tomaro-Duchesneau C, Saha S and Prakash S, **Shao W**, Kahouli I, Prakash S "Anti-inflammatory properties of probiotics: an *in vitro* investigation using a human colonic microbiota model and raw 264.7 macrophage cells", International symposium on innate immunity, October 7-9, 2013, France
3. **Shao W***, Paul A, Abbasi S, Chahal PS, Mena JA, Montes J, Montes J, Kamen A, Prakash S "Production of virus-like particles derived from adeno-associated virus for

potential biomedical applications", 9th World Congress of Biomaterial, June 1-5, 2012, Chengdu, China

4. **Shao W*** and Prakash S "Development of a carbon nanotube based drug delivery system" 2nd International Conference on Nanotechnology: Fundamentals and Applications, July 27-29, 2011, Ottawa, Ontario, Canada
5. **Shao W*** and Prakash S "Preparation and characterization of functionalized carbon nanotubes for potential biomedical applications" Multidisciplinary Approaches to Modern Therapeutics: Joining Forces for a Healthier Tomorrow, May 24 – 27, 2011, Montreal, QC, Canada
6. **Shao W*** and Saleh M "Identification of caspases substrates by diagonal gel approach and study on Caspase-1 substrates in glycolytic pathway", 50th Canadian Society for Biochemistry and Molecular Biology (CSBMCB) Annual Meeting, July 5 – 9, 2007, Montreal, QC, Canada
7. **Shao W*** and Saleh M "une caractérisation protéomique du digestome de la Caspase-1", 49e Congrès du CRCQ Sept. 20 – 22, 2007, Mont-Tremblant, QC, Canada

CONTRIBUTIONS OF CO-AUTHORS

As the first author of the original research articles included in this thesis, I was responsible for designing studies, conducting experiments, analyzing data, and writing the manuscripts. For all research articles, Dr. Satya Prakash, reported as the last author in all manuscripts, is a research advisor also the corresponding author. Specific contributions of the co-authors are listed below.

Chapter 3: Rana Imani helped with cell culture, discussion on the results and proofreading of the manuscript.

Chapter 4: Laetitia Rodes helped with cell culture and proofreading of the manuscript. Arghya Paul helped with *in vitro* lab technique for TUNEL. All the co-authors discussed the results and commented on the manuscript.

Chapter 5: Huiying Zeng provided assistance with discussion on the ratio of reactants, technical support of chemical synthesis and analysis of NMR spectrum of the polymer-drug. Arghya Paul helped with *in vitro* lab technique for DAPI staining. All the authors contributed in the discussion of the results and the proof reading of the manuscript.

Chapter 6: Laetitia Rodes helped with cell culture and proofreading of the manuscript. Bin Zhao helped with chemical synthesis of lipid-paclitaxel and analysis of NMR spectrum. Crystal Lee provided the assistance for the cell cycle analysis and proofreading of the manuscript. Arghya Paul helped with animal study. All the co-authors discussed the results and commented on the manuscript.

Original Research Article 1

CHAPTER 3 INVESTIGATION OF NONCOVALENT FUNCTIONALIZATION OF SINGLE-WALLED CARBON NANOTUBE USING VARIOUS POLYMERS: DISPERSION, STABILITY, TOXICITY AND INTRACELLULAR DRUG DELIVERY FEATURES

Wei Shao, Rana Imani and Satya Prakash*

Biomedical Technology and Cell Therapy Research Laboratory, Department of Biomedical Engineering, Faculty of Medicine, McGill University
3775 University Street, Montreal, Quebec, H3A 2B4, Canada.

* Corresponding author, Email: satya.prakash@mcgill.ca
Tel: 1 (514) 398-3676; Fax: 1 (514) 398-7461

Preface: The initial hurdle of biomedical applications of CNT has been its toxicity and poor solubility due to its hydrophobic nature. Proper surface modification of CNT, or CNT functionalization, so as to prepare well-dispersed CNT in biologically compatible solutions is a primary step for biomedical applications of CNT. The goal of this study is to examine noncovalent functionalization of SWNT with three different types of polymers: a lipid-conjugated polymer, an amphiphilic block polymer, and a polysaccharide. The three types of polymers could attach to SWNT through different types SWNT-polymer interactions. The obtained SWNT-polymers were examined and compared in terms of their SWNT dispersibility, surface properties, stability, cytotoxicity, and their cellular internalization.

The article was submitted to *Journal of Nanoscience and Nanotechnology* (2014).

3.1 Abstract

Single-walled carbon nanotube (SWNT) is a novel type of nanomaterials that has many features suitable for drug delivery applications. However, SWNT is not soluble in aqueous solutions, surface functionalization of SWNT so as to disperse it into aqueous solution becomes a primary step for its use in biomedical applications. In this study, for the first time, we compared the dispersibility, stability and other drug-delivery related properties of noncovalently functionalized SWNT using three polymers: a lipid-polymer phospholipid-polyethylene glycol (PL-PEG), a polybenzene ring containing polymer polystyrene-block-polyacrylic acid (PS-b-PAA) and a polysaccharide chitosan (CHI). We showed that the dispersity and stability of the SWNT functionalized by these polymers were much different. Transmission electronic microscopy (TEM) study revealed distinct morphology and much thicker polymer layer on SWNT-PS-b-PAA compared with other two SWNT-polymers. The higher level of polymer-coating ratio in SWNT-PS-b-PAA was confirmed by Thermogravimetric analysis (TGA) study, suggesting that PS-b-PAA could be attached to SWNT more densely than other two types polymers. The *in vitro* study showed that all three types of polymer coated SWNT cause little or no toxicity to the cells. All three types of polymer coated SWNT have shown to enter cancer cells as examined using FITC-labeled SWNT-polymers. The current study bridges SWNT with biological systems and establishes a foundation for the use of SWNT in drug delivery and other biomedical applications.

3.2 Introduction

Carbon nanotube (CNT) is a synthetic material made from all carbon atoms. Structurally, CNT can be viewed as a hollow tube rolled from layers of graphene sheets. Depending on the number of graphene layers, CNT is classified as single-walled carbon nanotube (SWNT) or multi-walled carbon nanotube (MWNT). CNT has attracted much attention since it was discovered in 1991 owing to its novel needle-like structure and remarkable physical properties, such as, ultrahigh surface area, distinct optical properties [64], and excellent electrical conductivity [65]. However, raw CNT is highly insoluble, and forms large bundles in aqueous solution due to strong inter-tube Van der Waals interaction. The initial hurdle of biomedical applications of CNT has been its poor solubility, particularly in biologically compatible buffers and conditions. In addition, toxicity studies have shown that raw CNT is toxic to mammalian cells and treated animals [68, 133, 135] due to its hydrophobicity. In contrast, the well-dispersed CNT does not cause apparent toxicity *in vitro* and *in vivo* [93, 131, 142, 144]. Thus, proper surface modification of CNT, or CNT functionalization, so as to prepare well-dispersed, biocompatible CNT is a critical step for biomedical applications of CNT [145]. The CNT surface modification methods are involved in covalent and non-covalent strategies. Covalent methods generate chemical bonds on the backbone of CNT, while noncovalent modification of CNT attaches water-soluble molecules on CNT surface by physical interactions. Both methods are effective for dispersion of CNT in aqueous solution. However, covalent modification disturbs sp^2 hybridization structure of CNT, thus, the optical or electronic properties of CNT could be destroyed [146]. In contrast, the noncovalent modification of CNT preserves the physical properties of CNT, which is important for biomedical applications of CNT in imaging and detection [11].

Raw CNT often forms tangled, rope-like structure due to high inter-tube Van der Waals binding energy. The Van der Waals force between the nanotubes is so great that high energy is needed to pry them apart. Ultrasonication is a commonly applied method for noncovalent functionalization of CNT, which provides sufficient energy to separate the aggregates. By mixing CNT with certain amphiphilic molecules with sonication, the CNT in solution would reconfigure to a new equilibrium state of lower energy by adsorption of

these interfacial molecules *via* hydrophobic interactions. Previously, many polymers have been examined for noncovalent functionalization of CNT. Typically, CNT-coating polymers can be categorized into three major types: 1) long chain lipid conjugated polymers *e.g.* phospholipid polyethylene glycol (PL-PEG) [70, 81, 82]; 2) polyaromatic chain-containing amphiphilic block polymers, *e.g.* polystyrene-block-polyacrylic acid (PS-b-PAA) [71, 83-85]; 3) polysaccharides, *e.g.* chitosan (CHI) [86-88] (Fig. 3.1). The lipid chains in the lipid-polymers could wrap to CNT through Van der Waals force and other hydrophobic associations; the poly aromatic chains could stick tightly to CNT through π-stacking; and the polysaccharides wrap spontaneously around the tubular CNT surface *via* favorable Van der Waals attraction, resulting in a compact, helical structure stabilized by an interlaced hydrogen-bond network [89]. Coating of these polymers on CNT remarkably improves dispersibility of CNT in aqueous solutions.

The goal of this study was to examine noncovalent functionalization of SWNT using the above-mentioned three types of polymers, and to investigate their dispersibility, surface properties, stability, cytotoxicity, and their cellular internalization for potential drug delivery and other biomedical applications.

3.3 Materials and methods

3.3.1 Reagents

All the reagents used in the experiments were purchase from Sigma Aldrich, Canada except otherwise indicated specifically.

3.3.2 Preparation of polymer-functionalized SWNT

SWNT-PL-PEG-NH_2: The SWNT functionalization procedure using PL-PEG-NH_2 followed the method reported by Liu, *et al* [81]. Briefly, PL-PEG-NH_2 (Avanti Polar Lipids, Inc. US) was dissolved in deionized (DI) water at a concentration of 0.5 mg/mL, Then 1 mg of SWNT (HiPco, Unidym Inc, USA) was added to 10 mL of PL-PEG-NH_2 solution, and sonicated continually for 1 hr in a tip sonicator (Microson^{TM}, XL2000,

100W, USA). During sonication, the sample was cooled in a water bath filled with ice-cold water to avoid overheating.

SWNT-PS-b-PAA: The functionalization of SWNT with PS-b-PAA followed the method developed by Kang et al [71] with minor modification. Briefly, PS-b-PAA (MW1.8k-b-6.0k Polymer Source, Montreal) was firstly dissolved in organic solvent DMF at a concentration of 4 mg/mL. 1 mg of SWNT was added in 10 mL of PS-b-PAA solution with brief sonication in a probe sonicator followed by adding 10 times DI water with continuous sonication for 1 hr with cooling with ice-cold water.

SWNT-CHI: The SWNT-CHI was prepared according to the previously developed procedure[86] with minor modification. Water-soluble CHI (Mesh 80, Jinan Haidebei Marine Bioengineering Co, China) was dissolved in DI water at a concentration of 2 mg/mL. Then SWNT (1 mg) was added to 10 mL of CHI solution and sonicated for 1 hr with cooling with ice-cold water.

After sonication, the preparation was centrifuged at 20k rpm (50Ti, Beckman Coulter, USA), and the well-dispersed SWNT-polymers were collected in supernatants. The samples were stored at 4 °C. Before use, the excess polymers and solvent were removed by three times of washing with DI water using centrifugation filtration units (Amicon, 100 kDa).

3.3.3 Characterization of polymer-functionalized SWNT

UV-NIR spectra of the functionalized SWNT solutions were obtained over the range of 190 – 850 nm in a UV-NIR spectrophotometer (Cary-100 bio, Varian Inc.) using 1 cm quartz cuvettes. Thermogravimetric analysis (TGA) was performed using Q500 (TA instruments Ltd, UK). Freeze dried SWNT-polymer samples were loaded in the sample holder and were heated up to 800 °C at a rate of 10 °C/min under nitrogen atmosphere. The weight loss and derivative weight (the rate of weight loss) were recorded continuously. The morphologies of the SWNT functionalized with different polymers were examined by Transmission electronic microscopy (TEM) (Philips169 CM200 200 kV). 5 μl of sample solution was deposited on carbon-coated copper grid and allowed to

dry for 10 mins. The surface charge of the functionalized SWNT was evaluated using zeta potential analyzer (Brookhaven Instruments Corporation, USA). 10 measurements were taken for each sample. The results were expressed as mean ± standard error.

3.3.4 Cell culture and cytotoxic study of polymer-functionalized SWNT

MCF-7 breast cancer cells (ATCC) were maintained in Dulbecco's modified Eagle's Medium (DMEM, Invitrogen, Canada) supplemented with 10% fetal bovine serum (FBS, Invitrogen, Canada). The cells were cultured in a humidified incubator with 5% CO_2 at 37 °C. The cytotoxicity of SWNT-polymer was evaluated in MCF-7 breast cancer cells using the Cell Titer 96® Aqueous Non-Radioactive Cell Proliferation MTS Assay kit (Promega). Briefly, triplicate of 1×10^4 cells were seeded in a 96-well plate and cultured for 24 hrs followed by treatment with polymer- functionalized SWNT at a concentration of 50 μg/mL at 37°C. The MTS assay was performed following the manufacture's instructions at varied time periods. The 3-(4,5-dimethylthiazol-2-yl)-5-(3-carboxymethoxyphenyl)-2-(4-sulfophenyl)-2H-tetrazolium (MTS) was reduced to form formazan by mitochondrial enzyme dehydrogenase in viable cells. The formazan concentration in the cell culture was measured at absorbance of 490 nm using 1420-040 Victor3 Multilabel Counter (Perkin Elmer, USA). The amount of formazan is proportional to the number of viable cells. The cell viability of SWNT-treated cells was calculated as the percentage of viable cells relative to that in untreated control group.

3.3.5 Preparation of FITC-labeled SWNT for cell internalization assay

The SWNT-polymers were diluted in PBS solution at a concentration of 100 μg/mL. The FITC stock solution (4 mg in ethanol) was added to SWNT-polymer solutions at a final concentration of 0.4 mg/mL, and then sonicated briefly followed by incubation at room temperature for overnight. The unbound FITC was removed by washing with DI water using a filtration column (100 kDa cut-off). For cell internalization assay, the MCF-7 cells were seeded in a 96-well plate at a density of 2×10^4 cells/well in 200μl medium at one night before the assay. The cells were incubated with FITC-labeled SWNT for 24

hrs, then washed and viewed under fluorescent microscopy (Nikon, Eclipse, Te2000-4, Japan).

3.4 Results and discussion

3.4.1 Characterization of SWNT-polymers

We observed that the raw SWNT was highly insoluble and formed large aggregation in water (Fig. 3.2A). To compare the SWNT-dispersibility by three polymers, we applied the same sonication/ultracentrifugation condition for SWNT functionalization using the same initial SWNT concentration. At experimental endpoint, the SWNT was dispersed in water by all three types of polymers. After removing precipitated SWNT bundles by ultracentrifugation, it was observed that different levels of SWNT dispersibility were obtained with the three types of polymers, in which, the SWNT-CHI solution exhibited black in color; the SWNT-PL-PEG showed clear grey in color, whereas, the SWNT-PS-b-PAA showed clear brownish solution (Fig. 3.2A).

It is known that SWNT has strong absorption in UV-NIR range, however, the bundled SWNT hardly absorbs in this range due to the photoluminescence quench [147]. UV-NIR spectrometry offers a precise measurement of SWNT concentration in solution [111]. The results showed that all three types SWNT-polymers displaying strong absorbance over the measured range of 190 – 850 nm (Fig. 3.2B-D), suggesting that the individually dispersed nanotubes formed. By comparing the absorbance of the SWNT-polymers at 400 nm, the ratio of the amount of SWNT dispersed in water was roughly 10:5:1 for CHI, PL-PEG and PS-b-PAA respectively.

Under TEM, it was observed that the nanotubes tangled together and formed large bundles Fig. 3.3A. After functionalization with polymers, single-dispersed nanotubes formed (Fig. 3.2B-C). The morphology of SWNT-PL-PEG and SWNT-CHI were similar, showing hollow nanotubes covered by a thin layer (less than 0.5 nm in thickness) of polymers (Fig. 3.3B & D); in contrast, the SWNT-PS-b-PAA showed a much thicker polymer layer (with a thickness ~ 15 nm, Fig. 3.3C). As we know, both PL-PEG and CHI

attach to SWNT by wrapping, therefore, only thin polymer layers were formed on SWNT; however, PS-b-PAA attached to SWNT *via* its hydrophobic PS portion with its hydrophilic PAA portion orderly aligned towards aqueous environment forming a brush-like thicker layer around the nanotubes (Fig. 3.3C).

The polymer-coating ratio in the three SWNT-polymers was investigated by TGA. The polymers pyrolysis before 500 °C under nitrogen condition, however, the SWNT is stable up to 1200 °C. Such a difference in thermal stability allows calculating the amount of the polymers coated on SWNT. Based on TGA result (Fig. 3.4), the polymer-coating ratios were calculated to be 48%, 94% and 80% w/w for SWNT-PL-PEG, SWNT-PS-b-PAA and SWNT-CHI respectively (the percentages of polymers were corrected by removing the weight of moisture from initial weight of samples). The result suggested that PS-b-PAA could be coated more densely on SWNT than the other two types of polymers, which is consistent with the TEM result that showed a thicker polymer layer on PS-b-PAA coated SWNT. The low polymer-coating ratio of SWNT-PL-PEG in our experiment was consistent with previous studies that showed pre-functionalized SWNT existed large uncoated surface that could be used for loading of a large amount of drug molecules [113, 120]. However, this direct drug-SWNT adsorption method might not be suitable for SWNT-PS-b-PAA drug carrier, since the uncoated surface area could be low in SWNT-PS-b-PAA. On the other hand, because of high polymer-coating ratio of PS-b-PAA on SWNT, high drug loading capacity on SWNT could be achieved by covalent conjugation of the drug molecules to the SWNT-coating polymers, which is especially useful for the bulky, hydrophobic drugs that are unable to be attached to SWNT sidewall.

As we know, in addition to stabilization of SWNT by steric hindrance of the coated polymers, the charges in the polymers also help to stabilize the dispersed SWNT-polymers in water. Zeta potential analysis indicated that the SWNT-CHI had a zeta potential of +60 ± 3 mv due to large number of highly cationic CHI; the SWNT-PS-b-PAA showed a zeta potential of -23 ± 3 mv because of the negative charged $-COO^-$ group; and the SWNT-PL-PEG-NH_2 had a positive charge of +12 ± 3 mv. As examined, all the three types of polymer-coated SWNT were stable in water at a SWNT

concentration up to 400 μg/ml. The stability of SWNT-polymers was further investigated in physiological buffer PBS and serum containing medium. The results showed that the SWNT-PL-PEG-NH_2 and SWNT-PS-b-PAA exhibited excellent stability with no aggregation observed by incubating in PBS (0.01M, PH7.4) and DMEM containing 10% FBS for 48 hrs at 37 °C. However, upon incubation of high concentration of SWNT-CHI (>100 μg/mL) with PBS and the cell culture medium, aggregation occurred. The differences in the stability of various polymer-coated SWNT could be due to different stabilization mechanisms. In SWNT-PL-PEG-NH_2 and SWNT-PS-b-PAA, the SWNT are stabilized by two factors: the charge and steric hindrance of the coated polymers. However, the steric hindrance of CHI on SWNT is minor since CHI wraps SWNT with its entire molecule, so the stability is largely supported by its highly positive charge (zeta of +60 mv). However, when the charges in CHI are neutralized by the ions existed in PBS and other physiological solutions, aggregation of SWNT could occur.

3.4.2 Cytotoxicity of SWNT-polymers

The cytotoxicity of SWNT-polymers was examined by MTS assay using MCF-7 cells. With treatment dosage of 50 μg/mL, no toxicity was observed in SWNT-PL-PEG-NH_2 and SWNT-CHI treated cells (viability close to 100%), which was consistent with the results obtained by other groups that PL-PEG functionalized SWNT is not toxic [118]. Minor toxicity was shown in SWNT-PS-b-PAA treated cells (viability of 86 ± 3% at 24 hrs and 82 ± 5% at 48 hrs, Fig. 3.5).

3.4.3 Cell internalization and localization of SWNT-polymers

The FITC-labeled SWNT-polymers were used to examine cell internalization. By incubation of the SWNT-polymers/FITC with MCF-7 breast cancer cells for 12 hrs, FITC fluorescence was observed under the microscope in the cells treated with all three types of SWNT-polymers, suggesting that all three types of SWNT-polymers could penetrate cancer cells (Fig. 3.6).

3.5 Conclusion

Since CNT is highly hydrophobic, it is critical to prepare well-dispersed and stable CNT solution prior to biomedical applications. Noncovalent functionalization of CNT with polymers renders CNT with good dispersity, and also improves their accessibility for further biomedical applications. We have shown that all three types of polymers used, PL-PEG, PS-b-PAA and CHI, could well disperse SWNT in aqueous solution, however, different level of SWNT dispersibility were obtained under the same level of sonication power and the same sonication time period. The three types of polymer coated SWNT were stable in water, however, high concentration of SWNT-CHI could form aggregation in PBS and cell culture medium, which might be related to different stabilization mechanisms. The polymer-coating ratio in SWNT-PS-b-PAA was much higher than that in SWNT-PL-PEG and SWNT-CHI. With different levels of polymer-coating ratio, the functionalized SWNT might be suitable for different schemes for drug loading to SWNT. For example, the PL-PEG functionalized SWNT, with the low level of polymer-coating ratio, large uncoated surface area exists, thus it is favorable for loading drugs directly onto SWNT sidewall for potential drug delivery applications; whereas, with high level of polymer-coating ratio in SWNT-PS-b-PAA, higher drug loading could be achieved by conjugation of drug molecules to SWNT functionalization polymers (PS-b-PAA). *In vitro* study has confirmed that the cell internalization capability of the three types of SWNT-polymers in breast cancer cells. Taking together, the current study interfaces the novel nanomaterials with biological systems and establishes a foundation for the use of SWNT in potential important applications in cancer detection, drug delivery, and other biomedical applications.

3.6 Acknowledgments

The authors acknowledge CIHR for project funding. W. Shao acknowledge the financial support from FRQS (Fonds de recherche du Québec - Santé) Doctoral award. The authors are grateful for the following assistances: Transmission Electron Microscopy imaging provided by X. Liu, (FEMR) Facility of Electron Microscopy Research at McGill

University; TGA assisted by P. Fiurasek, Centre for self-assembled Chemical Structures (CSACS).

3.7 Conflict of interest

The authors declare that no financial support or other compensation has been received relating to any aspect of this research or its publication that could be construed as a potential conflict of interest.

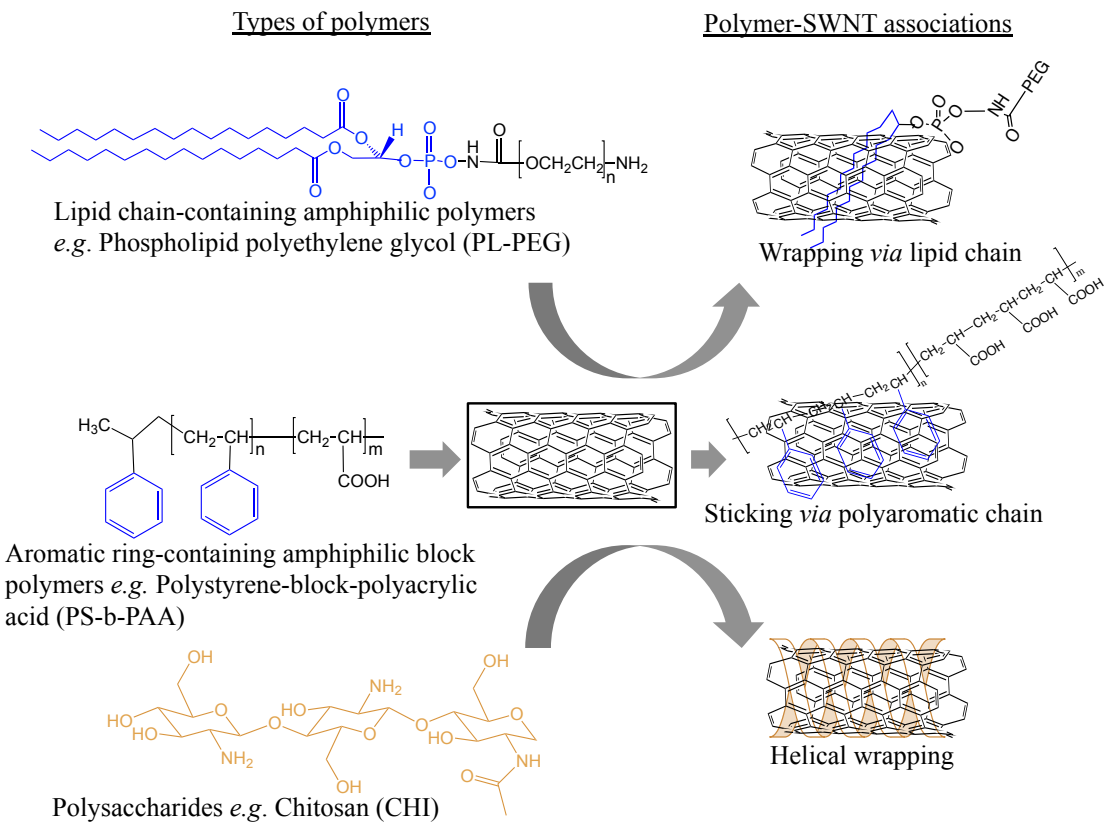

Figure 3.1 Non-covalent functionalization of SWNT using different types of polymers.

SWNT surface can be noncovalently functionalized using amphiphilic polymers that contain lipid chains or aromatic rings, or by polysaccharides that display helical structure. These polymers associate with SWNT through different SWNT-polymer interactions. The lipid chains in the lipid-polymer wrap to SWNT through Van der Waals force and other hydrophobic associations; the aromatic rings stick tightly to SWNT through π-stacking; and the polysaccharides wrap spontaneously around the SWNT surface, resulting in a compact, helical structure stabilized by an interlaced hydrogen-bond network.

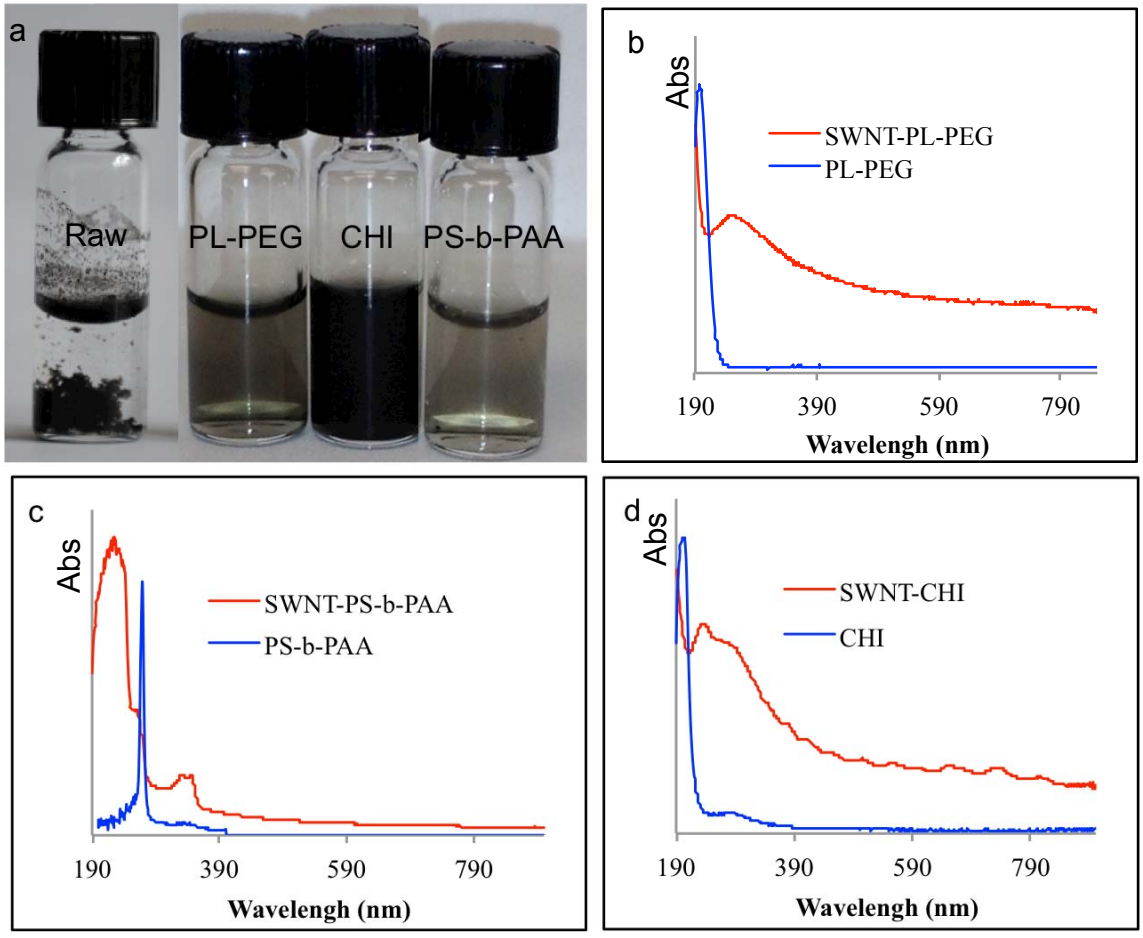

Figure 3.2 Characterization SWNT-polymers by UV-NIR spectrometry

(a) Photo graphs of raw and as prepared functionalized SWNT in water, and absorption spectra of (b) SWNT-PL-PEG (c) SWNT-PS-b-PAA (d) SWNT-CHI over the range of 190 – 850 nm.

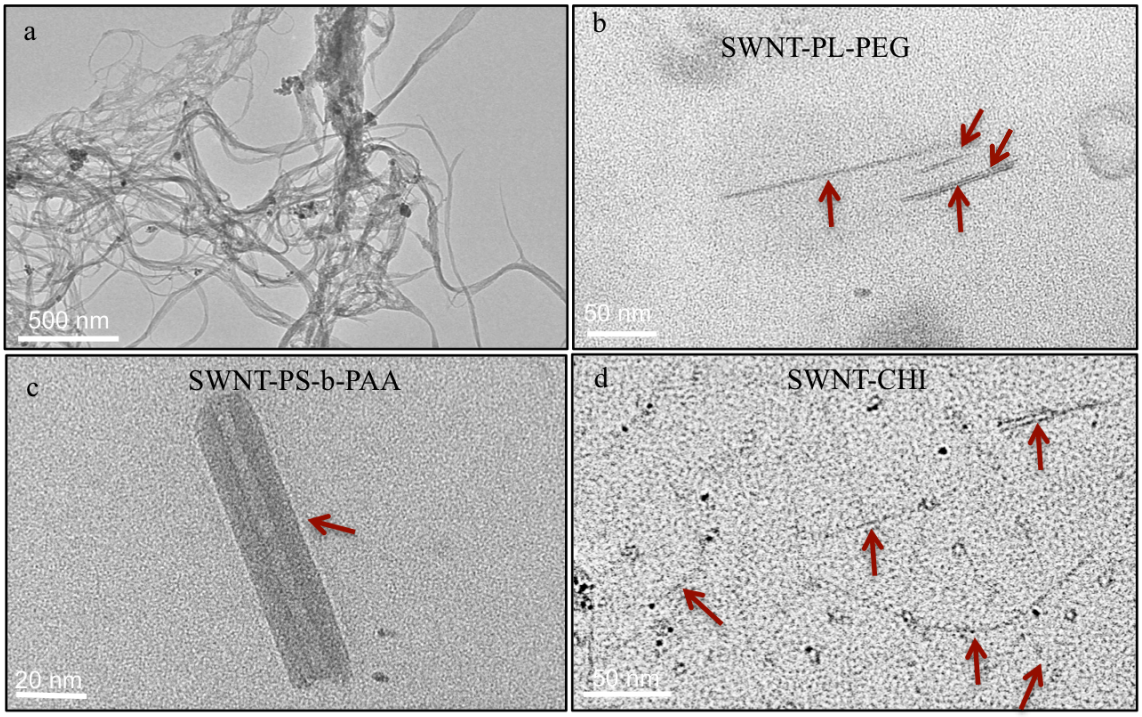

Figure 3.3 Characterization of SWNT-polymers by Transmission Electron Microscopy (TEM)

(a) Raw SWNT (b) SWNT-PL-PEG (c) SWNT-PS-b-PAA (d) SWNT-CHI
Red arrows indicated single-dispersed SWNT.

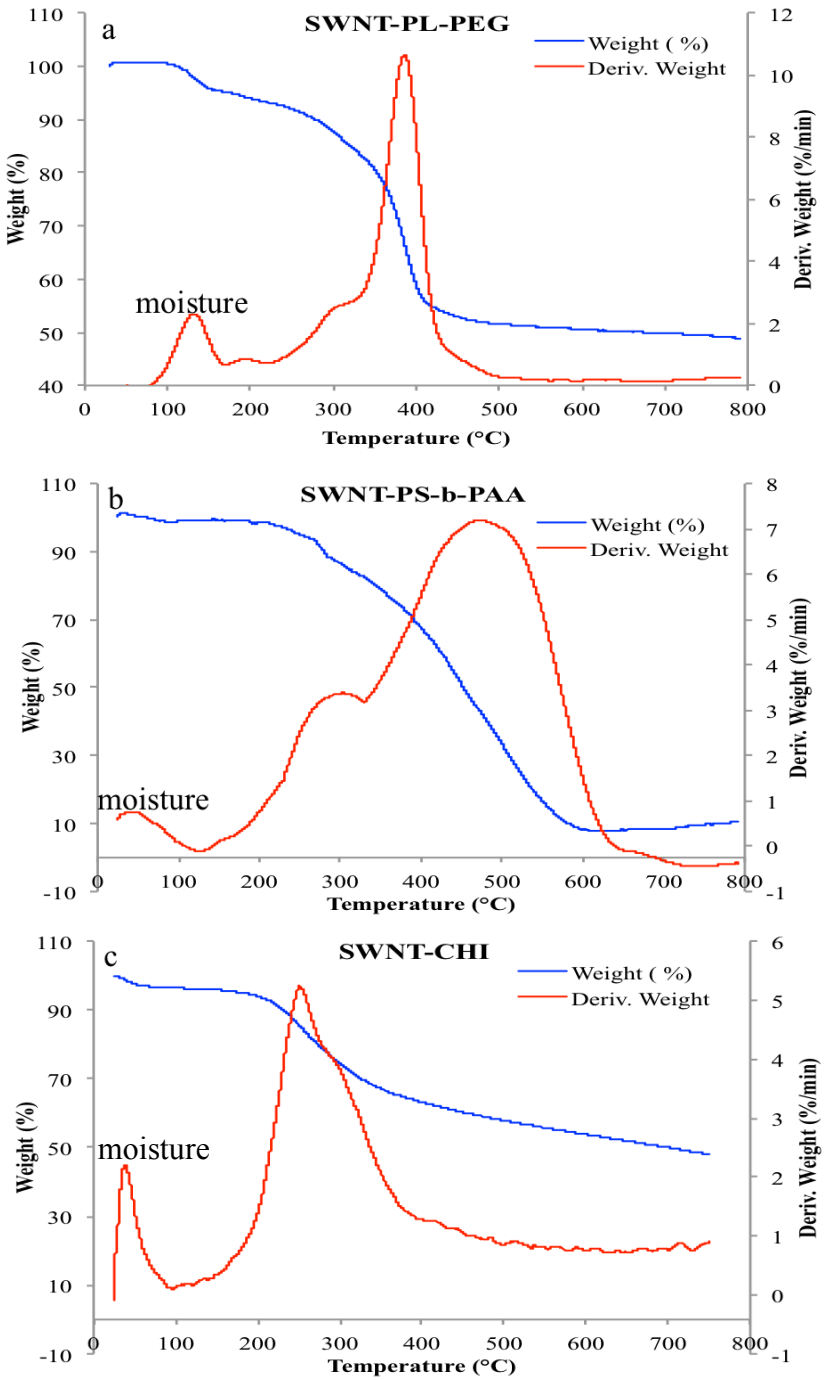

Figure 3.4 Characterization of SWNT-polymers by Thermogravimetric Analysis (TGA)

(a) SWNT-PL-PEG (b) SWNT-PS-b-PAA (c) SWNT-CHI
TGA was performed up to 800 °C under nitrogen atmosphere, weight loss and derivative weight of samples were recorded and plotted against temperature.

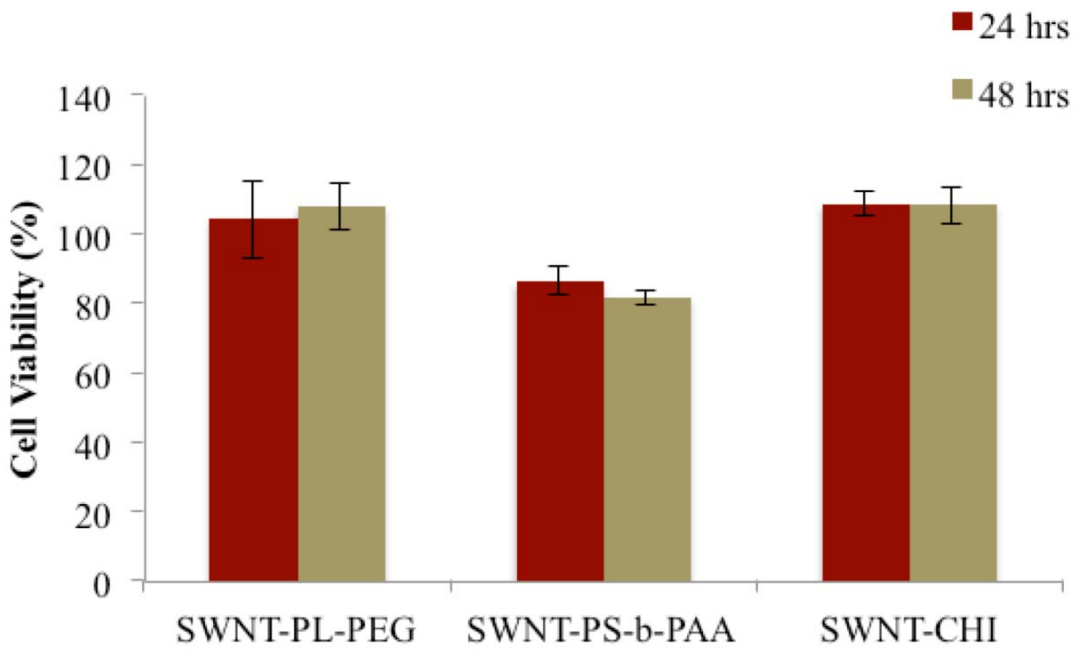

Figure 3.5 Cytotoxicity of SWNT-polymers in breast cancer cell line

MCF-7 cells were incubated with SWNT-polymers at 50 µg/mL for up to 48 hrs. Cell viability was measured by MTS assay. Cell viability in untreated control was assigned as 100% and its O.D from MTS assay was used to calculate cell viability in test groups.

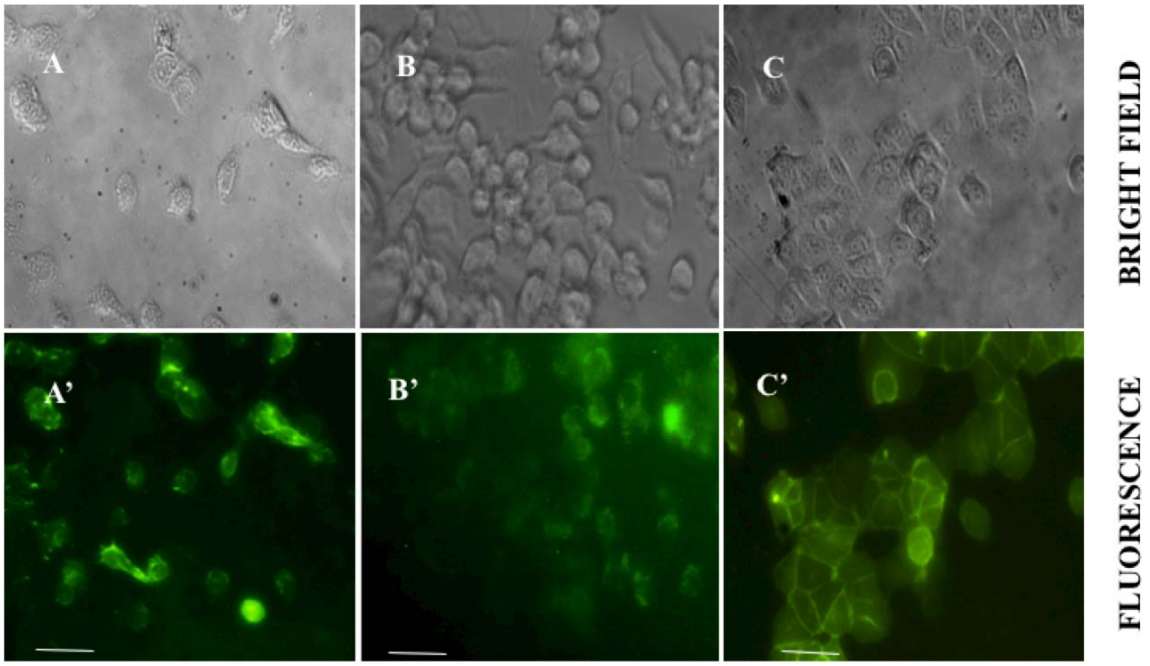

Figure 3.6 Cell internalization of SWNT-polymers in breast cancer MCF-7 cells

Microscopic images of (a) SWNT-PL-PEG (b) SWNT-PS-b-PAA (c) SWNT-CHI

MCF-7 cells were incubated with different SWNT-polymers/FITC respectively for 12 hrs and then the cells were washed and viewed under fluorescence microscopy.

Original Research Article 2

CHAPTER 4 A NOVEL HUMAN SERUM ALBUMIN NANOPARTICLE CONJUGATED CARBON NANOTUBE FOR INTRACELLULAR DELIVERY OF PACLITAXEL

Wei Shao, Arghya Paul, Laetitia Rodes, and Satya Prakash*

Biomedical Technology and Cell Therapy Research Laboratory, Department of Biomedical Engineering, Faculty of Medicine, McGill University
3775 University Street, Montreal, Quebec, H3A 2B4, Canada.

* Corresponding author, Email: satya.prakash@mcgill.ca

Tel: 1 (514) 398-3676; Fax: 1 (514) 398-7461

Preface: In this study, a new SWNT-based PTX delivery system was developed by conjugation of cross-linked human serum albumin (HSA) nanoparticles to functionalized SWNT for PTX delivery. The HSA is chosen because of its high binding affinity to PTX. The formulated SWNT-PTX enables removal of toxic delivery agents. The design strategy, preparation and characterization of SWNT-HSA-PTX were presented. The *in vitro* antitumour efficacy of SWNT-HSA-PTX was compared with free drug PTX and HSA nanoparticle only formulated PTX using MCF-7 breast cancer cells.

The article was submitted to *Cell Biochemistry and Biophysics* (2013). The manuscript has been tentatively accepted with minor revision.

4.1 Abstract

Paclitaxel (PTX) is one of the most important drugs for breast cancer, however, the drug effects are limited by its systematic toxicity and poor water solubility. Nanoparticles have been applied for delivery of cancer drugs to overcome their limitations. In this study, a novel single-walled carbon nanotube (SWNT)-based drug delivery system was developed by conjugation of human serum albumin (HSA) nanoparticles to SWNT for delivery of an antitumour agent paclitaxel (PTX). The SWNT-drug carrier was characterized by TEM, UV-NIR spectrometry, and TGA. The SWNT-drug carrier displayed high intracellular delivery efficiency (cellular uptake of >80%) in breast cancer MCF-7 cells, as examined by fluorescence labeled drug carriers. The PTX formulated with SWNT-HSA showed higher growth inhibition in MCF-7 breast cancer cells than the PTX formulated with HSA nanoparticle only after 48 hrs of drug incubation. The increased drug efficacy could be driven by SWNT-mediated cell internalization. These data suggested that the developed SWNT-based antitumour agent was effective. However, more studies for *in vivo* drug delivery efficacy and other properties are needed before this delivery system can be fully realized.

4.2 Introduction

Breast cancer is one of the most common causes of death worldwide. It accounts for almost 33% of all incident cases of cancer in women [1]. Chemotherapy in addition to the primary surgical removal of tumours is a necessary treatment for breast cancer. Widespread use of adjuvant chemotherapy in breast cancer has led to dramatic improvement in survival. Paclitaxel (PTX) is one of the most important anti-tumour reagents for breast cancer. It prevents microtubule disassembly, which disturbs the important cellular functions of microtubule, including mitosis, cell transport, and cell motility. Since the drug is not specific for cancer cells, it affects all fast dividing cells [148], therefore, it causes sever side effects [30, 31]. In addition, due to poor solubility of the drug, it is necessary to use surfactants, such as cremophor for delivery, which causes hypersensitivity reactions [33, 34]. The commercial PTX formulation, Taxol®, has to be infused intravenously over a long period of time. Abraxane®, a human serum albumin (HSA) nanoparticle formulated PTX, has been developed to solve the problems of PTX. The use of HSA nanoparticles allows removal of surfactant in the formulation, however, side effects still exist [5, 149, 150].

An effective cancer delivery system should be able to specifically deliver chemotherapy drugs to tumour tissues in order to reduce off-target toxicity. In addition, it is preferably able to carry drugs inside of cells to take effect. Nanoparticles have been shown to accumulate in tumour tissues due to permeability of leaky tumour vasculature to the nanoparticles. The phenomenon is termed as tumour-selective *Enhanced Permeability and Retention* (EPR) effect. The EPR effect is the basis for design of nanoparticle therapeutics for selective targeting tumours.

Carbon nanotube (CNT) is a novel type synthetic nanomaterials with unique hollow, cylindrical shape. Structurally, CNT can be viewed as rolled from layers of graphene sheets. CNT can be one layer (single-walled nanotube, SWNT) or multiple layers (multi-walled nanotube, MWCNT). CNT possesses many interesting properties as a drug carrier, such as, cell internalization due to its needle-like shape [12] and specific optical characteristics for *in vivo* detection and imaging. Since tumour accumulation of

functionalized CNT has been found in animal models [91], CNT has been widely investigated for delivery of anti-tumour agents, including DNA, siRNA, peptides and drugs [107, 146, 151-154].

CNT consists of supramolecular structure that is formed by covalent bonding between carbon atoms, so, drug loading to this pre-formed structure is very challenging. Owing to the hollow structure of nanotubes, small molecule drugs can be loaded into the interior of CNT through a simple capillarity-induced filling, however, the loading amount is usually very low [119]. Researchers have also found that CNT contains a large surface area that allows direct adsorption of some hydrophobic drugs, especially the drugs that contain flat, benzene ring structure, *e.g*, doxorubicin (DOX) [113]. However, for drugs with bulky structures, *e.g*. PTX, no effective drug-loading scheme is available.

To efficiently load of PTX to SWNT, in this study, we have developed a HSA nanoparticle conjugated SWNT for delivery of PTX. The design is based on the property of high binding affinity of PTX to HSA [155]. HSA is the most abundant plasma protein, which could act as a carrier in blood for certain hydrophobic molecules, such as long chain fatty acid, metal ions, and some drugs [7]. It was hypothesized that HSA could be used as a platform for loading of PTX onto SWNT.

4.3 Materials and methods

4.3.1 Noncovalent functionalization of SWNT with PL-PEG-NH_2

Noncovalent functionalization of SWNT (HiPco, Unidym Inc, USA) was prepared by a previously described method with minor modification [81]. The SWNT was firstly dispersed in organic solvent DMF by sonication for 5 mins in a bath sonicator (model 2510, Branson Ultrasonics, CT) at a concentration of 2 mg/ml. The amphiphilic lipid polymer, phospholipid polyethylene glycol (PL-PEG-NH_2, 2K Da, Avanti Lipid company, USA) was dissolved in deionized (DI) water at a concentration of 2 mg/ml. Ten times of volume of PL-PEG-NH_2 water was added to the solvent dispersed SWNT. The mixture was sonicated for 1 hr at room temperature with changing water every 20

min to avoid overheating. After sonication, the suspension was centrifuged at 20k rpm (50Ti, Beckman Coulter, USA) for 1 hrs at room temperature to remove SWNT bundles and impurities. Excess PL-PEG-NH_2 was removed by three times of washing using centrifugation filtration units (100 kDa cut-off) before use.

4.3.2 Preparation of HSA nanoparticles by cross-linking of the protein

The HSA nanoparticles were prepared by cross-linking of HSA proteins using EDC (Thermo Scientific), plus sulfo-NHS (Thermo Scientific) as cross-linking reagents following instruction provided by the manufacture. Briefly, EDC (30 mM) and sulfo-NHS (5mM) were dropwise added to 10 mL of HSA (20 mg/ml) in PBS buffer (PH 7.4). The mixture was incubated at room temperature for 2 hrs with shaking. The excess reagents in were removed by three times of washing with PBS using centrifugation filtration units (100 kDa cut-off).

4.3.3 Conjugation of HSA nanoparticles to SWNT-PL-PEG

Heterobifunctional linker molecule, NHS-PEG_4-Maleimide (SM-PEG_4, Thermo Scientific), was used for conjugation of cross-linked HSA nanoparticles to PL-PEG-NH_2 functionalized SWNT. The conjugation reaction was carried out in the following three steps. The first step was to link SM-PEG_4 to the amino end of SWNT-PL-PEG-NH_2, for which, 5 mL of SWNT-PL-PEG-NH_2 in PBS buffer (PH 7.4) mixed with 8 µl of 250 mM SM-PEG_4 and incubated at 4°C for 2 hrs, and then the excess linking reagent was removed by washing with PBS using centrifugation filtration units (100 kDa cut-off). The second step was to activate sulfhydryl group in HSA by Traut reagents (Sigma), for which, 20 mL of cross-linked HSA nanoparticles (5 mg/ml) in PBS buffer (PH 7.4) mixed with 100 µl of Traut reagent (50 mM), and 100 µl EDTA (0.5 M), and incubated at room temperature for 1 hr with shaking. The excess reagents were removed by washing with PBS using centrifugation filtration unit (2 kDa cut-off). In the third step, the SM-PEG_4 conjugated SWNT-PL-PEG-NH_2- mixed with sulfhydryl group activated HSA, and incubated at room temperature for 30 min with shaking. The SWNT-HSA conjugates

were purified by washing three times with DI H_2O using centrifugation filtration unit (100 kDa cut-off). The dry SWNT-HSA was obtained by freeze-drying process.

4.3.4 Characterization of SWNT-HSA drug carrier

UV-NIR spectra of PL-PEG-NH_2 functionalized SWNT were measured with 1 cm quartz cuvettes using UV-NIR spectrophotometer (Cary-100 bio, Varian Inc) over the range of 200 – 850 nm. The extinction coefficient was obtained by plotting the absorbance at 565 nm against SWNT concentration (mg/l) and subsequent linear regression analysis. TGA was performed using TGA Q500 (TA instruments Ltd, UK). Samples were loaded in the sample holder and the materials were heat up at a rate of 10 °C/min up to 800 °C under nitrogen. The weight loss and derivative weight were recorded continuously and plot against time. The size of cross-linked HSA nanoparticles was measured using dynamic light scattering (DLS) size analyzer (Brookhaven Instruments Corporation, USA). 10 measurements were taken for each sample and the results were expressed as mean ± standard error. The morphology of the functionalized SWNT and HSA conjugated SWNT were examined by TEM (Philips169 CM200 200 kV). 5 μl of sample was deposited on carbon-coated copper grid and allowed to dry for 10 mins. The excess liquid on grid was removed by touching the edge of the grid with filter paper.

4.3.5 Cell culture

MCF-7 breast cancer cells (ATCC) were maintained in Dulbecco's modified Eagle's Medium (DMEM, Invitrogen, Canada) supplemented with 10% Fetal Bovine Serum (FBS, Invitrogen, Canada). The cells were cultured in a humidified incubator with 5% CO_2 at 37 °C.

4.3.6 Labeling SWNT with fluorescence dye FITC and cell internalization assay

Fluorescent SWNT was prepared either by covalently linking fluorescein isothiocyanate (FITC) to PL-PEG-NH_2, and then used for coating of SWNT, or by physical attaching of

FITC on sidewall of nanotubes. For covalent labeling, FITC was conjugated to PL-PEG-NH_2 *via* its isothiocyanate group (–N=C=S) reacting with amino group in PL-PEG-NH_2 [81]. In general, 10 mg of PL-PEG-NH_2 was dissolved in 5 mL of 0.1 M $NaHCO_3$-Na_2CO_3 buffer solution (PH 9.0), and 100 µl of 13 mM FITC was added and incubated at room temperature in dark for one overnight. For physical attaching FITC on nanotubes, SWNT were firstly mixed with FITC in organic solvent DMF with 5 mins of sonication in a bath sonicator, and then functionalized with PL-PEG-NH_2 followed by further conjugation of HSA nanoparticles to PL-PEG-NH_2. The excess FITC was removed by dialysis using a membrane cassette with a cut-off of 100 kDa.

For cell penetration assay, the MCF-7 cells were seeded in a 96-well plate at a density of 2 x 10^4 cells/well in 200µl medium at one night before the assay. The cells were incubated with FITC labeled SWNT at a concentration of 1- 5 µg/mL (equivalent of SWNT amount) for 24 h. The cells were washed and viewed under fluorescence microscope.

4.3.7 Loading of PTX onto SWNT-HSA

Loading of PTX onto SWNT-HSA followed the procedure developed by Lay *et al* [124] with modifications. Briefly, PTX was firstly dissolved in methanol at a concentration of 4 mg/ml. SWNT-HSA dry powder was added to PTX methanol solution at a concentration of 15 mg/mL and sonicated for 30 min, and then, 10 times of volume of DI water was dropwise added to the SWNT-HSA/PTX methanol mixture. After water addition process, the mixture was sonicated for additional 1 hr with cooling using ice-cold water to prevent overheating. The mixture was equilibrated at room temperature for one overnight to allow unbound PTX to precipitate from the mixture. The dispersed SWNT-HSA/PTX in supernatant was carefully transferred to a fresh tube, and methanol in solution was removed by three times of washing with DI water using centrifugation filter units (100 kDa cut-off). The unbound PTX in precipitates was extracted with organic solvent dichloromethane and dried with a rotary evaporator, and then re-dissolved in methanol for quantification using UV spectrometry.

4.3.8 Cell viability assay

Cell viability was evaluated in MCF-7 breast cancer cells using the Cell Titer 96® Aqueous Non-Radioactive Cell Proliferation MTS assay kit (Promega). Briefly, triplicates of $1x10^4$ /well of cells in 96-well plates were treated with different PTX formulations at 37°C for varied time periods. MTS assay followed manufactory's instructions. The 3-(4,5-dimethylthiazol-2-yl)-5-(3-carboxymethoxyphenyl)-2-(4-sulfophenyl)-2H-tetrazolium (MTS) was reduced to form formazan by mitochondrial enzyme dehydrogenase present in viable cells, and the formazan concentration in cell culture was measured at absorbance of 490 nm using 1420-040 Victor3 Multilabel Counter (Perkin Elmer, USA). The amount of formazan is proportional to the number of viable cells. Cell viability was calculated as the percentage of absorbance relative to that in untreated control group.

4.3.9 Detection of apoptosis by TUNEL staining

The TUNEL staining of apoptotic cells upon drug treatment was performed using the DeadEnd Colorimetric TUNEL System (Promega) according to manufacturer's instruction. TUNEL detects DNA fragmentation of apoptotic cells. The ends of fragmented DNA are labeled by a modified TUNEL (TdT-mediated dUTP Nick-End Labeling). The terminal deoxynucleotidyl transferase (TdT) enzyme adds a biotinylated nucleotide at the 3'-OH ends of fragmented DNA, and the biotinylated nucleotides are conjugated with horseradish-peroxidase-labeled streptavidin. The peroxidase is then detected using its substrate, hydrogen peroxide, and the chromogen, diaminobenzidine (DAB). The nuclei of apoptotic cells are stained brown.

4.3.10 Statistical analysis

Statistical analysis was carried out using software SPSS software (Minitab Inc, State College, PA). Data were expressed as mean ± standard deviation (SD). Statistical significance was accepted at a level of $p < 0.05$. Differences between the groups were

tested through analysis of variance (ANOVA). Tukey's post-hoc analysis was applied to compare the differences between the groups.

4.4 Results and discussion

4.4.1 Design of SWNT-based drug delivery system for PTX

Previous study has shown that PTX can be directly adsorbed onto the nanotube sidewall for delivery, but with low loading efficiency [124], so it was designed to conjugate HSA nanoparticles to SWNT for more effective PTX loading. HSA was chosen for drug loading to SWNT because of its high binding affinity to PTX [155]. As illustrated in Fig. 4.1, SWNT, coated with PL-PEG-NH_2, serves as a drug-loading platform, on which, cross-linked HSA nanoparticles are conjugated to amino end group of PL-PEG-NH_2 for PTX loading. Both non-covalent and covalent approaches are applied to build SWNT-based drug delivery system. PL-PEG-NH_2 is non-covalently functionalized on SWNT so as to disperse SWNT in aqueous solutions. HSA is cross-linked to generate HSA nanoparticles, and then covalently linked to amino group in SWNT-PL-PEG-NH_2 to form SWNT-HSA drug carrier. PTX can be efficiently attached on SWNT-HSA *via* specific HSA-PTX interaction. It is expected that macromolecular structure of the SWNT-based drug could favor drug accumulation in tumour tissues through EPR effect, and cell internalization of SWNT-HSA-drug could be driven by needle-like SWNT.

4.4.2 Preparation of SWNT-HSA and the structural characterization

SWNT forms rope-like aggregation in water due to hydrophobic interaction between the nanotubes. In order to well disperse SWNT in water, lipid-polymer PL-PEG was applied for noncovalent functionalization of SWNT surface *via* a sonication process, which provides energy to break down the inter-tube interaction, and to allow the lipid-polymer to attach to SWNT surface. The PL-PEG functionalized SWNT was stable in aqueous solutions, including water, PBS and cell culture medium (insert in Fig. 4.2a). Single-dispersed SWNT with hollow tubular structure was clearly seen under TEM (Fig. 4.3a). Well-dispersed SWNT displayed strong absorption along the measured range of 200 to

850 nm (Fig. 4.2a). The dry SWNT-PL-PEG powder could be obtained by lyophilisation, and the dry powder could be easily re-dispersed in water solution with brief sonication after storage at 4 °C for up to three months. TGA was applied to evaluate the ratio of the polymer coated on SWNT since different thermal profile existed for SWNT and coated polymers, in which, SWNT is stable up to 1200 °C, and PL-PEG-NH_2 is fully degraded from 200 - 500 °C under nitrogen condition. TGA result showed that the polymer-coating ratio on SWNT was around ~50% w/w (the weight loss due to moisture of the sample was corrected, Fig. 4.2b).

To prepare SWNT-HSA drug carrier, HSA was firstly cross-linked to form nanoparticles. With the conjugation condition described in materials and methods section, it was formed small, homogenous HSA nanoparticles with a hydrodynamic diameter of 60.4 ± 1.1 nm as revealed by DLS. TEM image showed the morphology of the nanoparticles was either round or square in shape (Fig. 4.3c), and the HSA nanoparticles were densely attached on SWNT surface. With conjugation of HSA nanoparticles on SWNT, surface area and overall size (~ 100 nm in dia.) of the SWNT-drug carrier greatly increased (Fig. 4.3b).

4.4.3 Investigation of intracellular delivery efficiency of SWNT-HSA drug carrier

For cell internalization assay, fluorescent dye FITC was used to label SWNT-HSA. We firstly tried to conjugate FITC to HSA to make fluorescent nanoparticles. However, FITC conjugated HSA spontaneously formed the particles to ~500 nm as measured by DLS. The formation of bigger nanoparticles was possibly due to association of HSA molecules using hydrophobic FITC as molecular glue. Because the size of FITC conjugated HSA particles was too big even before cross-linking, we then changed FITC labeling method by adsorption of the flat benzene-containing FITC on the sidewall of SWNT. The formation of SWNT-HSA/FITC hybrid was confirmed by dialysis procedure using a membrane cassette of 100 kDa cutoff, in which, brown FITC-containing SWNT-HSA remained in cassette even with repeated changing water for 2 days. By incubation of cells with 1 – 5 μg/mL (equivalence of SWNT amount) of SWNT-HSA/FITC for 24 hrs, it

was obtained FITC cell internalization ratio of 72%, 80% and 81% for 1, 2.5 and 5 μg/mL of SWNT-HSA/FITC respectively, indicating that the SWNT-HSA drug carrier could deliver drugs inside of cancer cells in high efficiency (Fig. 4.4).

4.4.4 Examination of cytotoxicity of the SWNT-HSA drug carrier

The toxicity of PL-PEG functionalized SWNT and SWNT-HSA was examined using MCF-7 cells. The cells were treated with varied amounts of SWNT-HSA in range of 1 - 10 μg/mL for 24 hrs and cell viability was examined by MTS assay. Our result showed that cell viability was 97 ± 4%, 93 ± 7% and 93 ± 7% (mean ± s.d, n=3) for incubation with 1, 5 and 10 μg/mL of SWNT-PL-PEG respectively, which was similar to the result obtained in previous studies [118]. With conjugation of HSA nanoparticles to SWNT, we obtained the cell viability of 98 ± 4%, 91 ± 5% and 88 ± 6 % (mean ± s.d, n=3) for 1, 5 and 10 μg/mL of SWNT-HSA respectively (fig. 4.5). There was no statistic significance in cell viability between SWNT-PL-PEG and SWNT-HSA. So, we concluded that toxicity of SWNT-HSA was minor to cells, and therefore the SWNT-HSA is suitable as a drug carrier.

4.4.5 Evaluation of SWNT-HSA drug formulation

Since the water solubility of PTX is very low (~0.4 μg/ml), it is not possible to load PTX to SWNT-HSA directly in aqueous solution, so PTX was firstly dissolved in methanol for loading onto SWNT-HSA, then a large amount of DI water was dropwise added to SWNT-HSA/PTX methanol solution with sonication. During this process, the hydrophobic interaction would allow binding of PTX to SWNT-HSA. The PTX concentration in SWNT-HSA solution was calculated indirectly by subtracting the precipitated PTX from total amount of PTX added. It was estimated that PTX loading ratio of 135% w/w was obtained, which was much higher compared to 26% w/w of drug loading by direct adsorption of PTX to sidewall of SWNT-PEG [124].

4.4.6 Investigation of antitumour effect of SWNT-HSA formulated PTX

The antitumour effect of SWNT-HSA/PTX was investigated in breast cancer cell line MCF-7. The results showed that, within 72 hrs of drug treatment, free drug PTX dissolved in methanol showed slightly higher level of cell growth inhibition than PTX formulated with SWNT-HSA and HSA nanoparticle only, however the delivery vehicle methanol alone caused 12-14% cell death. Between HSA/PTX and SWNT-HSA/PTX groups, there was little difference in cell viability within 48 hrs of drug treatment, however, for 96 hrs of drug incubation, SWNT-HSA/PTX demonstrated stronger cell growth inhibition than HSA/PTX (cell viability of 53% *vs.* 62% $p < 0.05$, $n = 3$). The enhanced toxicity could be driven by SWNT-medicated cell internalization of the SWNT-HSA/PTX. The delayed drug effect could be due to slow release of PTX from SWNT-HSA, since only unbound PTX is pharmacologically active.

Apoptosis induced by different PTX formulations was examined using TUNEL staining. By counting the number of TUNEL-positive cells, it was obtained that the ratio of apoptotic cells was in range of 7-8% for all three PTX formulations ((Fig. 4.7). There was no statistic significance between them, suggesting the same mechanism of drug action could be responsible for all three PTX formulations.

4.5 Conclusion

In this study, a novel HSA nanoparticle-conjugated SWNT was developed for intracellular delivery of PTX for treatment of breast cancer. The SWNT-HSA/PTX formulation enables removal of toxic delivery agent Cremophor EL. As expected, the SWNT-HSA drug carrier demonstrated excellent intracellular drug delivery efficiency and the SWNT-HSA formulated PTX displayed stronger antitumour effect than HSA nanoparticle formulated PTX. The increased cancer cell inhibition effect could be driven by SWNT-mediated cell internalization. Thus, SWNT-HSA drug carrier is very

promising for delivery of PTX for treatment of cancer; thus, it is worthy for further *in vivo* application.

4.6 Acknowledgments

This work is supported by research grant to Satya Prakash from Canadian Institutes of Health Research (CIHR) (MOP 93641). W. Shao acknowledges the Excellence Award from Biomedical Engineering Department, McGill University and the financial support from FRQS (Fonds de recherche du Québec - Santé) Doctoral award. L. Rodes acknowledge the financial support from FRQS (Fonds de recherche du Québec - Santé) Doctoral award. A. Paul acknowledges the Alexander Graham Bell Post Graduate Scholarship-Doctoral from Natural Sciences and Engineering Research Council of Canada (NSERC). The authors are grateful for the assistance provided for transmission electron microscopy imaging by Xue-Dong Liu, Department of Physics, McGill University.

4.7 Conflict of interest

The authors declare that no financial support or other compensation has been received relating to any aspect of this research or its publication that could be construed as a potential conflict of interest.

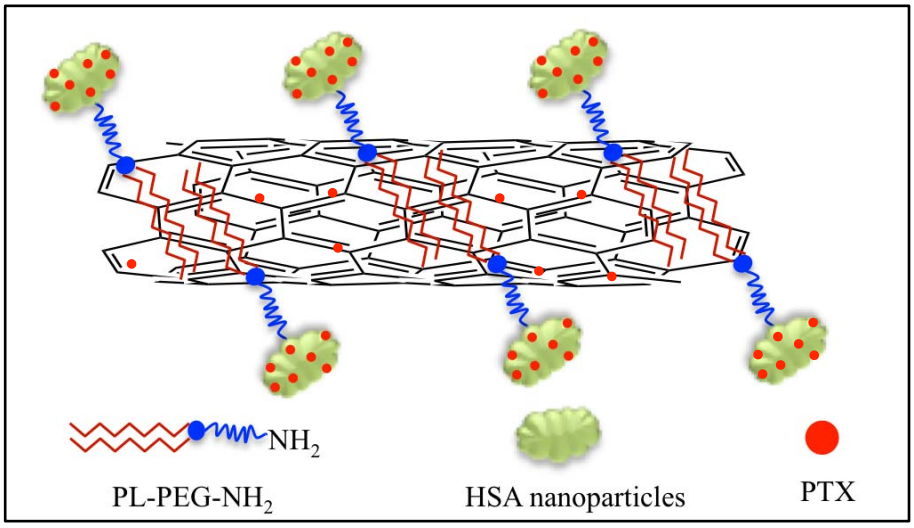

Figure 4.1 Schematic presentation of Human Serum Albumin nanoparticle conjugated SWNT for delivery of cancer drug paclitaxel.

SWNT, coated with PL-PEG-NH_2, serves as a drug-loading platform, on which, cross-linked HSA nanoparticles are conjugated to amino end group of PL-PEG-NH_2 for PTX loading. Both non-covalent and covalent approaches are applied to build SWNT-based drug delivery system. PL-PEG-NH_2 is non-covalently functionalized on SWNT so as to disperse SWNT in aqueous solutions. HSA is cross-linked to generate HSA nanoparticles, and then covalently linked to amino group in SWNT-PL-PEG-NH_2 to form SWNT-HSA drug carrier. PTX could be efficiently attached on SWNT-HSA *via* specific HSA-PTX interaction. It is expected that macromolecular structure of the SWNT-based drug could favor drug accumulation in tumour tissues through EPR effect, and cell internalization of SWNT-HSA-drug could be driven by needle-like SWNT.

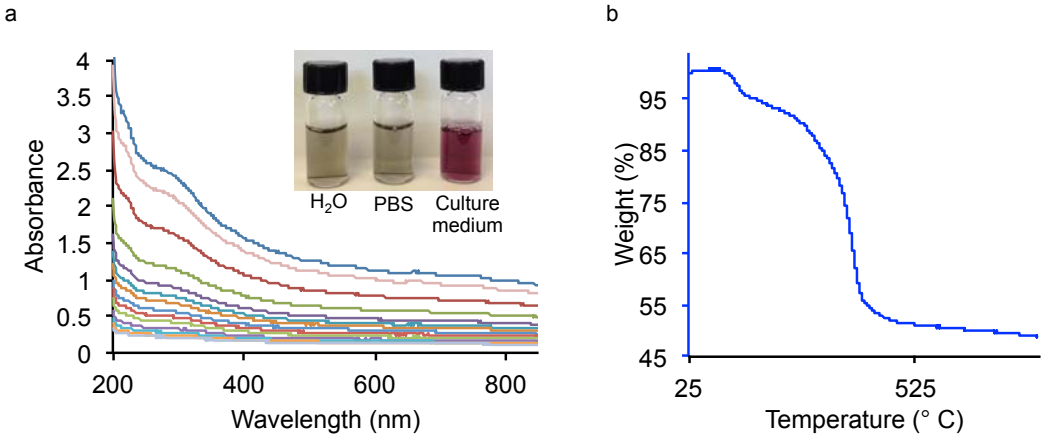

Figure 4.2 Characterization of the PL-PEG-NH_2 functionalized SWNT

(a) UV-NIR spectra of SWNT dispersed in water at various nanotube concentrations (b) Thermogravimetric analysis (TGA) of SWNT-PL-PEG. Insert in (a) is a photograph of SWNT-PL-PEG in water, PBS and cell culture medium

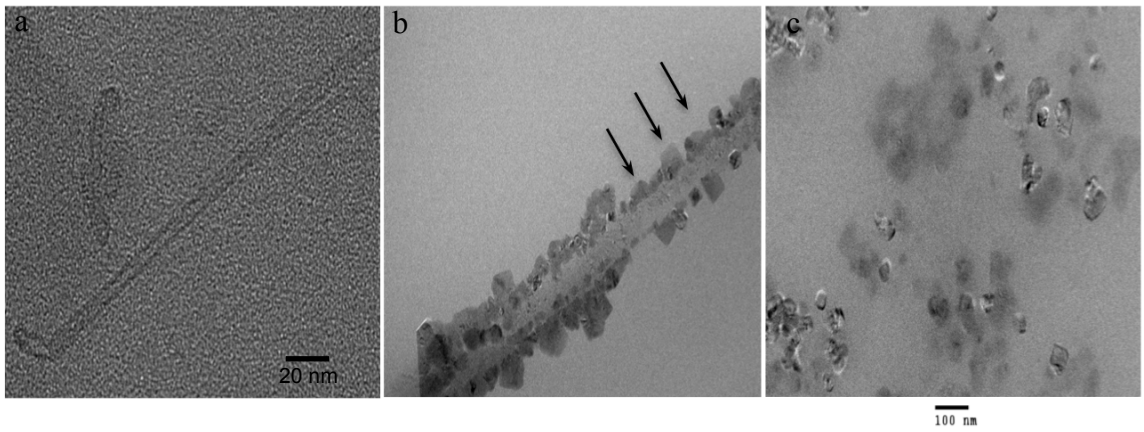

Figure 4.3 Characterization of SWNT-HSA drug carriers by Transmission Electron Microscopy (TEM)

(a) SWNT-PL-PEG-NH_2 (b) SWNT-HSA (c) HSA nanoparticles. HSA nanoparticles were conjugated to SWNT-PL-PEG-NH_2 using heterobifunctional linker SM-PEG_6. Arrowheads indicate the HSA nanoparticles conjugated to SWNT.

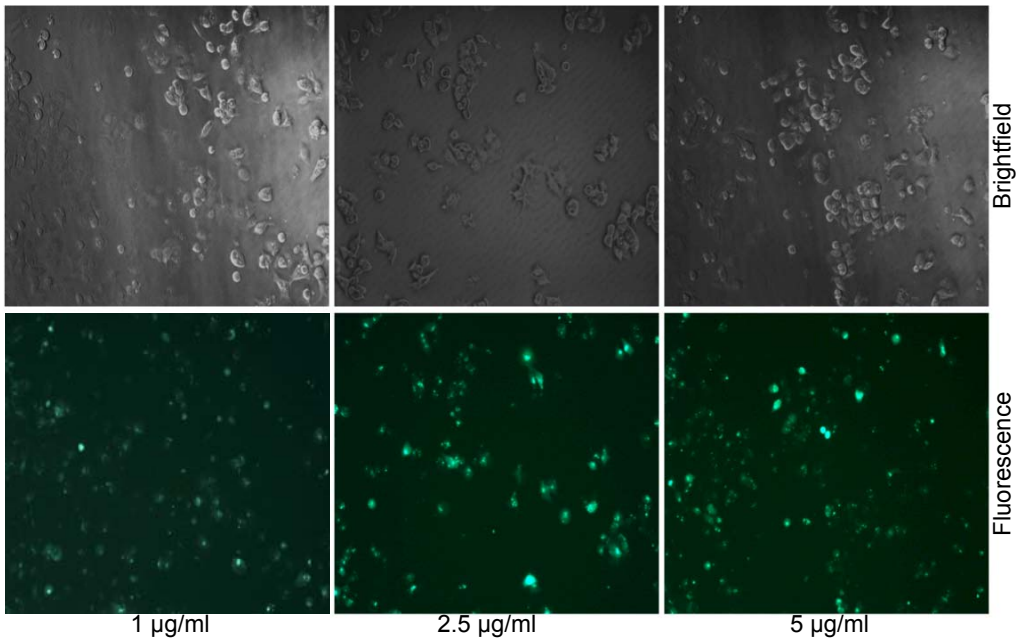

Figure 4.4 Drug delivery efficiency SWNT-HSA drug carrier evaluated by cell internalization assay

Microscopic images of MCF-7 cells incubated with fluorescent dye FITC labeled SWNT-HSA at a SWNT concentration of 1, 2.5, and 5 µg/mL respectively for 24 hrs. The percentage of fluorescence-positive MCF-7 cells were determined by counting cell numbers in five randomly selected views under microscope.

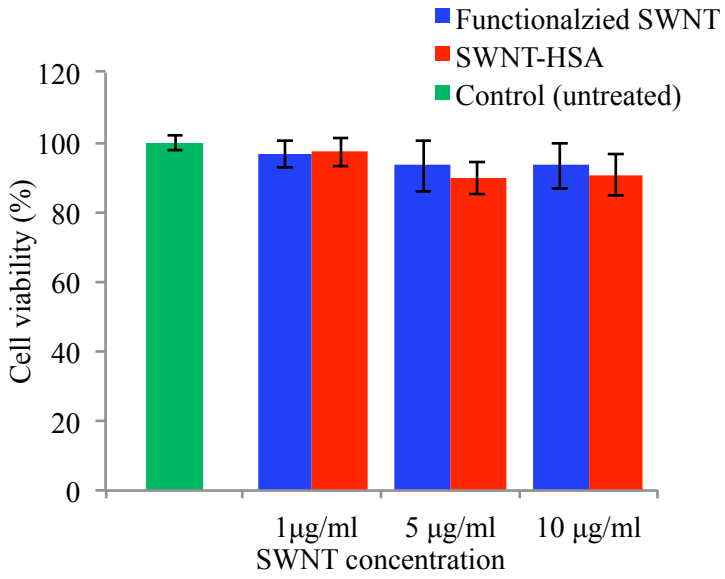

Figure 4.5 Investigation of cytotoxicity of the SWNT-HSA

MCF-7 cells were incubated with SWNT-HSA at different SWNT concentrations for 24 h. Cell viability was measured by MTS assay. Cell viability in untreated control was assigned as 100% and its O.D from MTS assay was used to calculate cell viability in test groups.

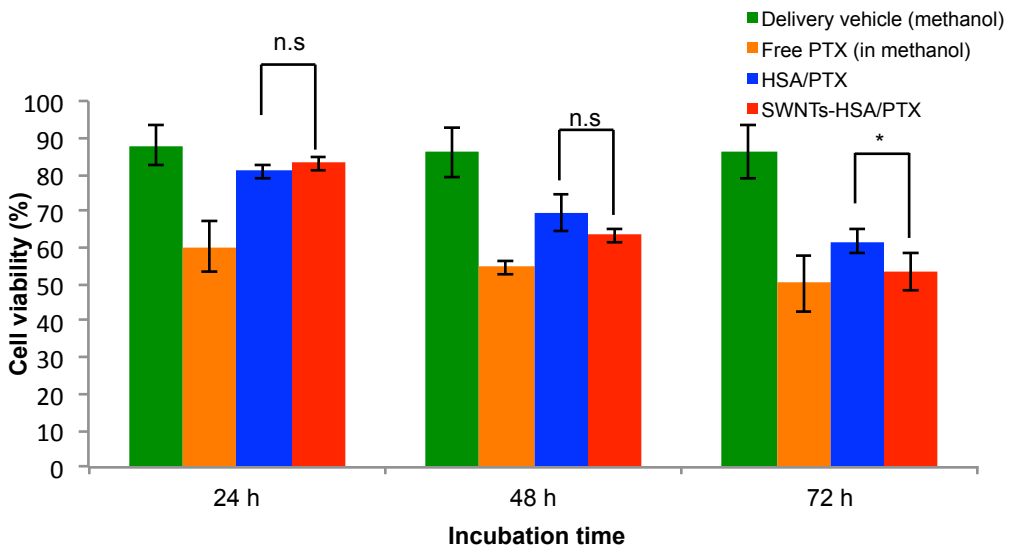

Figure 4.6 *In vitro* antitumour effect of SWNT-HSA/PTX formulation with time

MCF-7 cells were treated with 10 ng/mL (equivalent of PTX) in PTX (in methanol), HSA/PTX, or SWNT-HSA/PTX respectively for 24 – 72 hrs. Cell viability was measured by MTS assay. Cell viability in untreated control was assigned as 100% and its O.D from MTS assay was used to calculate cell viability in test groups. '*' indicates statistically significance between the two groups; 'n.s' indicates no statistically significance.

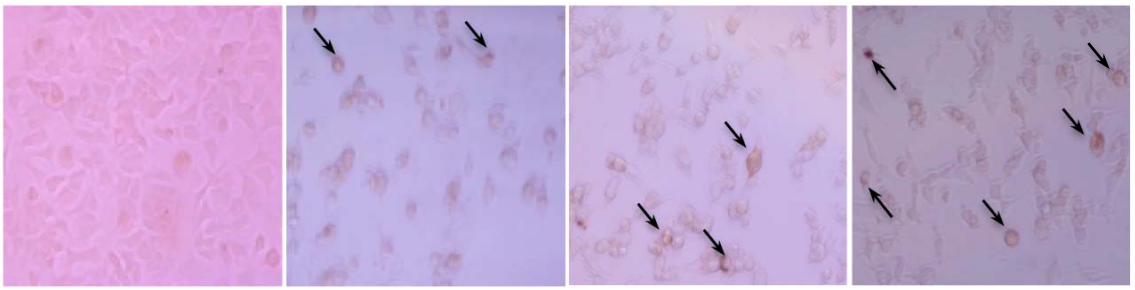

Untreated control Free PTX HSA/PTX SWNT-HSA/PTX

Figure 4.7 Apoptotic effect of SWNT-HSA/PTX formulation in breast cancer cells analyzed by TUNEL staining

Microscopic image of TUNEL staining of MCF-7 cells treated with free PTX, HSA/PTX and SWNT-HSA/PTX. The apoptotic cells were stained in dark brown. Arrowheads indicate the apoptotic cells.

Original Research Article 3

CHAPTER 5 DESIGN AND CONSTRUCTION OF A NEW CARBON NANOTUBE-BASED PACLITAXEL DELIVERY SYSTEM USING POLYMER-DRUG APPROACH

Wei Shao[1], Huiying Zeng[2], Arghya Paul[1] and Satya Prakash[1]*

[1]Biomedical Technology and Cell Therapy Research Laboratory,
Department of Biomedical Engineering, Faculty of Medicine, McGill University,
3775 University Street, Montreal, QC, H3A 2B4, Canada

[2]Department of Chemistry, McGill University
Otto Maass Building, 801 Sherbrooke Street West, Montreal, PQ, H3A 2K6

* Corresponding author, Email: satya.prakash@mcgill.ca
Tel: 1 (514) 398-3676; Fax: 1 (514) 398-7461

Preface: Previously, polymer-drug approach has been applied for conjugation of PTX to water-soluble polymers for delivery. In this study, SWNT-based PTX delivery system was constructed using polymer-drug approach, in which, PTX was grafted to an amphiphilic polymer polystyrene-block-acrylic acid, and used for noncovalent functionalization of SWNT. In this chapter, the design strategy, preparation, characterization, intracellular drug delivery capacity and *in vitro* drug effect of the SWNT-polymer-PTX were presented.

This article was submitted to *Journal of Biomaterial Applications* on Aug 1, 2014. It is currently under reviewing.

5.1 Abstract

Paclitaxel (PTX) is one of the most potent chemotherapy drugs for breast cancer, however, the drug efficacy is limited by its systematic toxicity. Nanoparticles have been applied for targeted delivery of chemotherapy drugs to tumour tissues, thereby reduce off-target toxicity. In this study, a carbon nanotube-based PTX delivery system was constructed using polymer-drug approach, in which, drug PTX was conjugated to an amphiphilic polymer polystyrene-block-acrylic acid (PS-b-PAA) for functionalization of single-walled carbon nanotube (SWNT). TEM study revealed that the polymer PS-b-PAA formed a thick layer on circumstance of the nanotubes. The polymer-coating ratio was ~18 molecules of polymer per 10 nm SWNT as estimated by TGA, which was much higher than that of other types of polymers. The high polymer-coating ratio ensured high drug loading on SWNT. We have shown that the FITC-labeled SWNT drug carrier was able to enter MCF-7 breast cancer cells in high efficiency, suggesting that the SWNT-PS-b-PAA could be a good intracellular drug carrier. Two PTX molecules could be grafted on PS-b-PAA, with which, the PTX-loading ratio in SWNT was estimated to be ~36 drug molecules per 10 nm of SWNT. *In vitro* study using MCF-7 breast cancer cells demonstrated that SWNT-polymer-PTX induced severe cellular damage by nuclear condensation – a typical action of PTX, suggesting that the SWNT-polymer-PTX was functional upon its cellular entry. Thus, the SWNT-polymer-PTX is a promising nano-drug delivery system for potential breast cancer treatment.

5.2 Introduction

Paclitaxel (PTX), a microtubule toxin, is one of the most potent drugs for breast cancer [25]. The binding of PTX to microtubules disturbs the dynamics of microtubules, therefore affecting the formation of a normal mitotic apparatus and leading to cell cycle arrests in the G2/M phase [156]. Like all other chemotherapy drugs, PTX is non-specific to cancer cells and affects all fast dividing cells, thus exhibits many side effects, such as leucocytopenias, alopecia, and diarrhoea and peripheral neuropathies etc. [148]. Moreover, PTX is very poor in water-solubility, so the clinical PTX formulation Taxol® is formulated with surfactant Cremophor EL, which is toxic and often causes complications due to hypersensitivity reactions [33, 34]. These severe side effects become dose-limiting factors that diminish the efficacy of PTX. There is a need to develop a new PTX formulation in order to overcome the problems of PTX.

Tumours, being fast growing tissues, display enhanced vascular permeability due to high demand for nutrients and possibly oxygen. The leaky tumour vasculature allows selective accumulation of nanoparticles in tumour tissues. This phenomenon is termed as *Enhanced Permeability and Retention* (EPR) effect. Small molecule drugs are formulated with nanoparticles made of liposomes, lipids or polymers to exert EPR effects [36]. Indeed, nanoparticle-drug formulations have demonstrated higher intratumoural drug concentration than their parental drugs [36]. The EPR effect is the basis for design of nano-drug delivery system for chemotherapy drugs.

Single-walled carbon nanotube (SWNT), a synthetic carbon-based nanomaterial, is among the most promising nanosized drug carriers since it offers many advantages over many other types of nanoparticles [146]. This includes intracellular drug delivery, large surface area for drug loading and intrinsic optical properties for detection and imaging, *e.g.* strong absorption in the near-infrared (NIR) range, photoluminescence and Raman shift [13, 64]. However, raw SWNT is highly hydrophobic, surface modification of SWNT, or SWNT functionalization as to disperse SWNT in aqueous solutions is necessary for its drug delivery and other biomedical applications [11]. Noncovalent functionalization of SWNT using biocompatible polymers is one of the most effective

methods for SWNT-dispersion [146]. Recent studies have shown that the polymer-coated, well-dispersed SWNT has a prolonged blood circulation and high tumour-to-tissue SWNT concentration [91, 92], which is highly favourable for delivery of chemotherapy drugs. Several types of amphiphilic polymers have been shown to well disperse SWNT in aqueous solutions, such as lipid chain-containing polymers *e.g.* phospholipid conjugated polyethylene glycol (PL-PEG) [70, 81, 82] and polyaromatic rings-containing amphiphilic block polymers, *e.g.* polystyrene-block-polyacrylic acid (PS-b-PAA) [71, 83-85]. Coating the polymers onto SWNT not only affords good dispersibility of SWNT, but also improves accessibility of the payloads to SWNT-based drug carriers.

Previously, PTX has been successfully conjugated to lipids or polymers for delivery [157-159]. Polymer-drug conjugate is made by covalent linking of small molecule drugs to polymers so as to improve the biodistribution or to overcome the hydrophobicity of the drugs [52]. Usually, drug molecules are conjugated to polymers *via* cleavable chemical bonds since the drug molecules have to be released to exert therapeutic effects. PTX contains a reactive hydroxyl group at C2′ position that are accessible for ester formation. Modification of PTX at the C2′ position has been shown to inactivate PTX [160], however, active PTX can be released through enzymatic degradation in circulation or following entry of the polymer drug conjugates into cancer cells [53].

In this study, an SWNT-based PTX delivery system was constructed utilizing polymer-drug approach, in which, PTX was conjugated to an amphiphilic polymer and then used for SWNT functionalization. For this purpose, an amphiphilic block polymer PS-b-PAA (MW1.8k-b-6.0k) was chosen since it contains multiple –COOH groups that can be used for drug conjugation *via* ester formation.

5.3 Materials and methods

5.3.1 Reagents

All the reagents used in the experiments were purchase from Sigma Aldrich, Canada, except otherwise indicated specifically.

5.3.2 Chemical Synthesis of the polymer drug (PS-b-PAA-PTX)

PTX (1 equiv), PS-b-PAA (0.3 equiv MW1.8k-b-6.0k Polymer Source, Montreal), and 4-N,N-dimethylaminopyridine (DMAP, trace) were dissolved in DMF. Then, diisopropylcarbodiimide (DIPC, 1.3 equiv) was added to the above DMF solution. The reaction was carried out at room temperature. The completion of the reaction was monitored by TLC using methanol/dichloromethane (1:10) as an eluent. The excess reagents and unreacted drug molecules in the product were removed by dialysis (2 kDa cut-off) against methanol: water (1:1) with changing the dialysate every 4 hrs. The complete removal of unreacted PTX was monitored by UV-NIR spectrometry showing no PTX peaks present in the dialysate. Then, the product was dialyzed against water for another day with changing water every 4 hrs. The final product was dried by lyophilisation. For NMR analysis, the final product was dissolved in DMSO-D and examined using 500 MHz Varian Mercury spectrometer. The NMR spectra showed characteristic peaks in PS-b-PAA-PTX as below: δ = 7.21-8.00 ppm for aromatic protons in PTX; δ= 6.66, 5.89, 5.61, 5.38, 5.30, 4.90,4.78, 4.63, 4.26, 4.16, 1.12-1.23 ppm for aliphatic protons in PTX; the resonances of PS-b-PPA at 7.06, 6.55, 3.35, 2.50, 2.21, 1.77, and 1.51 ppm; the appearance of a new peak at 4.78 ppm corresponded to C2'-H in acetylated PTX as the reported in literature [158]. The evidence of a shift from δ 4.72 ppm for the original C2'-H in PTX to the lower field of δ 4.78 ppm confirmed that the hydroxyl group of PTX was reacted with polymer PS-b-PAA.

5.3.3 Preparation of SWNT-polymer and SWNT-polymer-drug

Noncovalent functionalization of SWNT using PS-b-PAA or PTX conjugated PS-b-PAA-PTX followed the method developed by Kang et al [71] with minor modification. Briefly, polymer PS-b-PAA or PS-b-PAA-PTX was firstly dissolved in DMF and then mixed with SWNT (HiPco, Unidym Inc, USA) with brief sonication in the probe sonicator followed by adding 10 times of deionized (DI) water with continuous sonication for 1 hr with cooling using icy water. After sonication, the dispersed SWNT was centrifuged at 20k rpm (Beckman Coulter, USA). The supernatant that contains functionalized SWNT was carefully decanted to avoid disturbing the precipitated SWNT bundles in the bottom. The functionalized SWNT solutions were stored at 4 °C. Before use, the excess polymer and solvent were removed by washing 3 times with DI water using centrifugation filtration units (Amicon, 100 kDa).

5.3.4 Characterization of SWNT-polymer-drug

UV-NIR spectra of functionalized SWNT were obtained in UV-NIR spectrophotometer (Cary-100 bio, Varian Inc.) using 1 cm quartz cuvettes over the range of 200 – 850 nm. TGA was performed using TGA Q500 (TA instruments Ltd, UK). Freeze dried samples were loaded in the sample holder and were heated up to 800 °C at a rate of 10 °C/min under nitrogen atmosphere. The weight loss and derivative weight were recorded continuously. The size and morphology of functionalized SWNT were examined by TEM (Philips169 CM200 200 kV). The surface charge of the functionalized SWNT was measured by zeta potential analyzer (Brookhaven Instruments Corporation, USA). Ten measurements were taken for each sample. The results were expressed as means ± standard error (s.e).

5.3.5 Labeling SWNT with fluorescence dye Fluorescein isothiocyanate (FITC) for cell internalization assay

Fluorescent SWNT was prepared by adsorbing FITC molecules on the functionalized SWNT. The FITC stock solution (4 mg in ethanol) was added to SWNT-PS-b-PAA solution at a final concentration of 0.4 mg/ml. The mixture was sonicated briefly followed by incubation in dark at room temperature for one overnight to allow formation of SWNT-PS-b-PAA/FITC hybrid. The unbound FITC was removed by washing with DI water using a dialysis membrane cassette (100 kDa cut-off). For cell penetration assay, the cells were seeded in a 96-well plate at a density of 2 x 10^4 cells/well in 200µl medium at one night before the assay. The cells were incubated with SWNT-PS-b-PAA/FITC for 12 hrs, then washed with PBS, and viewed under fluorescence microscope (Nikon, Eclipse, Te2000-4, Japan).

5.3.6 DAPI staining for examination of PTX effects in MCF-7 cells

MCF-7 breast cancer cells (ATCC) were maintained in Dulbecco's modified Eagle's Medium (DMEM, Invitrogen, Canada) supplemented with 10% fetal bovine serum (FBS, Invitrogen, Canada). The cells were cultured in a humidified incubator with 5% CO_2 at 37 °C. The cells were incubated with PTX and SWNT-polymer-PTX for 48 hrs. Cells were washed and fixed with 4% paraformaldehyde and stained with 300 nM of nucleus staining fluorescent dye DAPI. Cells were visualized by fluorescence microscopy to examine nuclear condensations.

5.4. Results and discussion

5.4.1 Design strategy for the SWNT-polymer-drug

Noncovalent functionalization of SWNT by amphiphilic polymers is an effective way to disperse SWNT in aqueous solutions. An amphiphilic block polymer, polystyrene-block-acrylic acid (PS-b-PAA), was chosen for both SWNT dispersion and drug linkage. The hydrophobic portion (PS) of the polymer contains aromatic rings that could attach to

SWNT through π-stacking, and the hydrophilic portion (PAA) comprises multiple carboxyl groups that could link to PTX *via* ester bonding. As illustrated in Fig. 5.1, PTX is firstly conjugated to carboxyl groups of PS-b-PAA by esterification at C2′-hydroxl of PTX. Then, the polymer-PTX conjugate is used for SWNT surface-functionalization. Since PS-b-PAA can be coated densely around the nanotubes, it affords high drug-loading ratio on SWNT. Furthermore, the PAA contains multiple carboxylic groups, so multiple drug molecules could be potentially linked to one polymer molecule, which could further increase drug loading on SWNT.

5.4.2 Characterization of SWNT-drug carrier

The SWNT-drug carrier (SWNT-PS-b-PAA) was prepared *via* a simple sonication process. The sonication process provides energy to break down the interactions between nanotubes so as to allow attachment of polymers onto SWNT surface. Previous studies has shown that the bundled SWNT hardly absorbs due to photoluminescence quench in UV-NIR range, however, after dispersion, SWNT exhibits strong absorbance in this range [147]. As expected, the obtained SWNT-PS-b-PAA in water showed continuous absorbance over the measured range of 200 – 850 nm (Fig. 5.2a). In UV spectra of the SWNT-PS-b-PAA, a strong absorption peak before 230 nm corresponded to the absorption of PS-b-PAA with a slight blue shift (Fig. 5.2a). Under TEM, the SWNT-PS-b-PAA displayed single-dispersed status, and the polymer formed a thick layer on the circumstance of the nanotubes (Fig. 5.2b).

The differential thermo degradation profiles of SWNT and PS-b-PAA allow evaluation of the polymer-coating ratio on SWNT by TGA. Under nitrogen atmosphere, SWNT is stable up to 1200 °C, whereas, the PS-b-PAA degrades before 600 °C. Based on TGA of SWNT-PS-b-PAA (Fig. 5.2C), the polymer-to-SWNT ratio was estimated to be ~18 polymers per 10 nm of SWNT (assuming MW of 170 kDa for 200 nm and 1.5 nm of SWNT and MW of 7800 g/mol for PS-b-PAA). The obtained polymer-coating ratio was much higher than other types of polymer-coated SWNT (our unpublished data), such as PL-PEG and chitosan. For example, the polymer-coating ratio in SWNT-PL-PEG was

only ~3 per 10 nm of SWNT [113]. The differences in polymer-coating ratio could be attributed to distinct coating manor of the two polymers, since the PL-PEG wrapped to SWNT *via* its lipid chain, whereas, the PS-b-PAA packed on SWNT surface *via* its polyaromatic rings sticking onto SWNT with its hydrophilic portion of the polymer to be tidily aligned to form a dense polymer coating layer.

Since the PS-b-PAA is an anionic polymer, coating of the polymer on SWNT imparts negative charges on SWNT surface. As expected, the obtained SWNT-PS-b-PAA displayed a zeta potential of -24 ± 8 mV. By coating the charged polymers on SWNT, both steric hindrance of the polymer and electrostatic repulsion could prevent the SWNT from aggregation. Indeed, in our test, the SWNT-PS-b-PAA solution was stable in water, and did not aggregate in PBS and serum-containing cell culture medium.

5.4.3 *In vitro* evaluation of SWNT-drug carrier

The cytotoxicity of SWNT-drug carrier (SWNT-PS-b-PAA) was examined in MCF-7 cells. The cells were treated with varied concentrations of SWNT-PS-b-PAA in range of 10 - 50 μg/mL for up to 48 hrs. The cell viability was examined by MTS assay. Cell viability in untreated control group was assigned as 100% and its O.D from MTS assay was used to calculate the normalized cell viability in test groups. The result showed that cell viability was higher than 80% with the highest dosage treated (50 μg/mL), suggesting that the cytotoxicity of SWNT-PS-b-PAA was minor (Fig. 5.3A).

In next step, we evaluated the intracellular delivery capability of the SWNT-drug carrier. For this, the SWNT drug carrier was loaded with a fluorescent dye FITC by adsorption since FITC contains flat benzene ring that could efficiently adsorbed onto the surface of SWNT [113]. By incubation of SWNT-PS-b-PAA/FITC with MCF-7 breast cancer cells for 12 hrs, it was observed that FITC fluorescence was taken by the cells, suggesting that SWNT-PS-b-PAA could carry drugs inside of cancer cells (Fig. 5.3B).

5.4.4 Preparation of SWNT-polymer-PTX and characterization

Since the chosen PS-b-PAA contains around 80 units of carboxyl groups, it was expected that multiple drug molecules could be grafted in the polymer. Several PTX: polymer molar ratios (20, 10 and 3) were tested in the drug conjugation reaction, however, GPC analysis showed that only 2 PTX molecules were grafted in each polymer even with high PTX:polymer molar ratio (Fig. 5.4A). The synthesis of PS-b-PAA-PTX was confirmed by NMR and UV spectra (Fig. 5.4B). The limited drug-grafting ratio might be due to steric hindrance and/or possible hydrogen bonding formed between grafted PTX molecules with the polymer, which prevented accessing of the internal carboxylic groups by drug molecules.

The SWNT-polymer-PTX was prepared by functionalization of SWNT using PTX grafted polymer. Under TEM, the SWNT-PS-b-PAA-PTX showed similar morphology to SWNT-PS-b-PAA (data not shown), which suggested that grafting drug molecules to PS-b-PAA did not affect its SWNT functionalization effect. Based on 18 polymers attached to per 10 nm SWNT, the amount of drug loaded on SWNT was estimated to be ~36 PTX per 10 nm SWNT (assuming that grafting of drug molecules to the polymer does not affect its polymer-coating ratio on SWNT). This drug-loading ratio is much higher than PTX conjugated to SWNT-PL-PEG in another study, in which its was obtain ~15 molecules per 10 nm of SWNT [118]. The UV spectra of SWNT-PS-b-PAA-PTX showed a tremendous absorption before 250 nm, which could be due to the absorption of PS-b-PAA-PTX (Fig. 5.4 C). The SWNT-PS-b-PAA-PTX displayed zeta potential of -15 ± 5 mV, which is lower compared with zeta potential of -24 ± 8 mV in SWNT-PS-b-PAA. A decrease in surface negative charge could be due to neutralization of some of the negative charges in PAA by PTX conjugation. However, with the PTX-grafting ratio of 2, considerable negative charge remained, and therefore, the stability of the SWNT-polymer-drug did not be affected. Stability test confirmed that incubation of the SWNT-polymer-PTX with cell culture medium for 48 hrs at 37 °C did not cause noticeable aggregation.

5.4.5 *In vitro* anti-tumour drug effect of SWNT-polymer-PTX

The action of PTX is mediated through binding of the drug molecules to microtubules, which blocks progression of cell mitosis and induces cell cycle arrest in the G2/M phase [156]. Although PTX became inactive when it was conjugated to PS-b-PAA, we expected that active PTX could be released by degradation *via* lysosome enzymes following endocytosis of SWNT-polymer-drug in cancer cells. The antitumour effect of SWNT-polymer-PTX was examined using MCF-7 breast cancer cells. The cells were treated with SWNT-polymer-PTX at ~0.1 μg/mL (equivalent of PTX concentration). Clinical formulation Taxol (PTX dissolved in Cremophor EL) of the same concentration was used as a positive control. After 48 hrs, the cells were stained with cell permeable nucleus staining dye DAPI. Under microscopy, the formation of multinucleated cells due to mitotic pausing were dominant in both PTX and SWNT-polymer-PTX treated cells compared to untreated control (Fig. 5.5), confirming that PTX could be released from SWNT-polymer-PTX to exert effect inside of MCF-7 cells.

5.5 Conclusion

In this study, polymer-drug approach was applied for construction of SWNT-based PTX. PTX was grafted to amphiphilic polymer for SWNT functionalization to constitute SWNT-based drug. The chosen amphiphilic block polymer PS-b-PAA contains polyaromatic chain that could stick to SWNT sidewall *via* π-stacking so as to disperse SWNT in aqueous solution. The obtained SWNT-drug carrier was stable in water, PBS and serum containing cell culture medium, etc, therefore, is suitable for biomedical applications. TEM study revealed that the PS-b-PAA formed a thick polymer layer on the circumstance of the single-dispersed nanotubes. TGA also confirmed high coating ratio of PS-b-PAA on SWNT, which afforded high drug loading on SWNT. The chosen polymer contains multiple carboxylic groups that could be theoretically grafted with a large number of drug molecules, however, only two PTX molecules could be conjugated PS-b-PAA, which was possibly due to steric hindrance effect of PS-b-PAA. However,

owing to the high polymer-coating ratio of SWNT-PS-b-PAA, the high drug loading on SWNT was still achieved even with low drug-polymer grafting ratio. Cell internalization study showed that the SWNT-drug carrier could penetrate MCF-7 breast cancer cells. *In vitro* study demonstrated that SWNT-polymer-PTX was functional and induced severe cellular damage in MCF-7 breast cancer cells. This study introduced a new scheme for construction of SWNT-based drug delivery system that afforded high drug loading capacity.

5.6 Acknowledgments

The authors acknowledge CIHR for project funding. W. Shao acknowledges the financial support from FRQS (Fonds de recherche du Québec - Santé) Doctoral award. A. Paul acknowledges the financial support from FRQS (Fonds de recherche du Québec - Santé) - post-Doctoral fellowship. The authors are grateful for the following assistances: transmission electron microscopy imaging provided by X. Liu, (FEMR) Facility of Electron Microscopy Research at McGill University; NMR facility, Chemistry Department, McGill University; TGA tests provided by P. Fiurasek, Centre for self-assembled Chemical Structures (CSACS).

5.7 Conflict of interest

The authors declare that no financial support or other compensation has been received relating to any aspect of this research or its publication that could be construed as a potential conflict of interest.

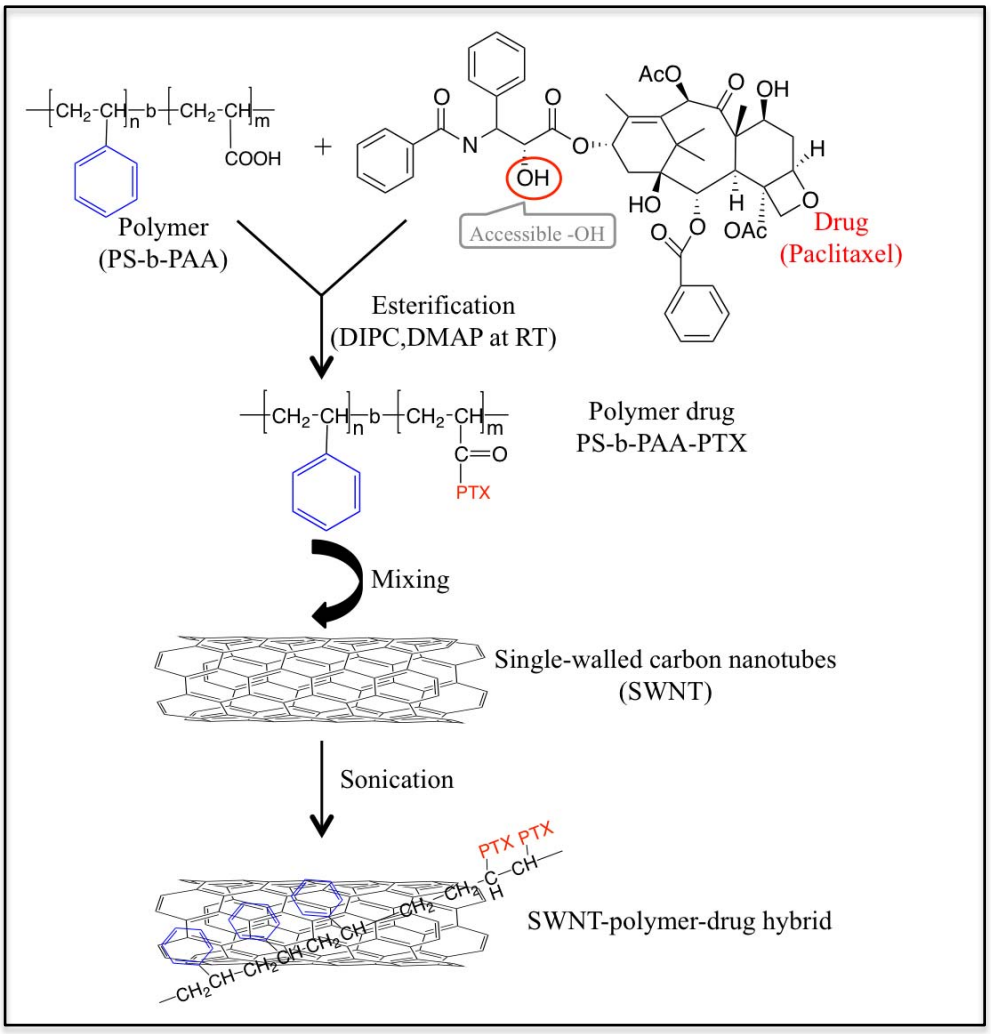

Figure 5.1 Construction of SWNT-polymer-PTX by polymer drug approach

An amphiphilic block polymer, polystyrene-block-acrylic acid (PS-b-PAA), was chosen for both SWNT dispersion and drug linkage. Drug PTX is firstly conjugated to carboxyl groups of PS-b-PAA by esterification at C2′-hydroxl of PTX. Then, the polymer-drug conjugate is used for SWNT surface-functionalization. High polymer-coating ratio on SWNT could be achieved exploiting strong π-stacking between the PS and SWNT benzene rings. In addition, the PAA contains multiple carboxylic groups, so multiple drug molecules could be potentially linked to one polymer molecule, which could further increase drug loading amount on SWNT.

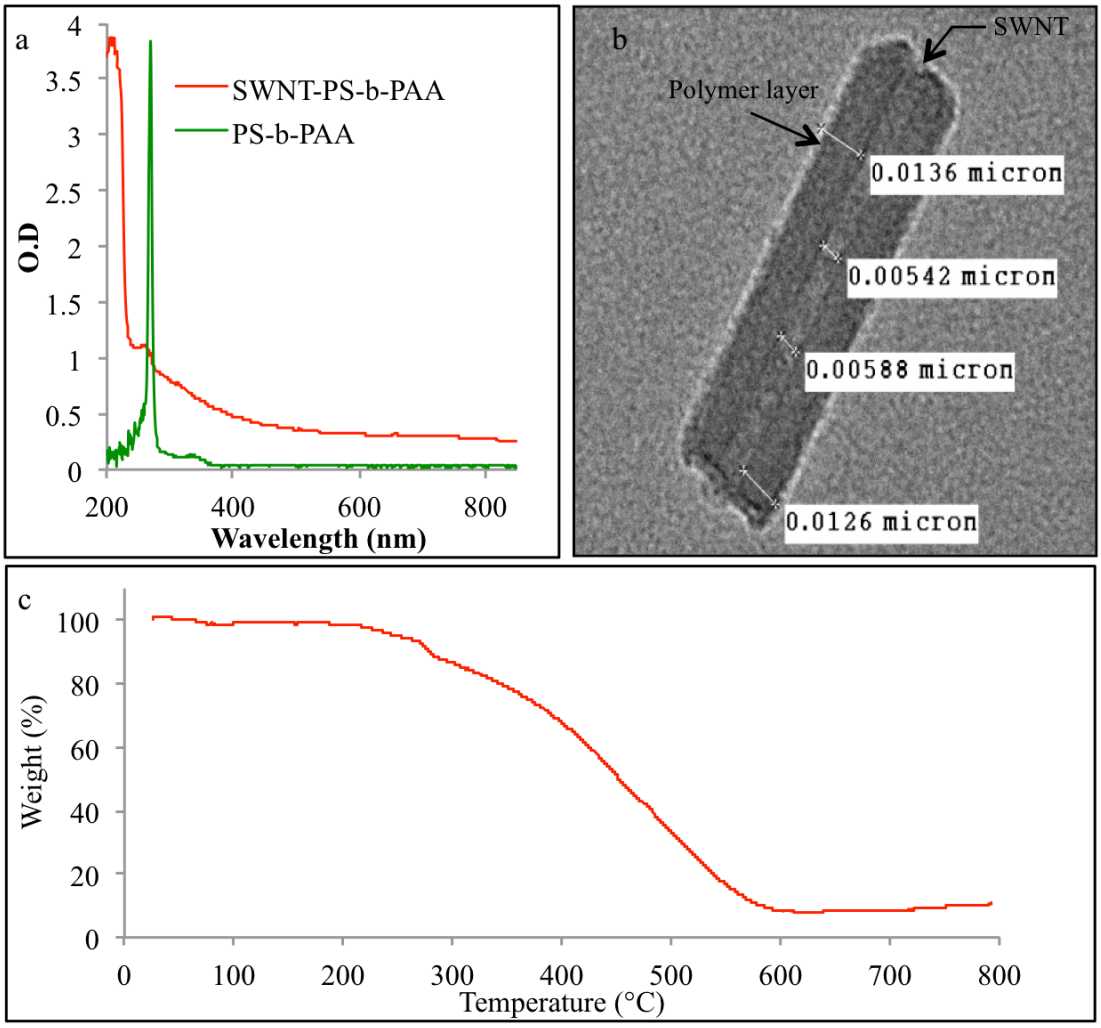

Figure 5.2 Characterization of SWNT-drug carriers by TEM, UV and TGA

(a) UV-NIR spectra of SWNT-PS-b-PAA (b) TEM image of SWNT-PS-b-PAA
(c) TGA of SWNT-PS-b-PAA

The absorption of the SWNT-PS-PAA in water was characterized by UV-NIR spectrometry over the range from 190 nm to 850 nm. For TGA, the dispersed SWNT-PS-b-PAA in water was dried by lyophilisation and the weight loss of SWNT-PS-b-PAA was measured up to 800 °C under nitrogen. For TEM, the sample was dried on a copper grid for imaging.

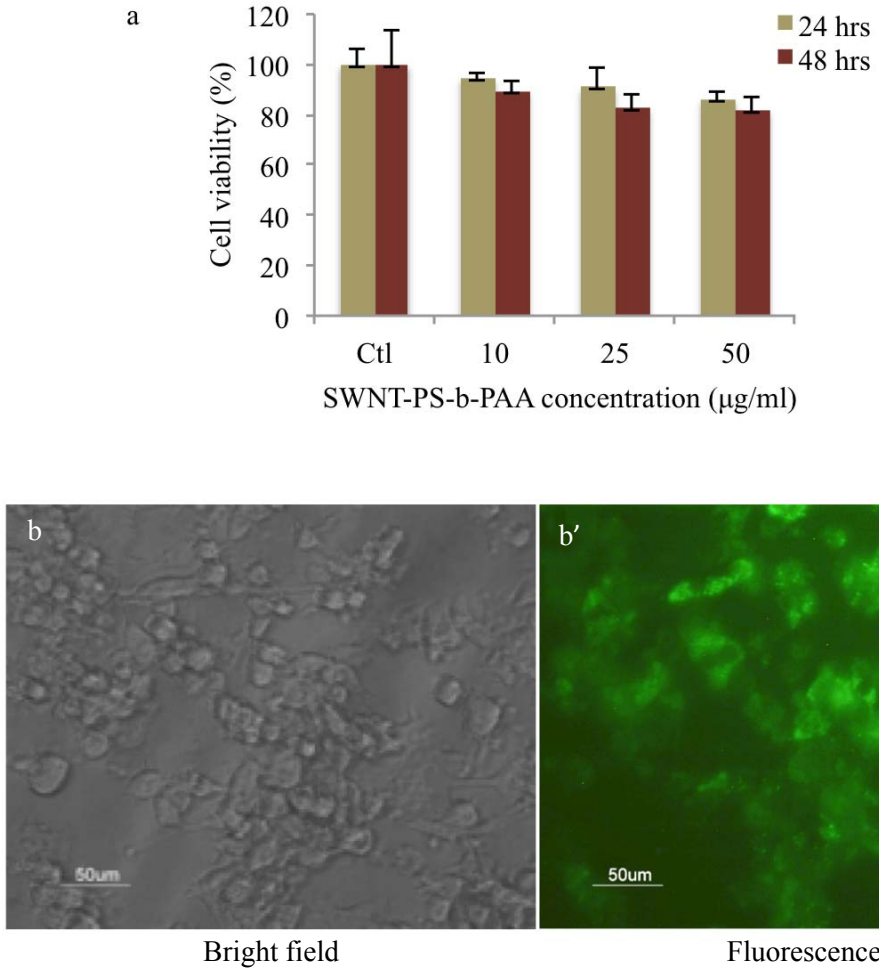

Figure 5.3 Toxicity and cell internalization of SWNT-drug carrier *in vitro*

(a) Cytotoxicity of the SWNT-drug carriers. MCF-7 cells were treated with SWNT-drug at a concentration ranged from 10 to 50 μg/mL for up to 48 hrs. Cells treated with PBS were used as a control. Cell viability was measured by MTS assay assuming that cell viability in PBS treated cells as 100% (b-b') Microscopic images of MCF-7 cells incubated with FITC labelled SWNT-drug carrier.

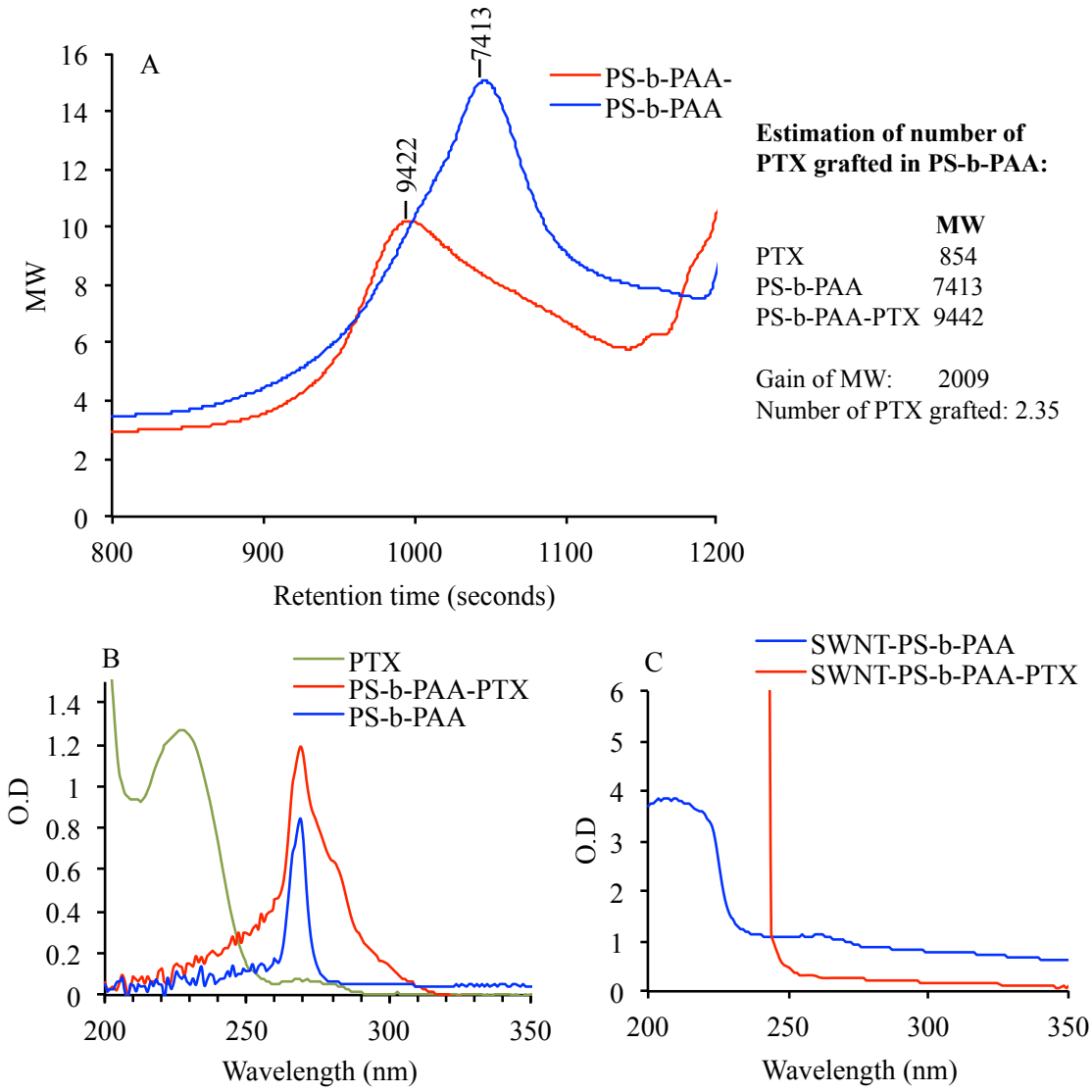

Figure 5.4 Characterization of SWNT-polymer-PTX by Gel Permeation Chromatography (GPC) and UV spectrometry

(a) Determination of drug-grafting ratio by GPC (b) UV spectra of PTX, polymer and polymer-PTX (c) UV spectra of SWNT-polymer-PTX

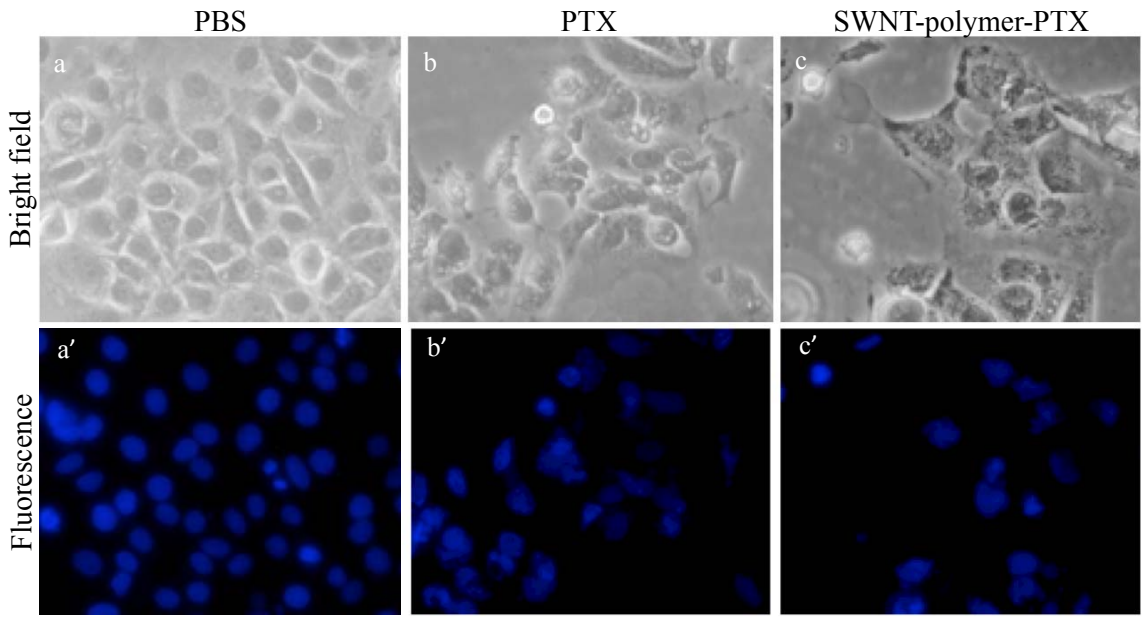

Figure 5.5 Antitumour efficacy of SWNT-polymer-PTX *in vitro*

Microscopy images of MCF-7 cells treated with (a-a′) PBS (b-b′) PTX and (c-c′) SWNT-polymer-PTX

MCF-7 cells were treated with SWNT-polymer-PTX at 0.1 μg/mL (equivalent of PTX concentration) for 48 hrs. Free drug PTX (dissolved in Cremophor EL) was used as a positive control. DAPI staining was applied to examine mitotic features of the cells.

CHAPTER 6 CARBON NANOTUBE LIPID DRUG APPROACH FOR TARGETED DELIVERY OF A CHEMOTHERAPY DRUG IN A HUMAN BREAST CANCER XENOGRAFT ANIMAL MODEL

Wei Shao[1], Arghya Paul[1], Bin Zhao[1], Crystal Lee[2], Laetitia Rodes[1] and Satya Prakash[1*]

[1]Biomedical Technology and Cell Therapy Research Laboratory, Department of Biomedical Engineering, Faculty of Medicine, McGill University
3775 University Street, Montreal, Quebec, H3A 2B4, Canada

[2] Department of Microbiology and Immunology, McGill University
3775 University Street, Montreal, Quebec, H3A 2B4, Canada

[*] Corresponding author Email: satya.prakash@mcgill.ca
Tel: 1 (514) 398-3676; Fax: 1 (514) 398-7461

Preface: This chapter introduces a new SWNT drug-loading method using lipid-drug approach. A proof-of-concept study was performed in breast cancer animal model using PTX as a model drug. The design strategies and advantages of the lipid-drug approach were fully described and discussed. The chemical synthesis of lipid-PTX and conjugation of tumour targeting molecule FA to SWNT-based drug carrier were confirmed by NMR and UV spectra. The SWNT-lipid-drug was characterized by Transmission Electron Microscopy (TEM), UV spectrometry and Thermogravimetric analysis (TGA). Intracellular drug delivery capacity and *in vitro* drug efficacy were evaluated using MCF-7 breast cancer cells. Finally, *in vivo* evaluation of the targeted SWNT-lipid-PTX in breast cancer xenograft mice model was presented and discussed.

Article published in *Biomaterial* (2013) 34 (38), 10109-10119

6.1 Abstract

Carbon nanotube (CNT) possesses excellent properties as a drug carrier. To overcome the challenge of drug functionalization with CNT, we have developed a novel lipid-drug approach for efficient drug loading onto CNT, in which a long chain lipid molecule is conjugated to drug molecule so that the lipid-drug can be loaded directly onto CNT through binding of the lipid 'tail' in the drug molecule to CNT surfaces *via* Van de Waal force and hydrophobic interaction. In our proof-of-concept study, drug paclitaxel (PTX) was conjugated with a biocompatible lipid molecule docosanol for functionalization with CNT. Folic acid was also conjugated to CNT for targeted drug delivery. High level of drug loading capacity on SWNT was achieved by lipid-drug approach. Conjugation of FA to SWNT-lipid-PTX led to an increase in cell penetration capacity, and the targeted SWNT-lipid-PTX showed improved drug efficacy *in vitro* in comparison to free PTX and non-targeted SWNT-lipid-PTX at 48 hrs (78.5% vs. 31.6% and 59.1% in cytotoxicity respectively, $p < 0.01$). *In vivo* analysis using a human breast cancer xenograft mice model confirmed improved anti-tumour drug efficacy *in vivo*. The targeted SWNT-lipid-PTX was found non-toxic at treatment dosage of 5mg/kg animal body weight as evaluated by biochemical analysis using blood samples, and by histological analysis of major organs.

6.2 Introduction

Conventional chemotherapeutic drugs distribute throughout the body and often cause severe side effects. The advances in nanotechnology and nanomedicine enable the revolutionary solutions in the field of drug delivery. One of the major reasons for using nanoparticle in chemotherapy drug delivery is that the nanoparticles preferentially accumulate in tumours through the *Enhanced Permeability and Retention* (EPR) effect. Indeed, nanoparticle drugs have demonstrated higher intratumoural drug concentration than their parental small-molecule counterparts [36]. In addition, nanoparticles, containing high surface area-to-volume ratio, can be potentially engineered into multifunctional nanoparticles that carry tumour-targeting molecules, tissue permeation enhancers, two or more types of therapeutics for more efficient cancer therapy [161]. Carbon nanotube (CNT), a new type of synthetic nanomaterial, offers opportunities for chemotherapy drug delivery. Structurally, CNT can be viewed as a tube rolled from layers of graphene sheets. Depending on the number of graphene layers, CNT is classified as single-walled carbon nanotube (SWNT) or multi-walled carbon nanotube (MWNT). Due to the well-organized structure, CNT presents remarkable physical properties, including ultra-high surface area, high tensile strength [94, 107, 162], excellent optical [64], electrical and thermal properties [81, 163, 164]. Besides, CNT is found easily penetrate all sorts of cells, including hard-to-transfect types of cells [12]. CNT is widely explored for potential biological applications because of its size, unique shape, and structure, as well as its attractive optical properties.

As a new type of nanomaterial, the toxicity of CNT has been intensively investigated *in vitro* and *in vivo*. It has been shown that appropriately functionalized CNT, *e.g.* polyethylene glycol (PEG) functionalized CNT does not cause noticeable toxicity to the treated animals [93]. Biodistribution of phospholipid-PEG (PL-PEG), functionalized SWNT showed that CNT is safe because it can be excreted *via* the biliary and renal pathways after intravenous injection [141, 165], With further conjugation of targeting ligands to SWNT, higher tumour accumulation could be achieved [91]. These results have paved the way for applications of CNT in cancer therapy. In recent years, SWNT has been applied in a variety of biomedical applications ranged from cancer drug

delivery, tumour imaging, detection and others [81]. Currently, the CNT-based siRNA formulation for cancer treatment is finalizing for moving into human trials [166].

Since CNT is pre-formed supramolecular nanotubes, the drug loading to this pre-formed structure is very challenging. SWNT can be filled with a large variety of compounds, including organic molecules [126, 127], and inorganic materials [128, 129]. Chemotherapeutic drugs are loaded into the interior of SWNT through a simple capillarity-induced filling. However, the loading amount is usually low [119]. Researchers have also investigated to load drugs on CNT sidewall, since they have found that pre-functionalized CNT still remains large uncoated surface area that allows for direct attachment some hydrophobic drugs that contain flat, benzene ring structures. One study has investigated the adsorption of doxorubicin on SWNT, in which, high loading amount was achieved (400% by weight) [113]. One advantage of this drug-loading method is that, when the drugs are loaded directly to CNT, the CNT-coating polymers are freed for conjugation of other functionalities, *e.g*. targeting molecules, antibodies, fluorescence molecule or other drugs for multifunctional delivery [113]. However, for drugs that have bulky structure, *e.g*. paclitaxel (PTX), the drug adsorption on nanotubes is not stable, so these bulky drugs are usually conjugated to CNT-dispersing polymers for delivery [167]. However, some limitations exist for the drug-polymer conjugation method. Firstly, the drug loading amounts on CNT were limited by the numbers of polymers that are attached CNT. In the case of PL-PEG functionalized CNT, PL-PEG only accounted for less than 10% of CNT surface, with which only ~3 PL-PEG was attached to each 10 nm of SWNT [113]. Secondly, when drugs occupied the CNT-dispersing polymers, there was no space for linking targeting molecules [118]. It is imperative to develop a more effective approach for construction of a multifunctional CNT-based drug delivery system, which is the main aim of this study.

6.3 Materials and methods

6.3.1 Reagents

All the reagents used in experiments were purchase from Sigma Aldrich, Canada except otherwise indicated specifically.

6.3.2 Chemical synthesis

Synthesis of lipid-acid [2-(2-(docosyloxy)-2-oxoethoxy)acetic acid]: The synthesis reaction followed the method developed by Arsell *et. al* [157]. Briefly, lipid docosanol (1 equiv) was dissolved in pyridine at room temperature, then diglycolic anhydride (3 equiv) was added. The reaction was carried out at room temperature with constant stirring for overnight. Then, the solvent was removed on a rotary evaporator. The residue was washed with 2N HCl, then extracted 3 times with dichloromethane. The combined extracts were dried over $MgSO_4$, and then filtered to remove $MgSO_4$. The filtrate was evaporated on a rotary evaporator. The product was dried under vacuum overnight.

Synthesis of lipid-PTX [2'-O-(5''-O-Docosanyldiglycoloyl) paclitaxel]: The synthesis reaction also followed the method developed by Arsell *et. al* [157]. PTX (1 equiv), lipid acid (2 equiv), and 4-N, N-dimethylaminopyridine (DMAP, 3 equiv) were dissolved in chloroform. Diisopropylcarbodiimide (DIPC, 1.3 equiv) was added to the above-mentioned solution and the reaction was carried out at room temperature. The completion of the reaction was monitored by thin layer chromatography (TLC) using methanol/dichloromethane (1:10) as an eluent. After the reaction completed, 2N HCl was added to quench the reaction. The aqueous mixture was extracted 2 times with chloroform. The extracts were combined and then washed with saturated $NaHCO_3$ solution. The product was purified by silica gel column using methanol/methylene. The final product was dried by lyophilisation. The success of the conjugation of lipid-PTX was confirmed by proton NMR (400 MHz Varian Mercury) using DMSO-D as a solvent.

Synthesis of PL-PEG-folate: Folic acid (3.5 mM) and 5 mM 1-ethyl-3-(3-dimethylamino-propyl) carbodiimide (EDC) were added to a solution of PL-PEG-NH_2 (2K Da, Avanti Lipid company, USA) at 0.35mM in 10 mM phosphate buffer at pH 7.5. The reaction was carried out at room temperature for 4 hrs with shaking. Then, the solution was dialyzed against phosphate buffer using a membrane cassette (molecular weight cut-off of 3k) for 3 days with frequent replacement of the buffer to remove excess folic acid and EDC.

6.3.3 Formation of SWNT-lipid-PTX

The procedure was adapted from the method reported by Liu, *et al* [81]. Lipid-PTX was dissolved in a water-miscible solvent, e.g. DMF or methanol. SWNT (HiPco, Unidym Inc, USA) was mixed with lipid-PTX in the solvent with brief. Then ten times of volume of PL-PEG water solution was added with sonication. The mixture was continually sonicated for 1 hr with cooling using icy water. SWNT bundles were removed by ultracentrifigation. Solvent and excess PL-PEG in solution were removed by three times of washing with deionized (DI) water using centrifugation filtration units (Amicon, 100 kDa) before use.

6.3.4 Characterization of SWNT-lipid-PTX by UV-NIR spectroscopy and thermal gravimetric analysis (TGA) and transmission electron microscope (TEM)

UV-NIR spectra of lipid-PTX, SWNT and SWNT-lipid-PTX were measured in 1 cm quartz cuvettes using UV-NIR spectrophotometer (Cary-100 bio, Varian Inc) over the range of 200 – 850 nm. The standard curve for quantification of lipid-PTX was obtained by plotting the absorbance at 278 nm against PTX concentration and subsequent linear regression analysis. TGA was performed using TGA Q500 (TA instruments Ltd, UK). Samples were loaded in the sample holder and the materials were heated up at a rate of 10 °C/min up to 800 °C under nitrogen. The weight loss and derivative weight were recorded continuously. The size and shape of functionalized SWNT-lipid-PTX were examined by TEM (Philips169 CM200 200 kV). 5 μl of sample solution was deposited

on carbon-coated copper grid and allowed to dry for 10 mins. The excess liquid on grid was removed by touching the edge of the grid with filter paper.

6.3.5 Labeling SWNT with fluorescence dye FITC and cell permeability assay

Fluorescent SWNT were prepared by adsorbing FITC directly on sidewall of nanotubes. SWNT were firstly mixed with FITC in organic solvent DMF by brief sonication, and 10 times of volume of PL-PEG solution was added with continuous sonication for 1 hr. The excess reagents were removed by dialysis using membrane cassette (100 kDa cut-off). For cell penetration assay, the cells were seeded in a 96-well plate at a density of 2 x 10^4 cells/well in 200 μl medium at one night before the assay. The cells were incubated with FITC labeled SWNT for 12-24 hrs. The cells were washed and viewed under fluorescence microscope. The intracellular delivery efficiency of SWNT was quantified by manually counting the percentage of cells up-taking fluorescence dye under microscopy.

6.3.6 Cytotoxic study

MCF-7 breast cancer cells (ATCC) were maintained in Dulbecco's modified Eagle's Medium (DMEM, Invitrogen, Canada) supplemented with 10% Fetal Bovine Serum (FBS, Invitrogen, Canada). The cells were cultured in a humidified incubator with 5% CO_2 at 37 °C. Cytotoxicity of SWNT-lipid-drug was evaluated in MCF-7 breast cancer cells by MTS assay using the Cell Titer 96® Aqueous Non-Radioactive Cell Proliferation MTS Assay kit (Promega). Briefly, triplicates of 1x10^4/well in 96-well plates were treated with different amounts of PTX formulations at 37°C at varied time period. The MTS assay was performed following the manufactory's instruction. The 3-(4,5-dimethylthiazol-2-yl)-5-(3-carboxymethoxyphenyl)-2-(4-sulfophenyl)-2H-tetrazolium (MTS) was reduced to form formazan by mitochondrial enzyme dehydrogenase in viable cells and the formazan concentration in the cell culture was measured at absorbance of 490 nm using 1420-040 Victor3 Multilabel Counter (Perkin Elmer, USA). The amount of formazan is proportional to the number of viable cells. Cytotoxicity was calculated as the percentage of dead cells relative to that in the untreated control group.

6.3.7 Cell cycle analysis

Cells were trypsinized and harvested by centrifugation at 200 g at 4 °C for 10 min. The cells were washed with ice-cold PBS and fixed in 75% ethanol in PBS at 4 °C for at least 30 min. Prior to analysis, cells were washed again with PBS and resuspended and incubated in a solution containing 0.05 mg/mL propidium iodide, 1 mM EDTA, 0.1% Triton-X-100 and 1 mg/mL RNAse A. After 30 min of incubation, the stained cells were examined by flow cytometry. Cells were acquired on a Becton Dickinson FACSCalibur (BD Bioscience) and DNA histograms were analyzed using CellQuest Pro software (BD Bioscience). The percentage of cells in the different cell cycle phases was calculated using ModFit LT 3.3.11 cell cycle analysis software (Verity Software House).

6.3.8 Animal studies

Female athymic nude mice (5-6 weeks old) were purchased from Charles River Laboratories. All animal experiments were performed under a protocol approved by McGill University Animal Care Committee. MCF-7 cells were harvested from subconfluent cultures with trypsin and washed with PBS. 4 $X10^6$ MCF-7 cells were mixed with Matrigel (BD Bioscience) and subcutaneously injected into the back flanks of a mouse on one side. Estradiol was dissolved in ethanol and supplemented in the drinking water at 1 mg/l. Drug treatment started in the mice when tumour volume reached at least 100 mm^3 (about one month after tumour cell inoculation). The mice were randomized according to their sizes. For the drug treatment, PTX was prepared by dissolving the drug in a vehicle solution (EtOH:cremophor, 50:50 v/v), and then diluted in physiologic saline. SWNT-lipid-PTX and FA-SWNT-lipid-PTX were diluted in physiologic saline. 100 to 200 mL of different PTX formulations were i.v injected into the mice *via* the tail vein every 6 days for 4 times. The injected doses were normalized to 5 mg PTX per kg of mice. The mice body weight and tumour sizes were measured by a calliper twice a week. Tumour volume was calculated as $\frac{1}{2} \times \text{width}^2 \times \text{length}$. Relative tumour volume was calculated as V/V_0 (V_0 was the initial tumour volume).

6.3.9 Blood sampling and tests

BALB/c mice were injected intravenously with either saline, SWNT only and SWNT-lipid-PTX. Blood was collected at 0, 4 hrs post-injection from the lateral saphenous vein of the mice. At endpoint of the experiments (42 days post-injection), the blood was collected by cardiac puncture. The blood was sent to Diagnostic Laboratory, McGill Animal Resource Centre for hematologic test and white blood cell differential.

6.3.10 Histology staining

For histological and TUNEL staining of tumour tissues, samples were collected at two experiment endpoints. One time point was on day 3 after last drug injection and another one was at 42 days post drug injection. At endpoint of 42 days, mice liver, kidneys, spleen heart, lungs and tumours were collected and fixed in 4% formaldehyde in phosphate buffer, embedded in paraffin, cut to a nominal thickness of approximately 5 μm and stained with haematoxylin and eosin (H&E). The tissue morphology was observed under a light microscope and the photomicrographs were taken by an AxioCam MRc (Carl Zeiss AG).

6.3.11 Examination of apoptotic cells

In H&E stain of tumour tissue, apoptotic cells were identified by cell shrinkage and condensed nuclei (darker). The apoptotic cells that are identified from H&E has been shown to be consistence with the apoptotic cells identified by the terminal deoxynucleotidyl transferase-mediated nick end labelling (TUNEL) methods [168, 169]. The number of tumour cells, apoptotic cells and non-apoptotic cells in 10 randomly selected fields at X400 were counted under microscope.

6.3.12 Statistical analysis

Statistical analysis was carried out using software SPSS software (Minitab Inc, State College, PA). Data were expressed as mean ± standard deviation (s.d). Statistical

significance was accepted at a level of $p < 0.05$. Equality of variances between groups was verified by Levene test. Differences between the groups were tested through analysis of variance (ANOVA), and Tukey's post-hoc test was applied to compare the difference between the groups.

6.4 Results and discussion

6.4.1 Design strategy of the targeted SWNT-lipid-drug delivery formulation

The raw CNT is highly hydrophobic, which causes difficulties for drug delivery applications. Previous studies have developed effective covalent and non-covalent CNT modification methods for dispersing CNT in aqueous solutions [69, 80, 170-173]. Among these approaches, the PL-PEG functionalized SWNT showed good dispersity in water and is stable in serum containing media. PL-PEG contains two long lipid chains, which lay flat on sp^2-conjugated graphitic nanotube structure and form strong hydrophobic interaction with SWNT. Inspired by this SWNT-lipid chain interaction, we have designed a lipid-drug approach by modification of a drug using a long chain lipid, and it was hypothesized that the lipid portion of the lipid-drug could tightly associate with SWNT in the same manner as PL-PEG does. As illustrated in Fig. 6.1, the drug molecule, *e.g*. PTX, is conjugated to a long chain lipid *via* a cleavable chemical bond. The SWNT-drug could be made exploiting the lipid 'tail' to form SWNT-lipid-drug complex through hydrophobic interaction. The SWNT-based drug is made targeted delivery using a tumour targeting molecule folic acid (FA), which binds to folate receptors (FR) that are overexpressed in a variety of cancer cells, including breast, colon, renal and lung tumours [47]. Binding of FA to FR leads to enhance cellular internalization of nanoparticles. This new method overcomes the existing challenges in loading drug molecules onto CNT and broadens their use in multifunctional deliveries.

6.4.2 Chemical synthesis of lipid-PTX conjugate and targeted polymer PL-PEG-FA

Lipid 1-docosanol was used for synthesis of lipid-PTX as reported previously [157]. 1-docosanol contains a 22-carbon lipid chain, which is similar to the lipid portion of the

polymer PL-PEG in structure, so, it could be compatible with PL-PEG for coating SWNT surface to form stable ternary structure. For chemical synthesis of the lipid-PTX, two steps were involved (1) forming a linker-lipid using a linker molecule diglycolic anhydride, (2) linking PTX to the linker-lipid by ester formation using diisopropylcarbodiimide (DIPC) in the presence of N, N-4-dimethylaminopyridine (DMAP) [157]. The final product was purified by chromatography and confirmed by NMR analysis (Fig. 6.2) and UV-NIR scan spectrometry (supplementary Fig. S6.1a). For synthesis of PL-PEG-FA, FA was conjugated to amino end group in PL-PEG-NH_2 *via* amide bonding using EDC [103]. The success of the conjugation reactions was verified by scan UV-NIR spectrometry (supplementary Fig. S6.2).

6.4.3 Formation of SWNT-lipid-drug and *in vitro* characterization

To form SWNT-lipid-drug, the lipid-drug conjugate was mixed with SWNT in water-miscible solvent firstly by brief sonication, then PL-PEG water solution was added to allow the formation of SWNT, lipid-drug and PL-PEG hybrids. To determine the optimized condition for loading of the lipid-drug, different lipid-drug/PL-PEG ratios were examined so as to achieve maximum drug loading and at the same time to maintain dispersibility of SWNT-drug. Lipid-drug/PL-PEG molar ratios ranged from 0.1 to 1 were tested. It was observed that, with molar ratios of smaller than 0.5, SWNT dispersibility did not affected; however, with the molar ratios of larger than 0.5, SWNT dispersibility dropped from ~ 40 μg/mL to < 10 μg/ml, which suggested that the addition of too much lipid-drug could disturb PL-PEG coating effect on SWNT, and thus affected the formation the SWNT-based drugs. So, in the following experiments, SWNT-lipid-PTX was prepared and characterized using lipid-drug/PL-PEG molar ratio of 0.5. The SWNT-lipid-PTX was found stable in PBS (PH 7.4) and serum containing solutions. No precipitation was observed in SWNT-lipid-PTX dispersed in water after storage at 4°C for three months. TEM image confirmed the single-dispersed nanotubes in SWNT-lipid-PTX in water (Fig. 6.3a).

The attachment of lipid-PTX and PL-PEG to SWNT was examined by Thermo Gravimetric Analysis (TGA). TGA provides thermal degradation profile of materials, and its derivative weight loss curve could differentiate the types of materials in the hybrids. Our result in TGA indicated that PL-PEG coated SWNT displayed one peak (at 380 °C), whereas, lipid-drug loaded SWNT showed two peaks (at 360 °C and 380 °C) in derivative weight loss curve (Fig. 6.3b). Since SWNT does not decompose within 800 under nitrogen condition, the two peaks presented in the lipid-drug loaded SWNT sample corresponded to two types of materials: the lipid-drug (360°C) and the PL-PEG (380°C), confirming that the lipid-drug was loaded on the SWNT. The formation of SWNT-lipid-PTX complex was further confirmed by UV-NIR spectrometry, in which the presence of lipid-PTX was evidenced by its characteristic peak at 278 nm on top of SWNT absorption spectrum (supplementary Fig. S6.1b). Based on UV-NIR absorbance of lipid-PTX and SWNT, the loading factor of lipid-PTX on SWNT was estimated in the range from 600-1000 (defined as lipid-PTX to SWNT molar ratio). By assuming SWNT having an average size of 200 nm in length and 1.5 nm in diameter, the percentage of lipid-PTX coverage on SWNT surface was 57-94% v/v (supplementary Fig. S6.2). The result suggested that high coverage lipid-drug on SWNT could be achieved by lipid-drug approach.

6.4.4 *In vitro* evaluation of SWNT-lipid-drug

As a new type of nanomaterial, the toxicity of CNT has been widely investigated. Previous results have showed that the toxicity of CNT is relevant to multiple factors, including size and length of the nanotubes [174], degree of impurities [68], and dispersion status [175] *etc*. Raw CNT has shown obvious toxicity *in vitro* and *in vivo*. In contrast, PL-PEG functionalized SWNT showed low toxicity because surface functionalization prevented aggregation of SWNT in aqueous solutions [93]. In view of the result, we chose to use PL-PEG functionalized SWNT as a drug loading platform in this study. We further examined the biocompatibility of SWNT-lipid-drug carrier (SWNT/lipid) using MCF-7 cells. The results showed that incubation of SWNT/lipid at

concentration of 10 μg/mL for up to 48 hrs did not cause any obvious toxicity compared with untreated control (Fig. 6.4a).

Then, we examined cell penetration capacity of SWNT-based drug carrier. FITC labeled SWNT and FA-SWNT were incubated with FR+ MCF-7 breast cancer cells for 24 hrs. The result showed that SWNT could carry FITC into cells and the percentage of FITC positive cells was 80 ± 2% (mean ± s.d, n= 5). With conjugation of FA to SWNT, the percentage of FITC positive cells increased to 95 ± 3% (mean ± s.d, n= 5). It was also noticed that, within a single cell, fluorescence intensity was significantly higher in cells treated with FA-conjugated SWNT than those without FA. The enhanced cell permeability was presumably due to cell surface receptor mediated cellular internalization (supplementary Fig. S6.4).

In next step, we examined therapeutic potential of the SWNT-lipid-PTX and the targeted SWNT-lipid-PTX using MCF-7 cells. Clinical formulation Taxol (PTX dissolved in Cremophor EL) was used as a positive control. We observed a time-related cell inhibition (Fig. 6.4b). The cytotoxicity in MCF-7 cells showed 25.1 ± 3.0%, 32.3 ± 4.3% and 44.1 ± 6.2% (mean ± s.d, n= 3) with 24 hrs incubation and 31.6 ± 2.9%, 59.1 ± 5.1% and 78.5 ± 2.1% (mean ± s.d, n= 3) with 48 hrs incubation for free PTX, SWNT-lipid-PTX and targeted SWNT-lipid-PTX respectively. At both time points, the two SWNT-lipid-PTX formulations were more effective than free PTX, and the targeted SWNT-lipid-PTX was more effective than non-targeted one. The improvement in drug efficacy could be attributed to higher degree of cellular penetration of the targeted SWNT-lipid-drug due to specific binding of FA to FR on cancer cell surface.

To determine the molecular mechanism of the cell death induced by SWNT-lipid-PTX, a cell cycle analysis was performed using flow cytometry with propidium iodide (PI) staining of DNA content in MCF-7 cells. It is known that cancer cell inhibition effect of PTX is mediated through binding of the drug molecule to the microtubules of cells so to prevent it from disassembly, which blocks the progression of cell mitosis and triggers initiation of cell cycle arrest in the G2/M phase [156]. Treatment of MCF-7 cells with

targeted SWNT-lipid-PTX cells induced substantial accumulation of 74% of arrest in G2/M phase compared with 0% in untreated control (Fig. 6.5). Treatment with PTX induced the same level of G2/M arrest, suggesting that SWNT-lipid-PTX induces cell death through the same mechanism as free PTX.

6.4.5 *In vivo* drug efficacy

In vivo drug efficacy of the targeted SWNT-lipid-PTX was evaluated using a breast cancer xenograft mice model. Compared with control group, both Taxol and the targeted SWNT-lipid-PTX showed tumour regression at different levels. Taxol showed evident tumour regression and obtained a relative volume of 1.35 ± 0.08 (*v.s* 1.49 ± 0.10 in control, $p < 0.001$) at post drug injection day 42. The targeted SWNT-lipid-PTX displayed evident tumour regression starting from day 7. At day 42, the targeted SWNT-lipid-PTX obtained relative volume of 1.14 ± 0.05 (*v.s* control, $p < 0.001$). Compared with control group, both treatment groups displayed significantly higher percentage of tumour inhibition at day 42 (9.0% for PTX *vs.* 23.5% for targeted SWNT-lipid-PTX respectively $p < 0.001$) (Fig. 6.6). To investigate the tumour suppression mechanism, we examined morphologic changes of the cells in tumour tissues and the level of apoptotic cells by H&E staining of tumour tissues. As we know, the morphologic changes of a cell undergoing apoptosis are distinguishable from other types of cells in H&E staining, such as nuclei condensation, membrane blebbing, *etc* [169, 176]. Our results showed that the treatment with the targeted SWNT-lipid-PTX led to a significantly increased level of apoptotic cells compared with PTX treatment. By counting the number of viable cells and apoptotic cells under microscope, we obtained the apoptotic cell fractions in tumour tissue were 1.3± 0.6%, 5.4 ± 2.4% and 20.7 ± 9.2% (mean ± s.d, n= 10) for saline, PTX and the targeted SWNT-lipid-PTX respectively, confirming that SWNT-based drugs exhibited more tumour inhibition effects by induce more apoptosis in tumour cells (Fig. 6.7). The limitation of this method is that the quantitative measurement may lacks objectivity and reproducibility and fewer apoptotic cells are usually detected under low magnification (*e.g.* 400X) [176].

6.4.6 *In vivo* toxicity study

Hematology analysis and histological evaluation of major organs were applied to evaluate toxicity of the SWNT-lipid-drugs. During the trial period, it was observed that SWNT-lipid-drug did not cause mortality with treatment dosage and no obvious adverse effects were noticed. No statistically significant differences in change of body weight were detected between test groups and control groups (Fig. 6.8a). Assessment of hematologic parameters, including hematocrit, hemoglobin, red blood cell count (RBC) and white blood cell count (WBC), also showed no difference between control and test groups ($p < 0.05$, Fig. 6.8b). Histological staining of major organs, including liver, heart, lung, and kidney, showed that no obvious tissue damage and no inflammatory cell infiltration occurred in all the groups (data not shown), confirming that both SWNT and SWNT formulated drugs did not cause any obvious toxic effects to blood and major organs at the injected dosage.

6.5 Conclusion

In this study, a lipid drug approach was proposed for preparation of SWNT-drug as to load drug directly onto SWNT sidewalls at a high loading efficiency. Using this approach, a targeted SWNT-lipid-drug formulation for PTX was made. The formation of SWNT-based drug was successively confirmed and characterized by TEM, TGA and UV-Vis spectrometry. Both SWNT-lipid-drug and FA-SWNT-lipid-drug (targeting folate receptor on tumor cell surface) exhibited excellent stability. The targeted SWNT-drug showed target specificity in vitro. The efficacies of the SWNT-lipid-PTX and targeted SWNT-lipid-PTX were examined in vitro using breast cancer cell lines. Both SWNT-lipid-PTX and targeted SWNT-lipid-PTX inhibited growth of breast cancer cells in vitro and had a significant improvement over free drug PTX. In vivo, the targeted SWNT-

lipid-PTX demonstrated significant tumor growth inhibition in a human breast tumor xenograft mouse model. The lipid-drug scheme can be applied to CNT-based delivery for other types of chemotherapy drugs by designing alternative chemical synthesis methods for cleavable drug-lipid linkages. The significance of the proposed lipid-drug approach also lies in that, when the drugs are loaded on SWNT sidewalls, the CNT-coating polymers can be free for conjugation of other molecules affording multi-functional drug delivery, e.g. conjugation of tumor-targeting molecules for targeted delivery, or conjugation of another type of drug molecule, siRNA, or antibodies for combination therapies.

6.6 Acknowledgments

The authors acknowledge CIHR for project funding. W. Shao and L. Rodes acknowledge the financial support from FRQS (Fonds de recherche du Québec - Santé) Doctoral award. A. Paul acknowledges the Alexander Graham Bell Post Graduate Scholarship-Doctoral from Natural Sciences and Engineering Research Council of Canada (NSERC). The authors are grateful for the following assistances: the approval of Animal Use Protocol provided by McGill Animal Care Committee; technical support for animal drug injection provided by A. Jimenez's group from Comparative Medicine & Animal Resources Centre; transmission electron microscopy imaging provided by X. Liu, (FEMR) Facility of Electron Microscopy Research at McGill University; NMR facility, Chemistry Department, McGill University; TGA tests provided by P. Fiurasek, Centre for self-assembled Chemical Structures (CSACS); FACs facility, Microbiology Department, McGill University.

6.7 Conflict of interest

The authors declare that no financial support or other compensation has been received relating to any aspect of this research or its publication that could be construed as a potential conflict of interest.

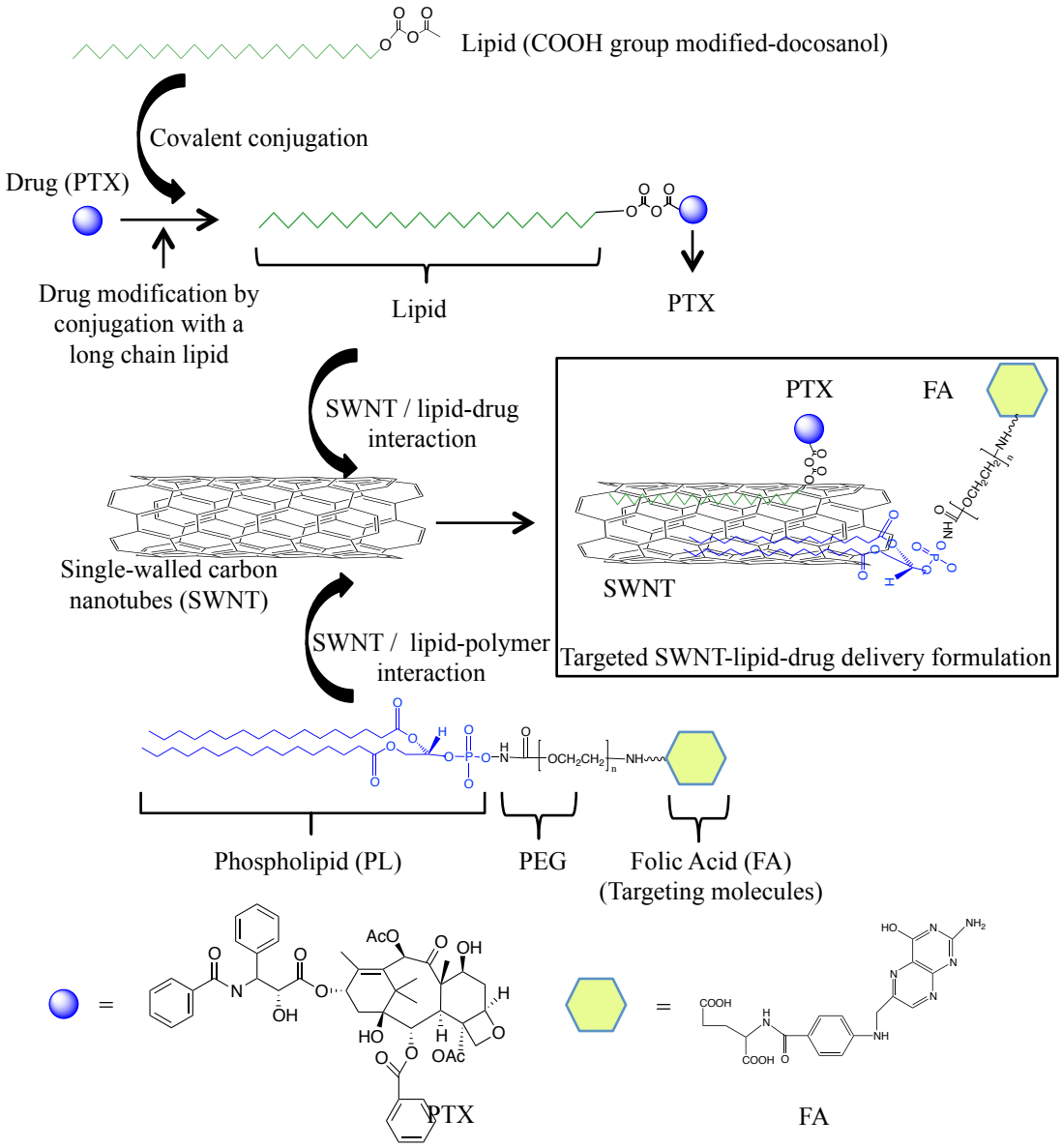

Figure 6.1 Design strategy of a novel targeted SWNT-lipid-drug delivery system

The drug molecule, *e.g.* paclitaxel (PTX), was conjugated to a long chain lipid *via* a reversible ester bond. The SWNT-lipid-drug was made by exploiting the lipid 'tail' in the drug to form lipid-drug/SWNT complex through strong hydrophobic interactions. The formulation was made multifunctional delivery using a tumor targeting molecule folic acid (FA) that was conjugated to the end of the PL-PEG exploiting an amide bond formed between amine group of PL-PEG and carboxyl group of FA. This formulation could overcome the existing challenges of CNT in drug deliveries and broadened their use for multifunctional deliveries. The Use of lipid molecule is unique and advantageous as it allows delivery of a range of drugs in multifunctional delivery applications.

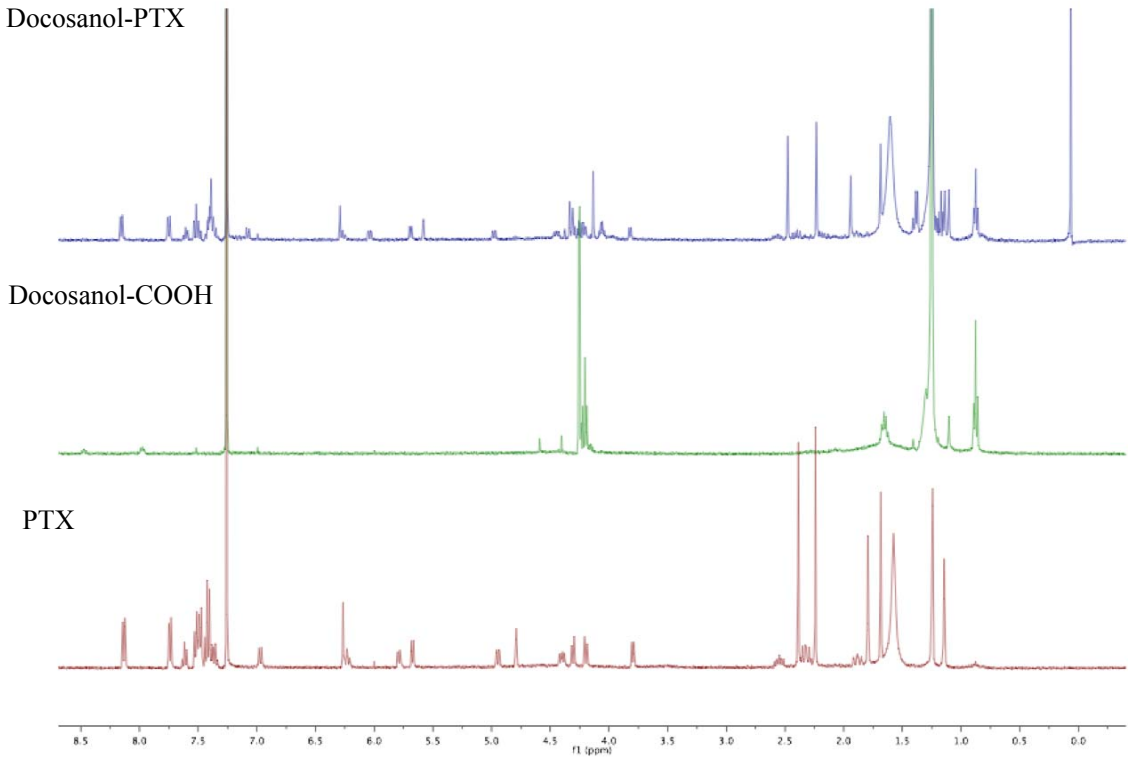

Figure 6.2 Examination of lipid-paclitaxel (PTX) synthesis by NMR

The reaction was carried out in chloroform in the presence of diisopropylcarbodiimide and *N*,*N*-4-dimethylaminopyridine. TLC was used to monitor the completion of the reaction. After reaction completed, the excess reagents, drug and solvent were removed by chromatography column. The conjugation product was verified by NMR. ^{1}H chemical shifts were reported relative to tetramethylsilane (TMS). The chemical shifts at δ 8.5-7.0 were derived from aromatic protons in PTX moiety; the doublet peaks at δ 6.9 were derived from NH group of PTX moiety; the chemical shifts at δ 4.2-4.0 were derived from CH_2OCH_2 group in docosanol moiety; the chemical shift at δ 1.2 were derived from the $CH_2C_{16}H_{32}CH_2$ group in docosanol moiety.

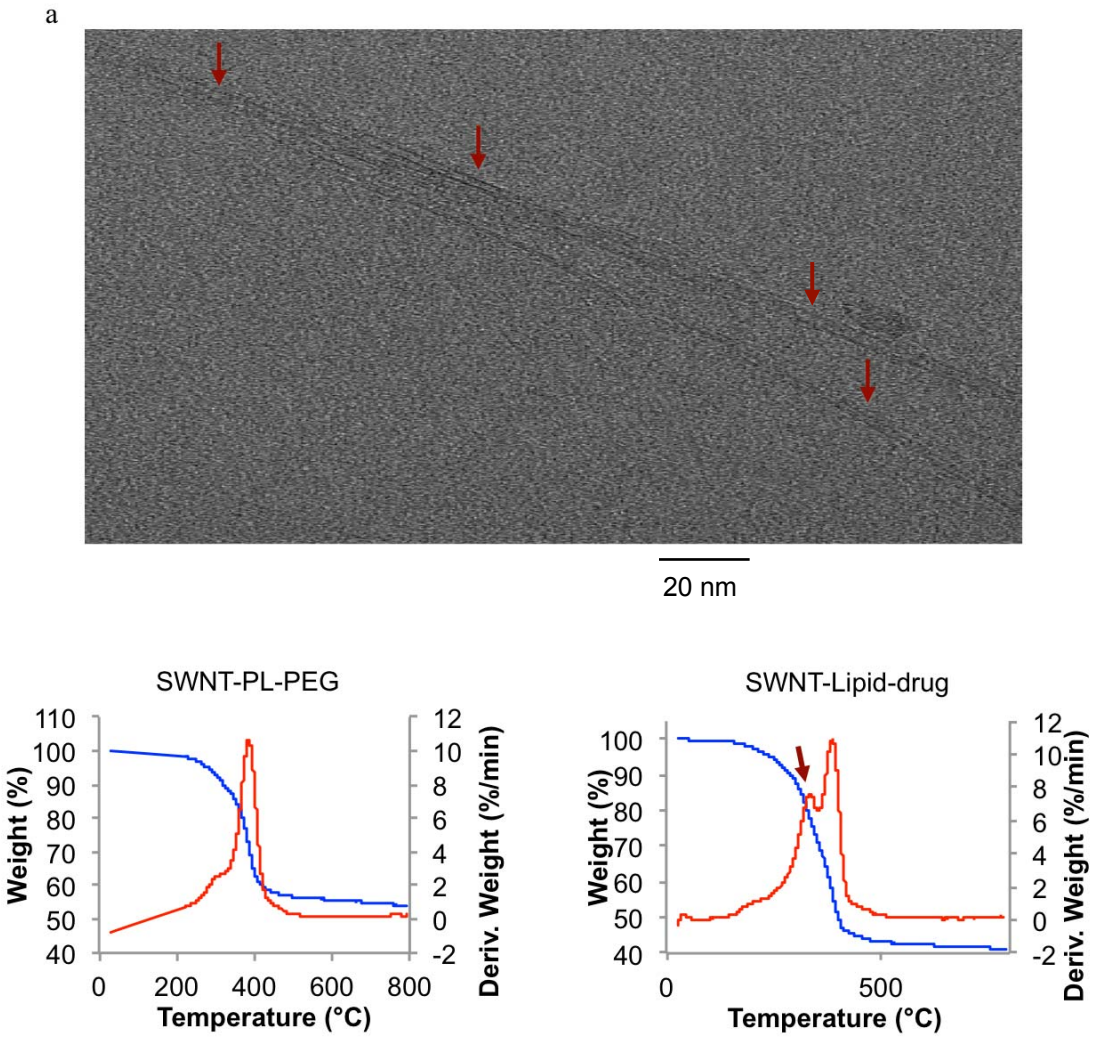

Figure 6.3 Characterization of SWNT-lipid-drug.

(a) Transmission electron microscopy (TEM) image of SWNT-lipid-PTX. Scale bar represents 20 nm. TEM showed single-dispersed lipid-PTX loaded nanotubes in water solution. (b) Evaluation of lipid-drug loading on SWNT by Thermogravimetric Analysis (TGA). SWNT were functionalized with PL-PEG only or with lipid-drug/PL-PEG. Samples were purified by filtration and then air-dried. TGA were performed from 25 to 800 ° C under nitrogen. Weight change (blue curve) and derivative weight (red curve) with temperature were recorded. TGA displayed extra peak at 320 ° C in derivative weight of SWNT-lipid-drug compared with SWNT-PL-PEG (marked by red arrow), confirming that lipid-drug was loaded on SWNT along with polymer PL-PEG.

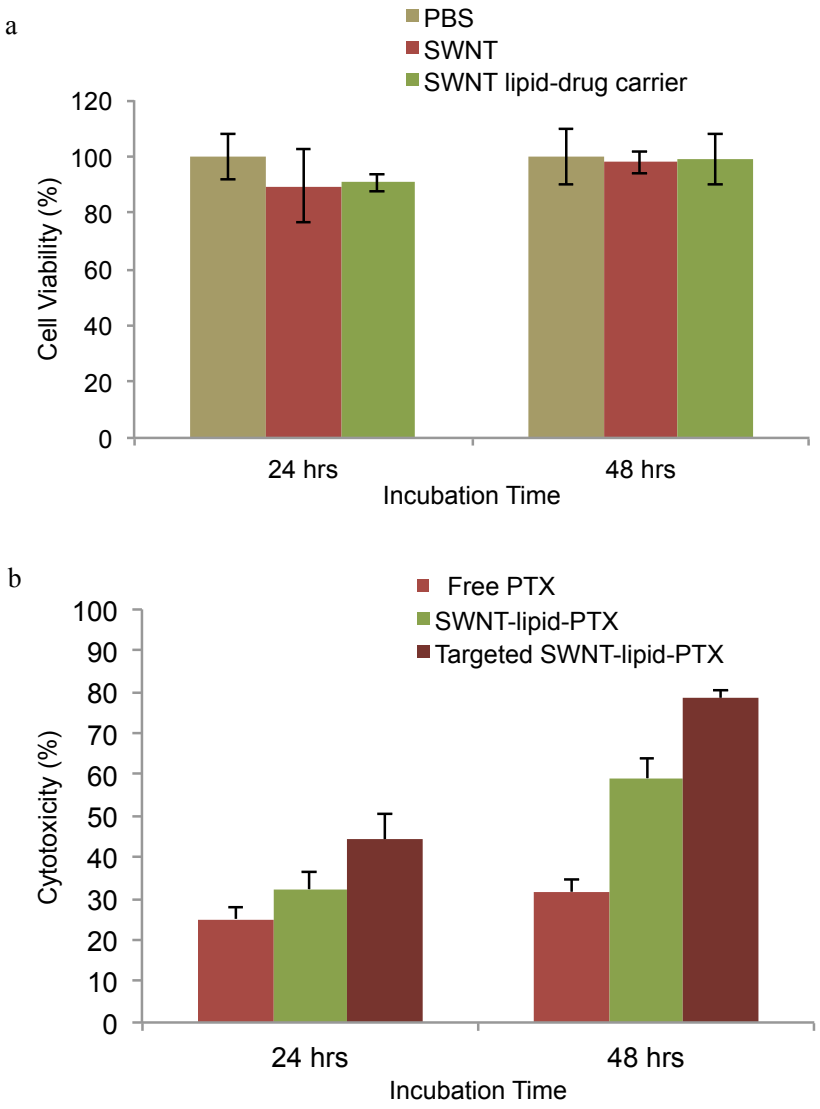

Figure 6.4 Investigation of *In vitro* drug effects of SWNT-lipid-PTX

(a) Cytotoxicity of SWNT-based drug carriers. MCF-7 cells were treated with SWNT or SWNT based lipid-drug carrier (SWNT/lipid) at 10 μg/ml for up to 48 h. Cells treated with vehicle PBS were used as a control. Cell viability was measured by MTS assay assuming that cell viability in PBS treated cells as 100%. (b) *In vitro*cancer cell inhibition of SWNT-lipid-PTX. MCF-7 cells were treated with PTX, SWNT-lipid-PTX or targeted SWNT-lipid-PTX at 20 nm for 24–48 h. Cell viability was evaluated by MTS assay. The data were presented in degree of cytotoxicity (%) assuming that cytotoxicity in untreated control as zero. The result showed that cytotoxicity was 25%, 32% and 44% for 24 h incubation and 32%, 59% and 78% at 48 h incubation for Taxol, SWNT-lipid-PTX and targeted SWNT-lipid-PTX respectively. At both time points, the SWNT-based PTX formulations were more effective than clinical formulation Taxol. More importantly, the targeted SWNT-lipid-PTX showed stronger cancer cell inhibition than SWNT-lipid-PTX. $n = 3$.

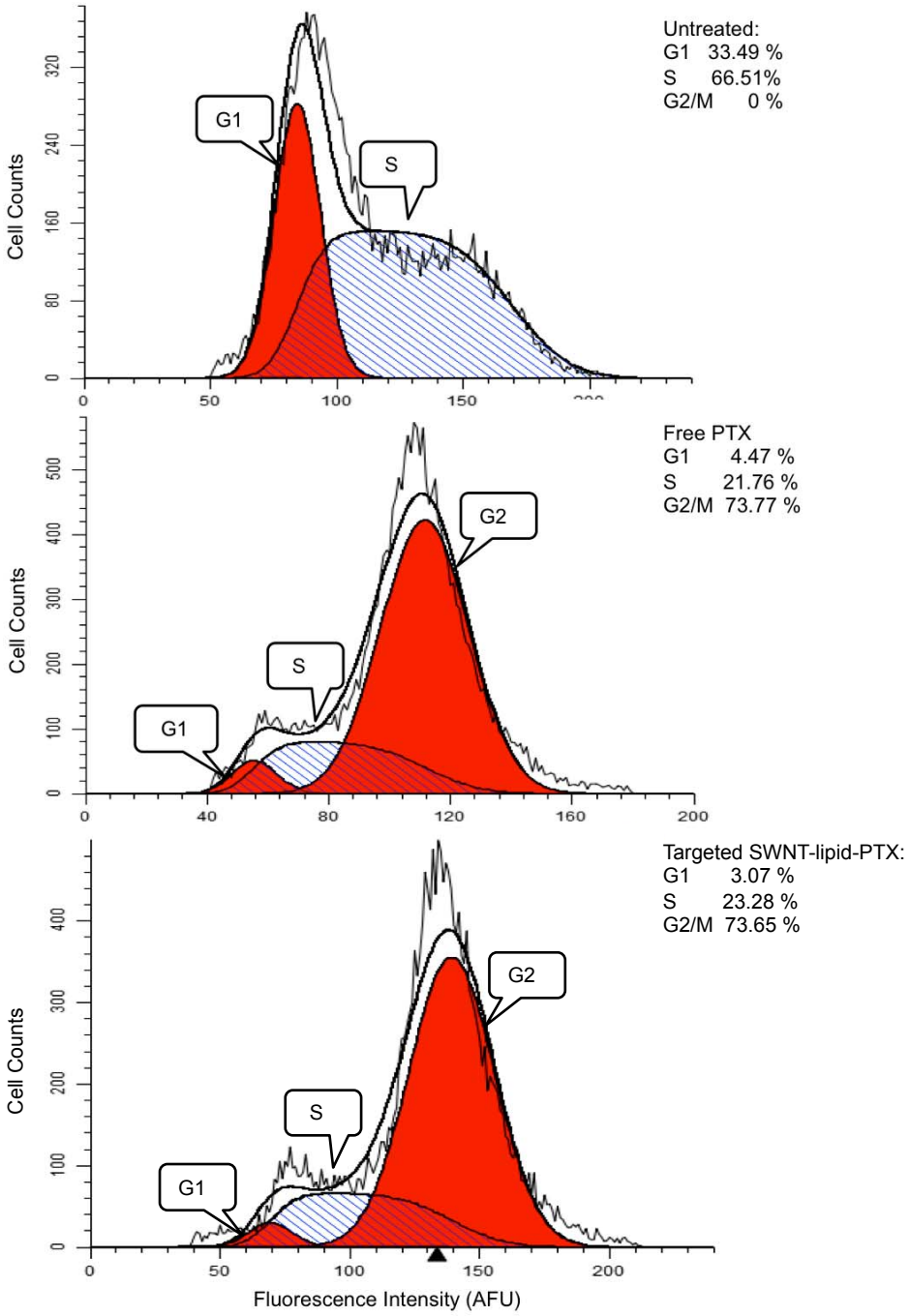

Figure 6.5 Cell cycle analysis of MCF-7 cells treated with targeted SWNT-lipid-PTX

Cells were treated with 20 nm Taxol and targeted SWNT-lipid-PTX respectively for 48 h. Cell cycle was analyzed by flow cytometry using PI staining of DNA contents. The percentage of cells in the different cell cycle phases was estimated using ModFit LT 3.3.11 cell cycle analysis software. Both PTX formulations induced similar level of cell cycle G1 arrest in MCF-7 cells (4.47% for Taxol and 3.07% for SWNT-lipid-PTX *vs*. 33.49% in untreated control).

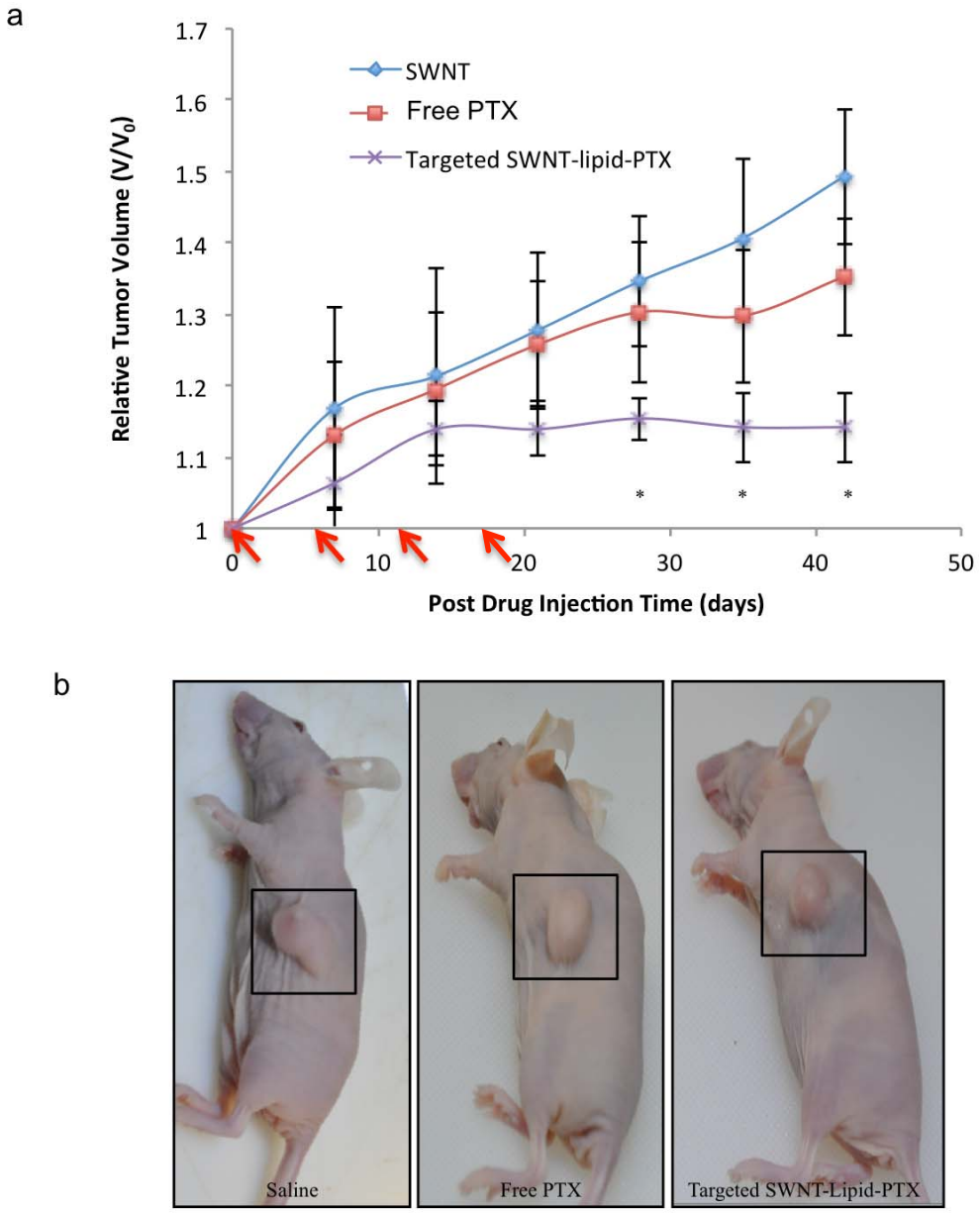

Figure 6.6 Tumour growth inhibition of targeted SWNT-lipid-PTX in MCF-7 xenograft breast cancer mice model

(a) Growth curve of tumors in MCF-7 tumor-bearing mice. Female athymic mice bearing s.c. inoculated MCF-7 tumors were injected with saline ($n = 8$), Taxol ($n = 7$), targeted SWNT-lipid-PTX ($n = 8$) at dosage of 5 mg/kg on day 0, 6, 12, 18. At post drug injection day 42, the relative tumor volume (V/V_0) were 1.49 $\pm$ 0.10, 1.35 $\pm$ 0.08 and 1.14 $\pm$ 0.05 for saline, Taxol and targeted SWNT-lipid-PTX respectively. The targeted SWNT-lipid-PTX showed significantly decreased tumor volume compared to both saline group and Taxol treated groups (*$p < 0.05$) (b) Photos of representative tumor-bearing mice from control and treatment groups at experimental end point. Tumors were indicated within black squares.

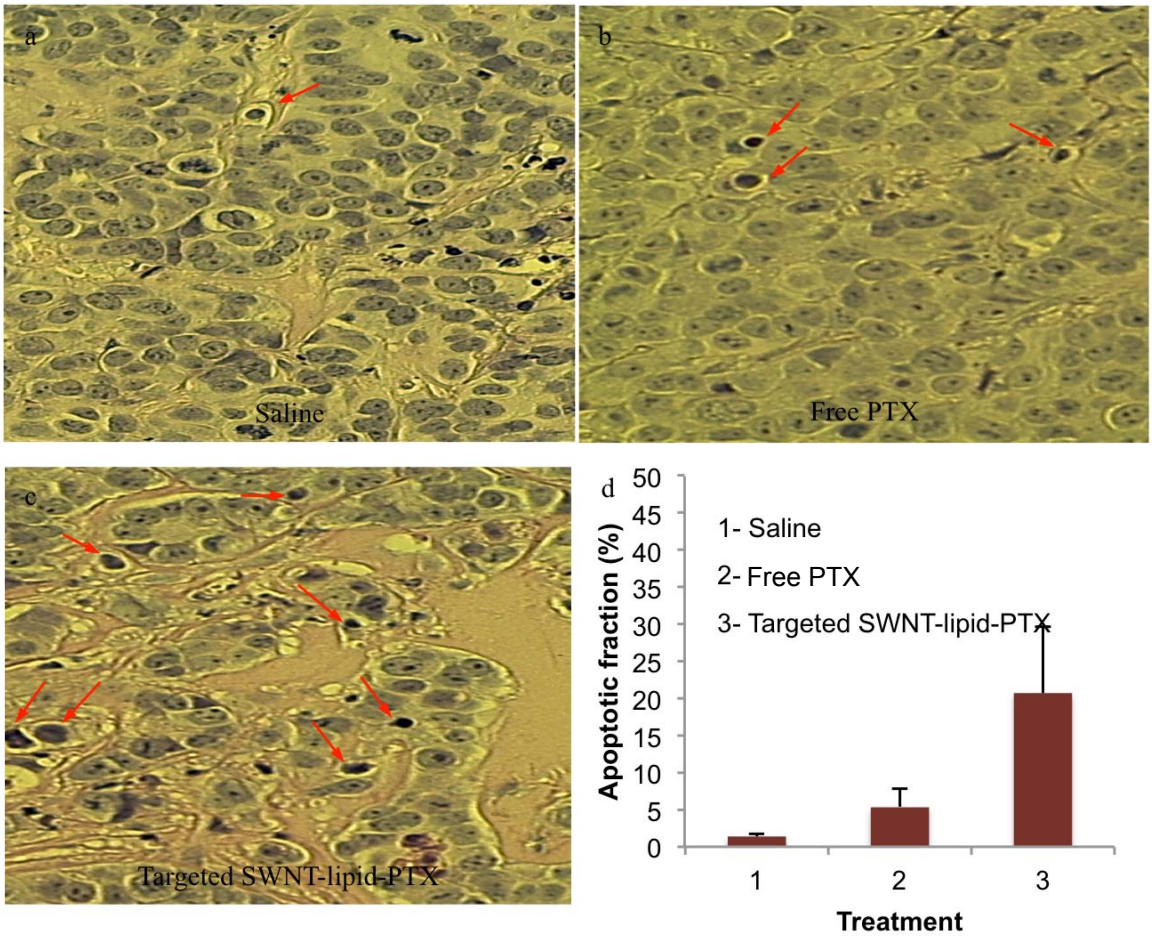

Figure 6.7 Morphologic changes and level of apoptosis in tumour tissues examined by H&E staining

Representative microscopic images of H&E staining of mice tumor tissues in (a) saline (b) Taxol and (c) targeted SWNT-lipid-PTX treatment groups. Mice tumors were excised on day 3 after last drug injection. H&E staining was performed to examine morphologic changes and the level of apoptosis in tumors. Apoptosis cells (indicated in black arrows) displayed characteristics of nuclei condensation, membrane blebbing, etc. (d) apoptotic cell fraction. Viable and apoptotic cells in H&E staining were counted under microscope field at 400× magnification. Apoptotic cell fraction was calculated. The tumors in saline group showed 1.3 ± 0.6% apoptosis. Taxol significantly increased apoptosis fraction to 5.4 ± 2.4% ($p < 0.05$). The targeted SWNT-lipid-PTX further increased the apoptotic fraction to 20.7 ± 9.2% ($p < 0.05$).

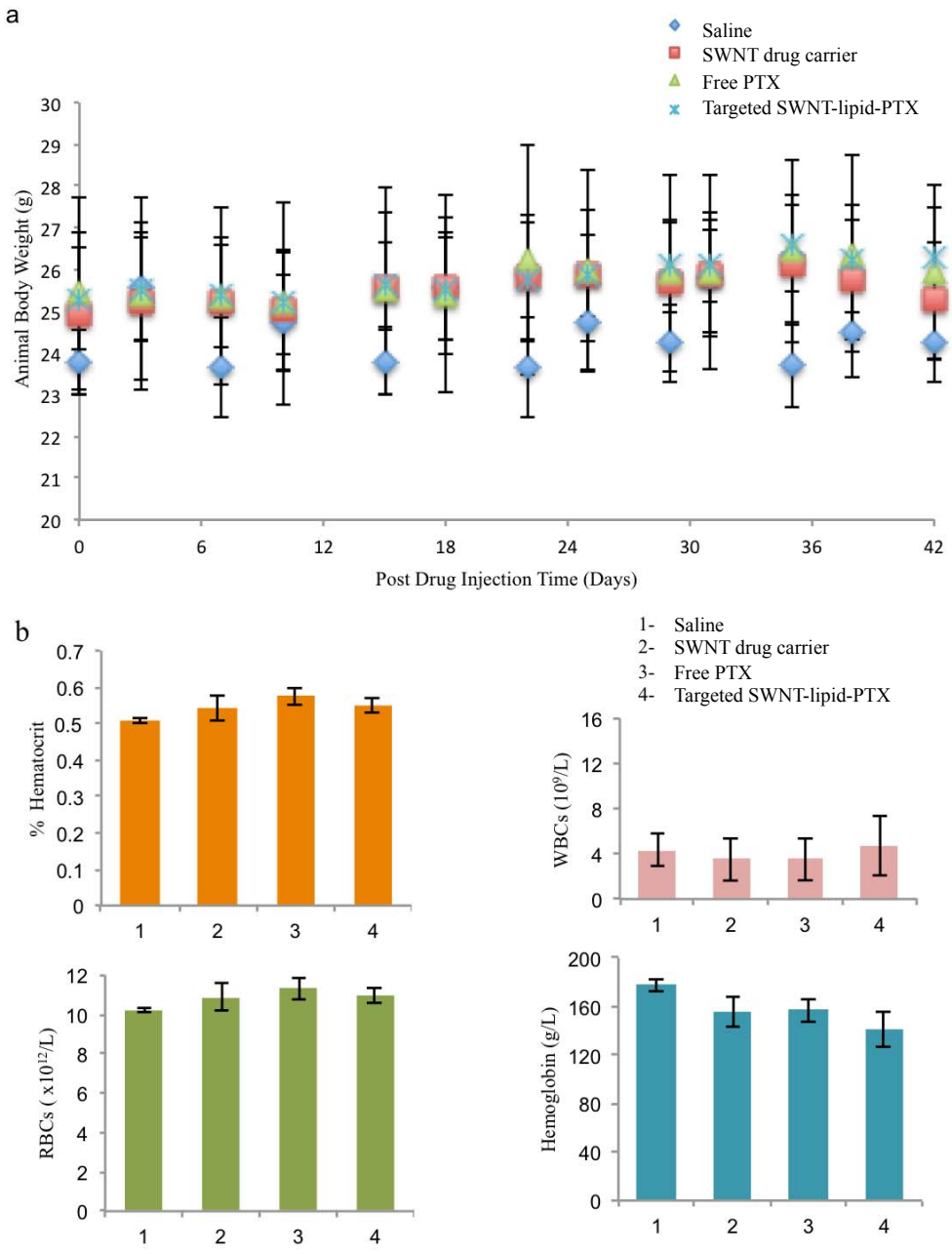

Figure 6.8 *In vivo* toxicity of SWNT-lipid-drug

(a) Toxicity examined by body weight. Female athymic mice were injected with saline ($n = 8$), SWNT drug carrier ($n = 3$) and Taxol ($n = 7$) and targeted SWNT-lipid-PTX ($n = 8$). The body weight of mice was monitored during the study period of 42 days. No significant differences in body weight were detected between test groups and control groups ($p < 0.001$) (b) Toxicity examined by hemotologic analysis. Blood was collected by cardiac puncture at experimental end point (post drug injection day 42). Hematologic parameters, including hematocrit, white blood cell count (WBC), red blood cell count (RBC) and hemoglobin were analyzed. The result showed no significant differences detected between test groups and control group ($p < 0.05$).

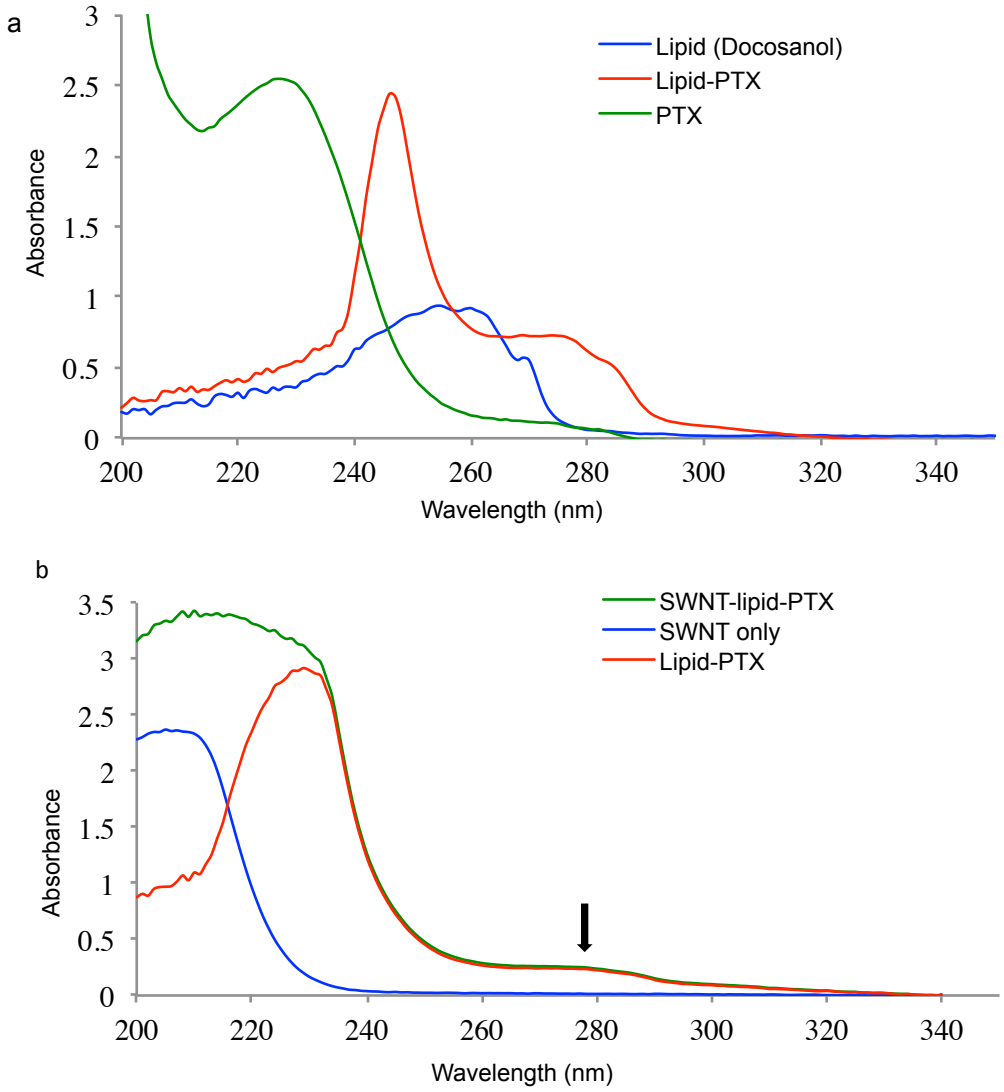

Figure S6.1 UV spectra of PL-PEG functionalized SWNT (SWNT-PL-PEG) and lipid-PTX loaded of SWNT-PL-PEG

(a) Characteristic peaks of lipid-PTX (red curve), lipid docosanal (blue curve) and PTX (green curve). Lipid-PTX showed characteristic absorbance peaks at 245 nm and 278 nm, which corresponded to lipid docosanol-COOH and PTX respectively, but with a slight shift due to the covalent bonding in between (red curve). (b) UV-NIR spectra of SWNT-PL-PEG before (blue curve) and after loading of lipid-PTX (green curve). The spectrum of lipid-PTX was obtained by subtracting the SWNT-PL-PEG spectrum from the lipid-drug loaded SWNT-PL-PEG spectrum (red curve). The absorbance peak of lipid-PTX at 245 nm was distorted, but the absorbance peak at 278 nm was maintained (indicated with a close arrow). The loading amount of lipid-PTX on SWNT-PL-PEG was calculated based on absorbance at 278 nm.

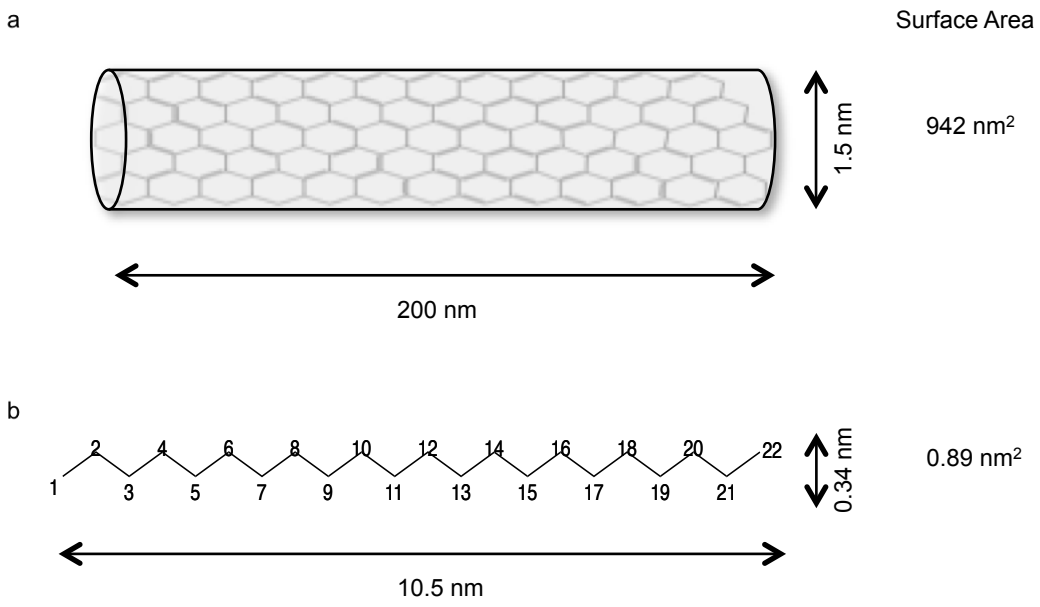

Figure S6.2 Estimation of lipid-PTX coverage on SWNT

(a) Estimation of the surface area of SWNT (b) estimation of the size of lipid chain of lipid-PTX. The total surface area for one SWNT nanotube was 942 nm^2 by assuming the average size of SWNT being 200 nm in length and 1.5 nm in diameter. The size of the lipid chain of lipid-PTX was estimated by Chem 3D software as 0.89 nm^2. Based on the result for number of lipid-PTX molecules attached to one SWNT molecule (ranged from 600 to 1000), the coverage of lipid-PTX on SWNT was calculated as 57 ～ 94% v/v.

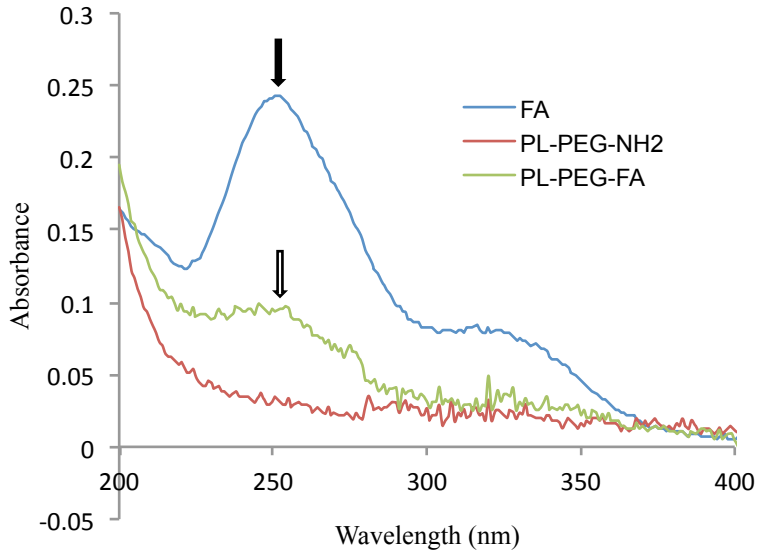

Figure S6.3 Chemical synthesis of targeted lipid-polymer PL-PEG-FA

(a) Scheme of chemical synthesis of PL-PEG-FA (b) examination of synthesis of PL-PEG-FA by UV-NIR scan Spectrometry. Targeting ligand folic acid (FA) was conjugated to amino end group in PL-PEG-NH_2 via amide bonding using EDC. After conjugation, the product was dialyzed to remove excess FA. FA presented a peak at 255 nm (indicated with a close arrow), whereas PL-PEG presented no peak at this position. After conjugation of FA to PL-PEG, a peak appeared at 255 nm (indicated with a open arrow) confirming the success of the conjugation.

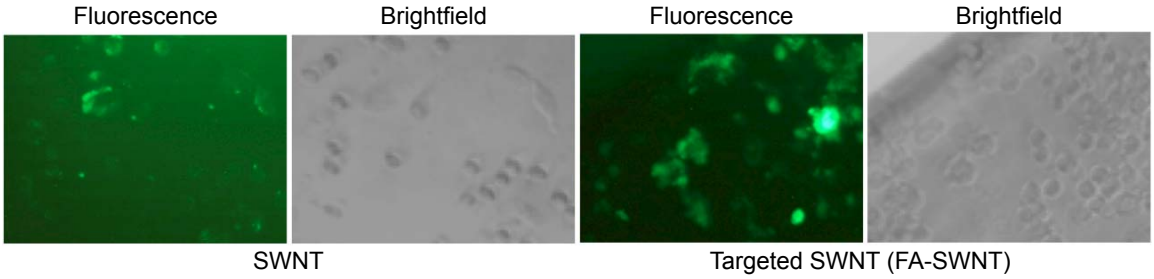

Figure S6.4 Intracellular drug delivery efficiency of SWNT drug carrier examined by cell internalization assay

MCF-7 cells incubated with 5 μg/mL of fluorescent dye FITC labelled SWNT or targeted SWNT (FA-SWNT), respectively. After 24 hrs of incubation, the cells were washed and observed under fluorescence microscope. The intracellular drug delivery efficiency was evaluated by counting the percentage of the cells uptaking the fluorescent dye. The percentages were 80 ± 2, % and 95 ± 2.5% (mean ± s.d, n = 5) for SWNT and targeted SWNT respectively. Moreover, by comparing the fluorescence intensity of a single cell, the cells treated with targeted SWNT were much brighter.

CHAPTER 7 GENERAL DISCUSSION

Chemotherapy is widely used as an adjuvant therapy for breast cancer. Widespread use of chemotherapy therapy in breast cancer has led to an improvement in survival. However, chemotherapy drugs are limited by their nonspecificity to cancer cells, as they target common cellular functions, such as DNA synthesis, mitosis and others, as summarized in **table 2.1**. Thus, these drugs cause damages in both cancer cells and normal cells that undergo rapid division. Conventional chemotherapy drugs distribute throughout the body; therefore, cause severe side effects. For example, drug PTX exhibits many side effects such as leucocytopenias, alopecia, and diarrhea and peripheral neuropathies, etc [148]. In addition to systematic side effects of PTX, the use of Cremophor EL for delivery due to the poor water-solubility of PTX causes hypersensitivity reactions [3, 4]. Nanoparticle formulations have been developed to replace the toxic delivery vehicle and to reduce the off-target toxicity. To date, a dozen of nanoparticle formulations for chemotherapy drugs have been approved for market, such as HSA nanoparticle formulated PTX (Abraxane®), liposomal DOX nanoparticles, and others [8]. It is evident that the nanoparticle therapeutics becomes an emerging modality for cancer.

CNT, a new type of synthetic nanomaterial, offers opportunities for chemotherapy drug delivery. CNT is superior to other types of nanoparticles in that the functionalized CNT is able to evade the endosomal compartment and translocate directly into the cytoplasm of different types of cells [12], which is useful for intracellular delivery of therapeutically active molecules. Large surface area of CNT allows loading large amounts of therapeutics, including a variety of small molecule drugs [177], siRNA [106], contrast agents [129], targeting or therapeutic antibodies [104], peptides [177] and proteins [178] to be loaded. In addition, the intrinsic optical and thermal properties CNT allow the development of CNT-based multifunctional drug carriers for simultaneous detection, diagnosis and treatment [60, 97, 102, 103, 141].

The initial hurdle of biomedical applications of CNT has been its hydrophobicity. It is critical to prepare well-dispersed CNT in aqueous solutions prior to the biomedical applications. Importantly, the functionalized CNT should sustain in physiologic

conditions, so as to prevent CNT agglomeration *in vivo*. Noncovalent functionalization of CNT with biocompatible polymers is an effective way to prepare well-dispersed CNT, and to improve their accessibility for further biomedical applications, as discussed in literature review (section 2.5.1). For the aimed drug delivery applications, we have firstly evaluated non-covalent functionalization of SWNT using various biocompatible polymers. Of the polymer tested, three types of polymers were able to well disperse SWNT in aqueous solutions, namely, PL-PEG, PS-b-PAA and CHI. As present in chapter 3, the three types of polymer-functionalized SWNT were compared in terms of dispersibility and stability, etc. We found that CHI displayed higher SWNT-dispersing capacity than PL-PEG-NH_2 and PS-b-PAA. However, in high concentration, the SWNT-CHI was less stable than the other two SWNT-polymers in salt containing solutions. All the three SWNT-polymers were able to penetrate cancer cells. Taking together, these SWNT-polymers, especially SWNT-PL-PEG and SWNT-PS-b-PAA, possess good biocompatibility, stability and excellent intracellular drug delivery capacity, and therefore, they are suitable for drug delivery applications.

On the other hand, although CNT contains large surface area for potential loading large amounts of drugs, the planar honeycomb lattice of sp^2 hybridized carbon atoms with no functional group present on CNT surface renders difficulty of loading drugs to this pre-formed CNT macromolecular structure, Currently, various methods have been developed for loading chemotherapy drugs to CNT. These methods include filling drugs inside of nanotubes, adsorption of drugs on CNT sidewall or covalent conjugation of drug molecules to CNT or CNT-dispersing polymers, as listed and discussed in **table 2.4**. Among all these methods, adsorption method offers high drug-loading capacity since the polymer-coated CNT still exists large uncoated surface area that could be used for adsorption of aromatic molecules [113]. Previous studies have shown that large amounts of DOX were loaded to SWNT for delivery by this method [113, 120, 177, 179-181]. However, this method is only suitable for drugs containing flat aromatic rings. For the drugs with bulky structure, *e.g.* PTX, no effective CNT-drug loading method is available. This study, in part, aimed to develop a more effective CNT-based delivery system for PTX.

In this thesis, three new schemes (denoted as **SWNT-HSA-PTX** and **SWNT-polymer-PTX, SWNT-lipid-PTX** respectively) have been designed for CNT-based delivery of PTX for treatment of breast cancer. Their advantages and limitations are discussed below.

In **SWNT-HSA-PTX** scheme, HSA was used as media for PTX loading utilizing its high binding affinity to PTX [7]. In addition, being an abundant protein present in blood, HSA coating could prevent elimination of SWNT-drug by immune system. Previously, HSA nanoparticle has been used for formulating with PTX (Abraxane®) and its clinical application has shown reduce the side effects [150]. However, pharmacokinetic studies showed that the clinical benefit from Abraxane might not due to the expected nanoparticle functioning, such as, improved pharmacokinetics and tumour targeting, etc. [5, 149, 150]. The SWNT-HSA-PTX scheme combines the HSA nanoparticle PTX with intracellular drug carrier SWNT. We have shown intracellular drug delivery capacity of the SWNT-HSA-drug carrer. *In vitro* study has shown better drug efficacy of SWNT-HSA-PTX than the PTX formulated with cross-linked HSA nanoparticle alone as tested in MCF-7 breast cancer cells. It was expected that SWNT-HSA-PTX could gain more benefits in terms of tumour-targeting by EPR effect and intracellular drug delivery than the clinical HSA nanoparticle PTX formulation. However, further *in vivo* study is required to investigate full potential of this scheme.

In the scheme of **SWNT-polymer-PTX**, polymer-drug approach was applied for construction of SWNT-based PTX. Polymer-drug approach is to covalently conjugate drugs to polymers *via* reversible linkers. This approach was first proposed in by Ringsdorf in the mid-1970 [52], further developed pre-clinically in the 1980s [182] and entered clinical pipeline in the 1990s [53]. Several polymer-PTX conjugates have been developed, such as PG-PTX, HMPA-PTX and others [53]. These Polymer-PTX conjugates were originally developed for removal of toxic delivery vehicle of PTX, Cremophor EL. Interestedly, the polymer-PTX conjugates have shown improved the plasma pharmacokinetics and tumour accumulation in experimental animal models [183]. PTX contains a reactive –OH group that can be linked to –COOH containing polymers

via ester bond. However, the polymer-conjugated PTX is inactive and the release of active PTX from the drug-carrying polymers is required [53]. The drug activation is through cleavage of the polymer-PTX by enzyme carboxylesterase [184], which is present in both cytosol and endoplasmic reticulum [184] of many types of cells including human tumours [185, 186]. Most polymer-PTX prodrugs are not cell permeable [53], which could limit their drug efficacy. Additional strategies that enable cell internalization of the polymer-PTX conjugates could allow exposure of the prodrugs to the activation enzymes, and therefore, could further enhance their antitumour drug effects. The SWNT-polymer-PTX scheme combines intracellular drug carrier SWNT with the polymer-PTX conjugates, which could allow intracellular delivery of the polymer-drug conjugates. We have also shown that the SWNT-polymer-PTX was functional *in vitro* using breast cancer cells, suggesting that the active PTX were released by enzymes present in breast cancer cells.

In **SWNT-lipid-PTX** scheme, PTX was modified by adding a "lipid tail" (a long chain lipid) *via* covalent conjugation. Such a drug modification was previously developed by Ansell *et al* in order to incorporate PTX better into micellar and lipophilic nanoparticles [157]. They have shown that the lipid-PTX was functional *in vivo,* and led to prolonged drug circulation half-life in experimental animal models. In our study, this lipid-drug was applied for facilitating drug loading to SWNT sidewall through its lipid-tail. Previously, PTX has been conjugated to SWNT dispersing polymer PL-PEG for delivery [167]. However this method is limited by drug-loading capacity because the coating ratio of PL-PEG on SWNT was low (~3 PL-PEG per 10 nm of SWNT) [113]. In addition, conjugation of hydrophobic drugs to CNT-dispersing polymers led to decreased blood circulation time [167]. Moreover, when the distal end of the polymer was occupied by the drug molecule, there was no space for targeting molecules [118]. In contrast, the lipid-drug approach developed in our study allows full utilization of different partitions of the SWNT-based drug carrier: CNT sidewall and the end of CNT-dispersing polymers. With the lipid-drug loaded onto nanotube sidewalls, the polymer end could be used for linking tumour targeting molecules or other functionalities. The lipid-drug scheme could

also be used for CNT-based for delivery of other types chemotherapy drugs by choosing alternative chemical synthesis approaches, as suggested in section of Recommendations.

As a new type of nanomaterial, CNT has demonstrated great promise in biomedical applications, especially in field of cancer therapy [91]. The studies in this thesis and from other research groups have shown tumour growth inhibition by CNT-based chemotherapy PTX [118, 187]. However, the lack of comparisons with clinical applied nanoparticles formulations, such as HSA-nanoparticle PTX (Abraxane ®) [188], or PG-PTX conjugates (CT-2103) [158] in the most studies limits the determination of the advantages of CNT over other existing technologies. Further work is needed to elucidate the true benefits of CNT over other types of well-established nanoparticle formulations.

Lastly, compared with clinical applied nanomaterials, such as liposomes, HSA nanoparticles, or some emerging types of nanocarriers that are derived from natural biological materials, *eg.* virus-like particles (VLPs) [189], the non-biodegradable nature of CNT raises the concern of long-term toxicity of CNT. Therefore, it is needed to clarify the overall toxicity profile of CNT, especially in animal models with specific mechanism under consideration, particularly in comparison with known toxins and other nanoparticle types.

CHAPTER 8 SUMMARY OF OBSERVATIONS AND CLAIMED ORIGNAL CONTRIBUTIONS TO KNOWLEDGE

8.1 Summary of observations

8.1.1 Design and preparation of SWNT for use in biomedical applications

The as-grown CNT is highly hydrophobic, which is the initial hurdle for the use of CNT in drug delivery. Non-covalent functionalization of CNT with certain polymers that contain amphiphilic properties is an effective way to disperse CNT in aqueous solutions. Three groups polymers, the lipid-polymers, amphiphilic block polymers, and polymers that display helical structure, *e.g.* polysaccharide or DNA, could attach to CNT *via* different manner of CNT-polymer interactions, such as Van de Waal force, π-stacking force, and hydrophobic interaction, etc. In our study, polymers PL-PEG, PS-b-PAA and CHI, are chosen from the above-mentioned three groups of polymers respectively for non-covalent functionalization of SWNT. We have shown that functionalization of SWNT with these polymers renders good SWNT dispersibility. All the three types of polymer-coated SWNT were stable in water, however, high concentration of SWNT-CHI (>100 μg/ml) could form aggregation in PBS and cell culture media, which might be related to different stabilization mechanism. The polymer-coating ratio in SWNT-PS-b-PAA was much higher than those in SWNT-PL-PEG and SWNT-CHI. With different level of polymer-coating ratio, the functionalized SWNT might be suitable for different drug delivery applications. For example, For PL-PEG functionalized SWNT, because of comparatively low level of polymer-coating ratio, large uncoated surface area on SWNT still exists, the PL-PEG functionalized SWNT is suitable for loading drugs directly onto SWNT sidewalls for potential drug delivery applications; whereas, with high level of polymer-coating ratio in SWNT-PS-b-PAA, high drug loading capacity could be achieved by conjugation of the drug molecules to SWNT-coating polymers for delivery. *In vitro* evaluation using MCF-7 cells has showed that all the three types of polymer-functionalized SWNT are able enter cancer cells in high efficiency.

8.1.2 HSA nanoparticle functionalized SWNT for intracellular delivery of PTX

The SWNT-based drug carrier displayed high intracellular delivery efficiency (percentage of cell uptake > 80 %) in breast cancer MCF-7 cells, which suggested that the needle-like SWNT-HSA drug carrier was able to transport drugs across cell membrane despite its macromolecular structure. The PTX formulated with SWNT-HSA showed higher growth inhibition in MCF-7 breast cancer cells than the PTX formulated with HSA nanoparticle only (cell viability of 53% *vs.* 62% with 72 hrs of drug incubation). The increased drug efficacy could be driven by SWNT-mediated cell internalization. These data suggest that the developed SWNT-based PTX is functional. However, more studies for *in vivo* drug delivery efficacy and other properties are needed to examine the full potential of the SWNT-HSA-PTX.

8.1.3 Polymer-drug approach for construction of SWNT-polymer-PTX

Polymer-drug conjugates have been previously applied for delivery of PTX so as to improve biodistribution or to overcome hydrophobicity of PTX. In this study, PTX was grafted to an amphiphilic polymer PS-b-PAA in first step, and then used for SWNT functionalization. Characterization with TEM and TGA revealed the PS-b-PAA coating ratio on SWNT was ~18 polymer molecules per 10 nm SWNT, which is much higher than other types of polymers, *e.g.* PL-PEG (~3 PL-PEG molecules per 10 nm SWNT). It was found that two PTX molecules could be grafted in each PS-b-PAA molecule, with which, the PTX-loading ratio in SWNT-PS-b-PAA-PTX was estimated to be ~36 PTX molecules per 10 nm of SWNT. *In vitro* study using MCF-7 breast cancer cells demonstrated that SWNT-polymer-PTX could induce severe nuclear condensation – a typical drug effect of PTX, suggesting that the SWNT-polymer-PTX was functional upon its cellular entry.

8.1.4 Novel lipid-drug approach for SWNT-based targeted delivery of PTX

PTX was successfully conjugated to a long chain lipid docosanol for loading to SWNT. High level of drug loading capacity onto SWNT was achieved by the lipid-drug

approach. Further more, targeted SWNT-lipid-PTX was made by conjugation of a tumour-targeting molecule FA to the PL-PEG. Conjugation of FA to SWNT-lipid-PTX led to an increase in cell penetration capacity, and targeted SWNT-lipid-PTX showed much improved drug efficacy *in vitro* in comparison to Taxol (PTX dissolved in surfactant Cremophor EL) and non-targeted SWNT-lipid-PTX (78.5% vs. 31.6% and 59.1 % respectively in cytotoxicity at 48 hrs, $p < 0.01$). *In vivo* study using a human breast cancer xenograft mice model showed an average relative volume (V/V_0) of 1.49 ± 0.10, 1.35 ± 0.08 and 1.14 ± 0.05 on day 42 for saline, PTX and targeted SWNT-lipid-PTX groups respectively. Compared with control group, the treatment groups displayed significantly higher tumour inhibition at day 42 (9.0% for PTX *vs.* 23.5% for targeted SWNT-lipid-PTX respectively $p < 0.001$) (Fig. 6.6). The *in vivo* drug efficacy was also confirmed by apoptotic cell fractions in tumour tissue (1.3± 0.6%, 5.4 ± 2.4% and 20.7± 9.2% for saline, PTX and targeted SWNT-lipid-PTX respectively). Biochemical analysis using blood samples and histological analysis of major organs conformed that the SWNT-lipid-PTX did not show obvious toxicity in treated animals.

8.2 Claims to original contributions

8.2.1 Design and development of lipid-drug approach for construction of SWNT based, targeted PTX delivery system

1. A novel lipid-drug approach has been proposed for construction of SWNT-based drug delivery system.

2. An effective SWNT-lipid-PTX delivery system has been developed using lipid docosanol conjugated PTX. Its application has been demonstrated *in vitro* and *in vivo.*

3. A targeted SWNT-lipid-PTX has been made by conjugation of FA to polymer PL-PEG. Conjugation of FA to the SWNT-lipid-PTX has led to an increase in cell internalization capacity *in vitro* compared to the SWNT-lipid-PTX without FA.

4. The targeted SWNT-lipid-PTX has shown much improved drug efficacy *in vitro* in comparison to free drug PTX and the non-targeted SWNT-lipid-PTX (cytotoxicity of 78.5% *vs.* 31.6% and 59.1% at 48 hrs respectively, n= 3).

5. The targeted SWNT-lipid-PTX has shown significantly higher tumour inhibition in a breast cancer xenograft mice model (9.0% *vs.* 23.5% of tumour inhibition over untreated control for free PTX and targeted SWNT-lipid-PTX respectively, n= 8, $p < 0.001$).

6. The targeted SWNT-lipid-PTX did not cause obvious toxicity in major organs of the mice at treated concentration (5mg PTX/kg mice body weight).

8.2.2 Design and development of a HSA nanoparticle-conjugated SWNT based drug delivery system for PTX

7. A novel HSA nanoparticle-conjugated SWNT (SWNT-HSA-PTX) has been developed for delivery of PTX.

8. The SWNT-HSA drug carrier has demonstrated good stability and excellent intracellular drug delivery capacity.

9. The PTX formulated with SWNT-HSA showed higher growth inhibition in MCF-7 breast cancer cells than that with HSA nanoparticle only (cell viability of 53% *vs.* 62% with 72 hrs of drug incubation). The increased drug efficacy could be driven by SWNT-mediated cell internalization.

8.2.3 Design and development of polymer-drug approach for construction of SWNT based PTX delivery system

10. The amphiphilic block polymer PS-b-PAA has shown much higher polymer-coating ratio on SWNT compared to PL-PEG functionalized SWNT (~18 molecules of PS-b-PAA *vs.* ~3 molecules of PL-PEG per 10 nm of SWNT). The high polymer-coating ratio

is beneficial for drug loading scheme *via* conjugation of drug molecules to SWNT-coating polymers for delivery.

11. The PS-b-PAA functionalized SWNT has been shown to penetrate MCF-7 cancer cells, and therefore, the SWNT-PS-b-PAA is suitable as an intracellular drug carrier.

12. Two PTX molecules could be grafted to PS-b-PAA using chosen chemical synthesis scheme.

13. A new SWNT-polymer-PTX delivery system has been developed by functionalization of SWNT using drug-grafted amphiphilic block polymer PS-b-PAA.

14. The SWNT-polymer-PTX has been shown functional *in vitro* and could induce severe cellular damage in MCF-7 cells.

CHAPTER 9 RECOMMENDATIONS

The CNT study in this thesis as well as studies from others research groups have demonstrated great potential in the field of drug delivery for treatment of breast cancer and other drug delivery applications. However, further investigation is needed to be able to realize its full potential in clinical applications. This includes methods for CNT functionalization, toxicity study for absorption, metabolism and excretion of functionalized CNT, etc. In this section, I briefly summarize my recommendations with regards to future studies required to make this thesis observation cohesive, importantly, to extend the use of SWNT-drug schemes presented in this thesis to other drug delivery applications.

9.1 Investigation of SWNT-drug biodistribution and pharmacokinetics in breast cancer animal models

In general, nanoparticles are employed to provide protection and reduced renal clearance of small molecule drugs. By formulating with nanoparticles, longer drug circulation time is usually achieved, which would lead to enhanced bioavailability of delivered drugs in tumour sites. In the lipid-drug approach (presented in chapter 6), by applying both passive and active tumour-targeting strategies to the SWNT-based PTX delivery system, we have shown increased anti-tumour efficacy in a breast cancer animal model compared to free drug, however, the mechanism of enhanced therapeutic efficacy by this approach remains unrevealed. It is necessary to evaluate drug concentration in all major tissues following drug administration over a period of time until elimination phase. The pharmacokinetics and biodistribution of drug formulated SWNT would provide information to understand the mechanisms of targeting, drug release, degradation, as well as to predict side effects of SWNT-drugs.

9.2 Investigation of size effect of CNT on tumour penetrating and suppression efficacy

One problem of using CNT in drug delivery relates to the irregularity in its size, since the diameter of CNT could vary from less than 1 nm to several nm and the length could span from 10 nm to μm. As we know, application of nanoparticles for cancer therapy employs the favorable size of the nanoparticles for leaking into tumour vasculature by EPR effect. As presented in this thesis, the *in vivo* study with H&E staining of tumour tissues has clearly demonstrated apoptotic cells inside of tumours treated by SWNT-drugs (Fig. 6.7), and the studies from other groups have also revealed that the SWNT-based drugs could penetrate blood vessels and enter tumour vasculature [118]. However, *in vivo* tumour inhibition effect achieved in these studies just represents the overall targeting efficacy of the CNT-drug carriers with a broad distribution of sizes. Furthermore, except tumour blood vessel wall, many other barriers present in tumour microenvironment, which include low interstitial pressure, low extracellular pH and central hypoxia region, etc [190]. These barriers prevent therapeutic agents from diffusing deeper into tumour tissues. The huge variation in the size of CNT could possibly counteract their effect in overcoming these barriers. Thus, it is important to examine the size, especially the length, effect of CNT on tumour-targeting efficacy. However, the available synthesis methods cannot produce homogeneous CNT by precise control of sizes. One solution to obtain homogeneous CNT is through separation technique. Currently, various separation methods have been investigated for sorting CNT by the size and length, which include size exclusion chromatography [191], capillary electrophoresis [192], and flow-flow fractionation [193] and others. In future study, it is worth exploring systematically size effect of CNT on efficacy of targeted drug delivery in cancer therapy.

9.3 Further investigation of lipid-drug approach as a generalized method for CNT-based delivery of other chemotherapy drugs

The lipid-drug approach presented in this thesis is developed for targeted delivery of PTX (chapter 6). This approach could be applied for CNT-based delivery of other chemotherapy drugs, since, similar to PTX, most chemotherapy drugs are small molecules that contain reactive functional groups, such as -COOH, $-NH_2$ or -OH, etc. By choosing alternative chemical synthesis schemes, different chemotherapy drugs can be

conjugated to long chain lipids to form lipid-drugs. For example, drug DOX comprises an -NH_2 that can be conjugated to -COOH containing lipid *via* amidation reaction; drug MTX contains a reactive –COOH group that can be linked to a lipid alcohol *via* ester formation; drug 5-FU could be linked to a lipid alcohol through its intermediate acid derivative 5-FU-1-acetic acid, which is prepared from 5-FU and bromoacetic acid following a known method [194] (Fig. 9.1). Like lipid-PTX, the above-mentioned linkages between lipid and the drugs are cleavable, which ensure release of active drugs inside of cancer cells.

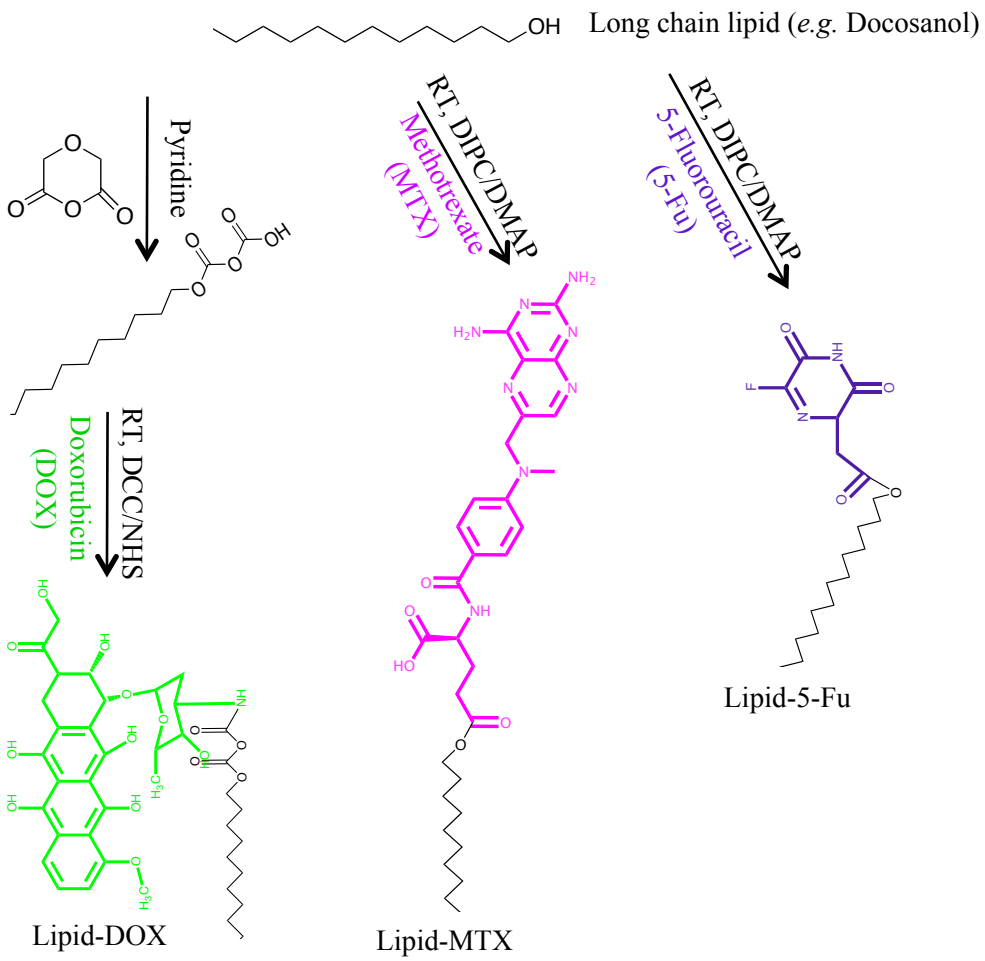

Figure 9.1 Examples of chemical synthesis schemes of lipid-drug conjugates

9.4 Investigation of lipid-drug approach for CNT-based combination therapy for breast cancer

Combination therapy is an effective way for treatment of breast cancer [195]. The use of chemotherapy drugs in combination with other breast cancer agents allows enhanced killing effect on cancer cells *via* different molecular pathways [196]. Several regimens of combination therapy for treatment of breast cancer have been well defined clinically [22]. For example, Trastuzumab, a monoclonal antibody against the extracellular domain of HER-2, has been shown to be active against HER-2-overexpressing metastatic breast cancer either as a single agent or used in combination with chemotherapy drugs. In preclinical models, Trastuzumab has shown additive and even synergistic anti-tumour activity with some active chemotherapeutic agents for treatment of breast cancer. Currently, Trastuzumab has been routinely combined with anthracycline, taxane and 5-Fluorouracil (5-FU) for treatment of HER-2 positive breast cancer [22], and the results have shown increased response rate and survival when compared to chemotherapy alone [22]. If formulating these agents in the same drug carrier, it could possible overcome the differences in pharmacokinetics and biodistribution of combined therapeutics [197], thus further increases treatment efficacy.

As illustrated in Fig. 9.2A, co-delivery of HER-2 antibody with one or more chemotherapy drugs could be realized in CNT-based delivery system using lipid-drug approach. For example, therapeutic HER-2 antibody Trastuzumab is conjugated to lipid-polymer PL-PEG-NH_2 for non-covalent functionalization of SWNT. By conjugation of different chemotherapy drugs, *e.g.* DOX, PTX, 5-FU etc., to the same type of long chain lipids respectively (Fig. 9.1and 9.2B), it is possible to load one or two types of lipid-drugs in combination of HER-2 antibody in the same CNT carrier for combination therapy (Fig. 9.2C).

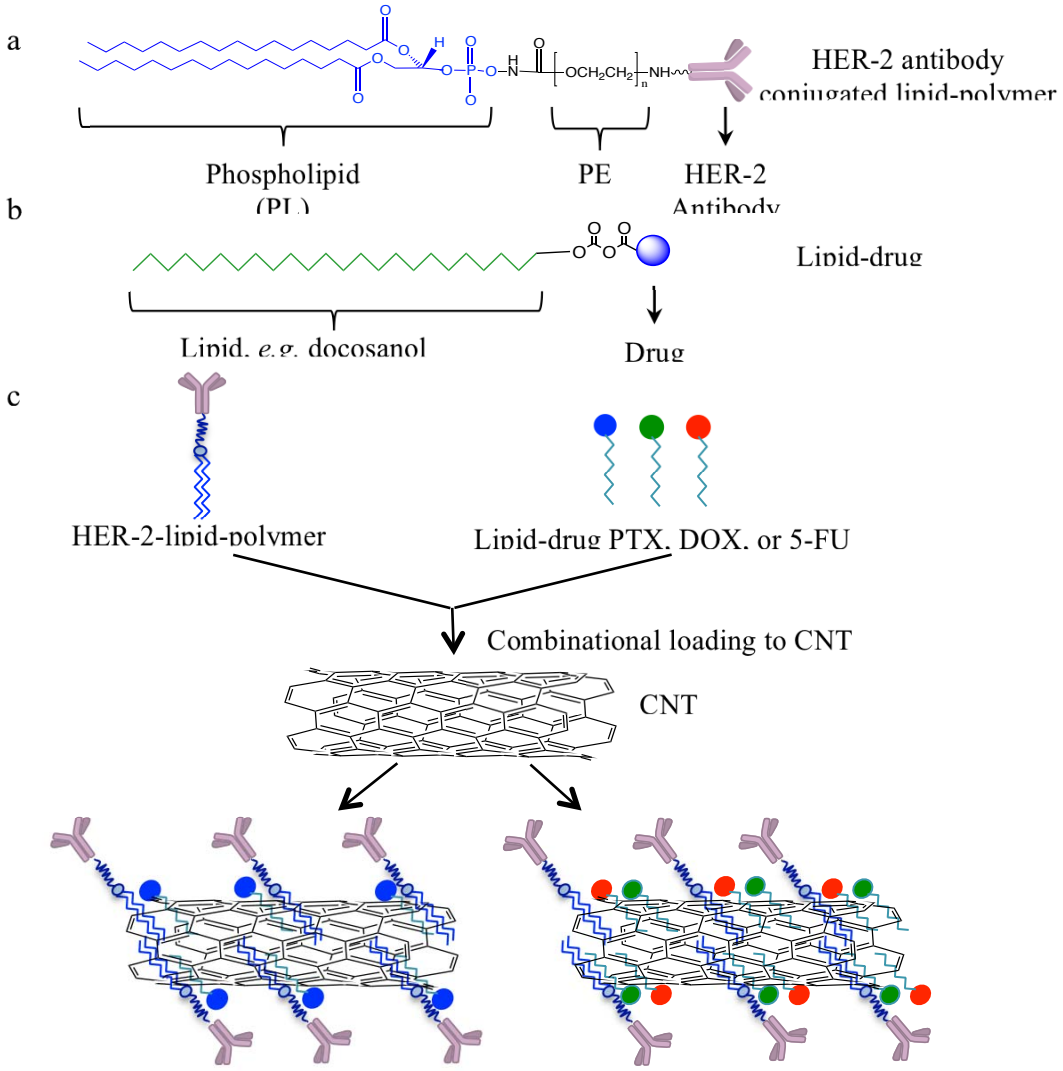

Figure 9.2 Schemes of carbon nanotube based HER-2 antibody therapy in combination of chemotherapy drugs for treatment of breast cancer

In summary, CNT holds great potential in breast cancer therapy and other biomedical applications due to its excellent features. This includes cell penetration capacity, ultrahigh surface area for loading multiple therapeutics for multifunctional drug delivery, and the intrinsic optical properties for detection and imaging, as well as for hyperthermia cancer therapy. The SWNT-drug delivery strategies developed and proposed in this thesis would definitely contribute to our knowledge to this new type of drug carrier. However, only after the uncertainty on CNT toxicity is resolved, the CNT-based therapeutics can be possibly applied clinically.

BIBLIOGRAPHY

[1] Lester J. Breast cancer in 2007: incidence, risk assessment, and risk reduction strategies. Clin J Oncol Nurs. 2007;11:619-22.
[2] Jemal A, Bray F, Center MM, Ferlay J, Ward E, Forman D. Global cancer statistics. CA: a cancer journal for clinicians. 2011;61:69-90.
[3] Tsavaris NB, Kosmas C. Risk of severe acute hypersensitivity reactions after rapid paclitaxel infusion of less than 1-h duration. Cancer Chemother Pharmacol. 1998;42:509-11.
[4] Sendo T, Sakai N, Itoh Y, Ikesue H, Kobayashi H, Hirakawa T, et al. Incidence and risk factors for paclitaxel hypersensitivity during ovarian cancer chemotherapy. Cancer Chemother Pharmacol. 2005;56:91-6.
[5] Davis ME, Chen ZG, Shin DM. Nanoparticle therapeutics: an emerging treatment modality for cancer. Nature reviews Drug discovery. 2008;7:771-82.
[6] Sutton D, Nasongkla N, Blanco E, Gao J. Functionalized micellar systems for cancer targeted drug delivery. Pharmaceutical research. 2007;24:1029-46.
[7] Kratz F. Albumin as a drug carrier: design of prodrugs, drug conjugates and nanoparticles. Journal of controlled release : official journal of the Controlled Release Society. 2008;132:171-83.
[8] Peer D, Karp JM, Hong S, Farokhzad OC, Margalit R, Langer R. Nanocarriers as an emerging platform for cancer therapy. Nature nanotechnology. 2007;2:751-60.
[9] Iijima S. Helical microtubules of graphitic carbon. Nature. 1991;354.
[10] M. M, V. K. Who should be given the credit for the discovery of carbon nanotubes? Carbon. 2006;44:1621-3.
[11] Shao W. PA, Prakash S. Carbon Nanotubes in Cancer and Stem Cell Therapeutics. Selective Topic in Nanomedicine, World Scientific. 2013.
[12] Kostarelos K, Lacerda L, Pastorin G, Wu W, Wieckowski S, Luangsivilay J, et al. Cellular uptake of functionalized carbon nanotubes is independent of functional group and cell type. Nature nanotechnology. 2007;2:108-13.
[13] Ando Y. Carbon nanotube: the inside story. Journal of nanoscience and nanotechnology. 2010;10:3726-38.
[14] Elnashar AT, Ali el SM, Gaber A. The prognostic value of triple negative in stage II/III breast cancer. Journal of oncology pharmacy practice : official publication of the International Society of Oncology Pharmacy Practitioners. 2012;18:68-75.
[15] Alberg AJ, Singh S, May JW, Helzlsouer KJ. Epidemiology, prevention, and early detection of breast cancer. Curr Opin Oncol. 2000;12:515-20.
[16] Breidenbach M, Rein DT, Schondorf T, Khan KN, Herrmann I, Schmidt T, et al. A new targeting approach for breast cancer gene therapy using the heparanase promoter. Cancer Lett. 2006;240:114-22.
[17] Goss R. Substrate specificity of the violaxanthin de-epoxidase of the primitive green alga Mantoniella squamata (Prasinophyceae). Planta. 2003;217:801-12.
[18] Winer EP, Hudis C, Burstein HJ, Bryant J, Chlebowski RT, Ingle JN, et al. American Society of Clinical Oncology technology assessment working group update: use of aromatase inhibitors in the adjuvant setting. J Clin Oncol. 2003;21:2597-9.

[19] Higgins MJ, Wolf AC. Adjuvant endocrine therapy for premenopausal hormone receptor-positive breast cancer; much done, more to do. Oncology (Williston Park). 2009;23:40, 2, 4.
[20] Castiglione-Gertsch M, O'Neill A, Price KN, Goldhirsch A, Coates AS, Colleoni M, et al. Adjuvant chemotherapy followed by goserelin versus either modality alone for premenopausal lymph node-negative breast cancer: a randomized trial. Journal of the National Cancer Institute. 2003;95:1833-46.
[21] Ganz PA, Greendale GA, Petersen L, Kahn B, Bower JE. Breast cancer in younger women: reproductive and late health effects of treatment. J Clin Oncol. 2003;21:4184-93.
[22] Montemurro F, Valabrega G, Aglietta M. Trastuzumab-based combination therapy for breast cancer. Expert opinion on pharmacotherapy. 2004;5:81-96.
[23] Li J, Gonzalez-Angulo AM, Allen PK, Yu TK, Woodward WA, Ueno NT, et al. Triple-negative subtype predicts poor overall survival and high locoregional relapse in inflammatory breast cancer. The oncologist. 2011;16:1675-83.
[24] Steponaviciene L, Lachej-Mikeroviene N, Smailyte G, Aleknavicius E, Meskauskas R, Didziapetriene J. Triple negative breast cancer: adjuvant chemotherapy effect on survival. Advances in medical sciences. 2011;56:285-90.
[25] Bergh J, Jonsson PE, Glimelius B, Nygren P. A systematic overview of chemotherapy effects in breast cancer. Acta Oncol. 2001;40:253-81.
[26] Minotti G, Menna P, Salvatorelli E, Cairo G, Gianni L. Anthracyclines: molecular advances and pharmacologic developments in antitumour activity and cardiotoxicity. Pharmacological reviews. 2004;56:185-229.
[27] Binks SP, Dobrota M. Kinetics and mechanism of uptake of platinum-based pharmaceuticals by the rat small intestine. Biochemical pharmacology. 1990;40:1329-36.
[28] Cheung-Ong K, Giaever G, Nislow C. DNA-damaging agents in cancer chemotherapy: serendipity and chemical biology. Chemistry & biology. 2013;20:648-59.
[29] Jordan A, Hadfield JA, Lawrence NJ, McGown AT. Tubulin as a target for anticancer drugs: agents which interact with the mitotic spindle. Med Res Rev. 1998;18:259-96.
[30] Kavallaris M, Verrills NM, Hill BT. Anticancer therapy with novel tubulin-interacting drugs. Drug Resist Updat. 2001;4:392-401.
[31] Eniu A, Palmieri FM, Perez EA. Weekly administration of docetaxel and paclitaxel in metastatic or advanced breast cancer. The oncologist. 2005;10:665-85.
[32] Ren Y, D'Ambrosio MA, Garvin JL, Wang H, Carretero OA. Possible mediators of connecting tubule glomerular feedback. Hypertension. 2009;53:319-23.
[33] Sun M, Lughezzani G, Perrotte P, Karakiewicz PI. Treatment of metastatic renal cell carcinoma. Nature reviews Urology. 2010;7:327-38.
[34] Menard-Moyon C, Kostarelos K, Prato M, Bianco A. Functionalized carbon nanotubes for probing and modulating molecular functions. Chemistry & biology. 2010;17:107-15.
[35] Cancer multidrug resistance. Nature biotechnology. 2000;18 Suppl:IT18-20.
[36] Ojima I. Guided molecular missiles for tumour-targeting chemotherapy--case studies using the second-generation taxoids as warheads. Accounts of chemical research. 2008;41:108-19.
[37] Lammers T, Hennink WE, Storm G. Tumour-targeted nanomedicines: principles and practice. British journal of cancer. 2008;99:392-7.

[38] Brigger I, Dubernet C, Couvreur P. Nanoparticles in cancer therapy and diagnosis. Adv Drug Deliv Rev. 2002;54:631-51.
[39] Cedervall T, Lynch I, Foy M, Berggard T, Donnelly SC, Cagney G, et al. Detailed identification of plasma proteins adsorbed on copolymer nanoparticles. Angew Chem Int Ed Engl. 2007;46:5754-6.
[40] Haag R, Kratz F. Polymer therapeutics: concepts and applications. Angew Chem Int Ed Engl. 2006;45:1198-215.
[41] van Vlerken LE, Vyas TK, Amiji MM. Poly(ethylene glycol)-modified nanocarriers for tumour-targeted and intracellular delivery. Pharmaceutical research. 2007;24:1405-14.
[42] Ruggiero A, Villa CH, Holland JP, Sprinkle SR, May C, Lewis JS, et al. Imaging and treating tumour vasculature with targeted radiolabeled carbon nanotubes. International journal of nanomedicine. 2010;5:783-802.
[43] Boyer JC, Manseau MP, Murray JI, van Veggel FC. Surface modification of upconverting NaYF4 nanoparticles with PEG-phosphate ligands for NIR (800 nm) biolabeling within the biological window. Langmuir. 2010;26:1157-64.
[44] Ke S, Wright JC, Kwon GS. Avidin-biotin-PEG-CPA complexes as potential EPR-directed therapeutic protein carriers: preparation and characterization. Bioconjug Chem. 2007;18:1644-50.
[45] Krauss WC, Park JW, Kirpotin DB, Hong K, Benz CC. Emerging antibody-based HER2 (ErbB-2/neu) therapeutics. Breast disease. 2000;11:113-24.
[46] Garanger E, Boturyn D, Dumy P. Tumour targeting with RGD peptide ligands-design of new molecular conjugates for imaging and therapy of cancers. Anti-cancer agents in medicinal chemistry. 2007;7:552-8.
[47] Lu Y, Low PS. Folate-mediated delivery of macromolecular anticancer therapeutic agents. Adv Drug Deliv Rev. 2002;54:675-93.
[48] Dosio F, Milla P, Cattel L. EC-145, a folate-targeted Vinca alkaloid conjugate for the potential treatment of folate receptor-expressing cancers. Curr Opin Investig Drugs. 2010;11:1424-33.
[49] Yezhelyev MV, Gao X, Xing Y, Al-Hajj A, Nie S, O'Regan RM. Emerging use of nanoparticles in diagnosis and treatment of breast cancer. The lancet oncology. 2006;7:657-67.
[50] Lotem M, Hubert A, Lyass O, Goldenhersh MA, Ingber A, Peretz T, et al. Skin toxic effects of polyethylene glycol-coated liposomal doxorubicin. Archives of dermatology. 2000;136:1475-80.
[51] Elbayoumi TA, Torchilin VP. Tumour-specific antibody-mediated targeted delivery of Doxil reduces the manifestation of auricular erythema side effect in mice. International journal of pharmaceutics. 2008;357:272-9.
[52] Ringsdorf H. Structure and properties of pharmacologically active polymer. J Polymer Sci Polymer Symp. 1975;51:135-53.
[53] Li C, Wallace S. Polymer-drug conjugates: recent development in clinical oncology. Adv Drug Deliv Rev. 2008;60:886-98.
[54] Zamboni WC. Liposomal, nanoparticle, and conjugated formulations of anticancer agents. Clinical cancer research : an official journal of the American Association for Cancer Research. 2005;11:8230-4.

[55] Gao X, Cui Y, Levenson RM, Chung LW, Nie S. In vivo cancer targeting and imaging with semiconductor quantum dots. Nature biotechnology. 2004;22:969-76.
[56] Thomas R, Park IK, Jeong YY. Magnetic iron oxide nanoparticles for multimodal imaging and therapy of cancer. International journal of molecular sciences. 2013;14:15910-30.
[57] Cai W, Gao T, Hong H, Sun J. Applications of gold nanoparticles in cancer nanotechnology. Nanotechnology, science and applications. 2008;1:17-32.
[58] Zhao M, Beauregard DA, Loizou L, Davletov B, Brindle KM. Non-invasive detection of apoptosis using magnetic resonance imaging and a targeted contrast agent. Nature medicine. 2001;7:1241-4.
[59] Yang L, Peng XH, Wang YA, Wang X, Cao Z, Ni C, et al. Receptor-targeted nanoparticles for in vivo imaging of breast cancer. Clinical cancer research : an official journal of the American Association for Cancer Research. 2009;15:4722-32.
[60] Keren S, Zavaleta C, Cheng Z, de la Zerda A, Gheysens O, Gambhir SS. Noninvasive molecular imaging of small living subjects using Raman spectroscopy. Proceedings of the National Academy of Sciences of the United States of America. 2008;105:5844-9.
[61] Jain S, Hirst DG, O'Sullivan JM. Gold nanoparticles as novel agents for cancer therapy. The British journal of radiology. 2012;85:101-13.
[62] Alexis F, Pridgen EM, Langer R, Farokhzad OC. Nanoparticle technologies for cancer therapy. Handbook of experimental pharmacology. 2010:55-86.
[63] Harris PJF. Carbon nanotubes and Related Structures. Cambridge University Press1999.
[64] Chen Z, Zhang X, Yang R, Zhu Z, Chen Y, Tan W. Single-walled carbon nanotubes as optical materials for biosensing. Nanoscale. 2011;3:1949-56.
[65] Bekyarova E, Itkis ME, Cabrera N, Zhao B, Yu A, Gao J, et al. Electronic properties of single-walled carbon nanotube networks. Journal of the American Chemical Society. 2005;127:5990-5.
[66] Kim JE, Lim HT, Minai-Tehrani A, Kwon JT, Shin JY, Woo CG, et al. Toxicity and clearance of intratracheally administered multiwalled carbon nanotubes from murine lung. J Toxicol Environ Health A. 2010;73:1530-43.
[67] Zhao X, Liu R. Recent progress and perspectives on the toxicity of carbon nanotubes at organism, organ, cell, and biomacromolecule levels. Environment international. 2012;40:244-55.
[68] Kagan VE, Tyurina YY, Tyurin VA, Konduru NV, Potapovich AI, Osipov AN, et al. Direct and indirect effects of single walled carbon nanotubes on RAW 264.7 macrophages: role of iron. Toxicology letters. 2006;165:88-100.
[69] O'Connell MJ, Bachilo SM, Huffman CB, Moore VC, Strano MS, Haroz EH, et al. Band gap fluorescence from individual single-walled carbon nanotubes. Science. 2002;297:593-6.
[70] Richard C, Balavoine F, Schultz P, Ebbesen TW, Mioskowski C. Supramolecular self-assembly of lipid derivatives on carbon nanotubes. Science. 2003;300:775-8.
[71] Kang Y, Taton TA. Micelle-encapsulated carbon nanotubes: a route to nanotube composites. Journal of the American Chemical Society. 2003;125:5650-1.
[72] Hu H, Zhao B, Itkis ME, Haddon RC. Nitric Acid Purification of Single-Walled Carbon Nanotubes. The Journal of Physical Chemistry B. 2003;107:13838-42.

[73] Tasis D, Tagmatarchis N, Georgakilas V, Prato M. Soluble carbon nanotubes. Chemistry. 2003;9:4000-8.
[74] Tasis D, Tagmatarchis N, Bianco A, Prato M. Chemistry of carbon nanotubes. Chemical reviews. 2006;106:1105-36.
[75] Tagmatarchis N, Prato M. Functionalization of carbon nanotubes via 1,3-dipolar cycloadditions. Journal of Materials Chemistry. 2004;14:437-9.
[76] Georgakilas V, Tagmatarchis N, Pantarotto D, Bianco A, Briand JP, Prato M. Amino acid functionalisation of water soluble carbon nanotubes. Chem Commun (Camb). 2002:3050-1.
[77] Kostarelos K. The long and short of carbon nanotube toxicity. Nature biotechnology. 2008;26:774-6.
[78] Prato M, Kostarelos K, Bianco A. Functionalized carbon nanotubes in drug design and discovery. Accounts of chemical research. 2008;41:60-8.
[79] Kostarelos K, Bianco A, Prato M. Promises, facts and challenges for carbon nanotubes in imaging and therapeutics. Nature nanotechnology. 2009;4:627-33.
[80] Sang Won Kim TK, Yern Seung Kim, Hong Soo Choi, Hyeong Jun Lim, Seung Jae Yang, Chong Rae Park. Surface modifications for the effective dispersion of carbon nanotubes in solvents and polymers. Carbon. 2012;50:30.
[81] Liu Z, Tabakman SM, Chen Z, Dai H. Preparation of carbon nanotube bioconjugates for biomedical applications. Nature protocols. 2009;4:1372-82.
[82] Park S, Yang HS, Kim D, Job K, Jon S. Rational design of amphiphilic polymers to make carbon nanotubes water-dispersible, anti-biofouling, and functionalizable. Chem Commun. 2008:2876-8.
[83] Petrov P, Stassin F, Pagnoulle C, Jerome R. Noncovalent functionalization of multi-walled carbon nanotubes by pyrene containing polymers. Chem Commun (Camb). 2003:2904-5.
[84] Chen RJ, Zhang YG, Wang DW, Dai HJ. Noncovalent sidewall functionalization of single-walled carbon nanotubes for protein immobilization. Journal of the American Chemical Society. 2001;123:3838-9.
[85] Kang YJ, Taton TA. Micelle-encapsulated carbon nanotubes: A route to nanotube composites. Journal of the American Chemical Society. 2003;125:5650-1.
[86] Zhang X, Meng L, Lu Q. Cell behaviors on polysaccharide-wrapped single-wall carbon nanotubes: a quantitative study of the surface properties of biomimetic nanofibrous scaffolds. ACS nano. 2009;3:3200-6.
[87] Jiang L, Liu C, Jiang L, Peng Z, Lu G. A chitosan-multiwall carbon nanotube modified electrode for simultaneous detection of dopamine and ascorbic acid. Analytical sciences : the international journal of the Japan Society for Analytical Chemistry. 2004;20:1055-9.
[88] Liu Y, Chipot C, Shao X, Cai W. Solubilizing carbon nanotubes through noncovalent functionalization. Insight from the reversible wrapping of alginic acid around a single-walled carbon nanotube. The journal of physical chemistry B. 2010;114:5783-9.
[89] Liu Y, Chipot C, Shao X, Cai W. Edge effects control helical wrapping of carbon nanotubes by polysaccharides. Nanoscale. 2012;4:2584-9.
[90] Zheng M, Jagota A, Semke ED, Diner BA, McLean RS, Lustig SR, et al. DNA-assisted dispersion and separation of carbon nanotubes. Nature materials. 2003;2:338-42.

[91] Liu Z, Cai W, He L, Nakayama N, Chen K, Sun X, et al. In vivo biodistribution and highly efficient tumour targeting of carbon nanotubes in mice. Nature nanotechnology. 2007;2:47-52.
[92] Yang ST, Fernando KA, Liu JH, Wang J, Sun HF, Liu Y, et al. Covalently PEGylated carbon nanotubes with stealth character in vivo. Small. 2008;4:940-4.
[93] Liu Z, Davis C, Cai W, He L, Chen X, Dai H. Circulation and long-term fate of functionalized, biocompatible single-walled carbon nanotubes in mice probed by Raman spectroscopy. Proceedings of the National Academy of Sciences of the United States of America. 2008;105:1410-5.
[94] Xie SS, Li WZ, Pan ZW, Chang BH, Sun LF. Mechanical and physical properties on carbon nanotube. J Phys Chem Solids. 2000;61:1153-8.
[95] Strano MS, Jin H. Where is it heading? Single-particle tracking of single-walled carbon nanotubes. ACS nano. 2008;2:1749-52.
[96] Jin H, Heller DA, Strano MS. Single-particle tracking of endocytosis and exocytosis of single-walled carbon nanotubes in NIH-3T3 cells. Nano letters. 2008;8:1577-85.
[97] Welsher K, Liu Z, Daranciang D, Dai H. Selective probing and imaging of cells with single walled carbon nanotubes as near-infrared fluorescent molecules. Nano letters. 2008;8:586-90.
[98] Welsher K, Liu Z, Sherlock SP, Robinson JT, Chen Z, Daranciang D, et al. A route to brightly fluorescent carbon nanotubes for near-infrared imaging in mice. Nature nanotechnology. 2009;4:773-80.
[99] Zavaleta C, de la Zerda A, Liu Z, Keren S, Cheng Z, Schipper M, et al. Noninvasive Raman spectroscopy in living mice for evaluation of tumour targeting with carbon nanotubes. Nano letters. 2008;8:2800-5.
[100] Liu Z, Tabakman S, Sherlock S, Li X, Chen Z, Jiang K, et al. Multiplexed Five-Color Molecular Imaging of Cancer Cells and Tumour Tissues with Carbon Nanotube Raman Tags in the Near-Infrared. Nano research. 2010;3:222-33.
[101] Berber S, Kwon YK, Tomanek D. Unusually high thermal conductivity of carbon nanotubes. Physical review letters. 2000;84:4613-6.
[102] De la Zerda A, Zavaleta C, Keren S, Vaithilingam S, Bodapati S, Liu Z, et al. Carbon nanotubes as photoacoustic molecular imaging agents in living mice. Nature nanotechnology. 2008;3:557-62.
[103] Kam NW, O'Connell M, Wisdom JA, Dai H. Carbon nanotubes as multifunctional biological transporters and near-infrared agents for selective cancer cell destruction. Proceedings of the National Academy of Sciences of the United States of America. 2005;102:11600-5.
[104] Chakravarty P, Marches R, Zimmerman NS, Swafford AD, Bajaj P, Musselman IH, et al. Thermal ablation of tumour cells with antibody-functionalized single-walled carbon nanotubes. Proceedings of the National Academy of Sciences of the United States of America. 2008;105:8697-702.
[105] Wang L, Zhang M, Zhang N, Shi J, Zhang H, Li M, et al. Synergistic enhancement of cancer therapy using a combination of docetaxel and photothermal ablation induced by single-walled carbon nanotubes. International journal of nanomedicine. 2011;6:2641-52.
[106] Bartholomeusz G, Cherukuri P, Kingston J, Cognet L, Lemos R, Leeuw TK, et al. In Vivo Therapeutic Silencing of Hypoxia-Inducible Factor 1 Alpha (HIF-1alpha) Using

Single-Walled Carbon Nanotubes Noncovalently Coated with siRNA. Nano research. 2009;2:279-91.
[107] Liu Y, Wu DC, Zhang WD, Jiang X, He CB, Chung TS, et al. Polyethylenimine-grafted multiwalled carbon nanotubes for secure noncovalent immobilization and efficient delivery of DNA. Angew Chem Int Ed Engl. 2005;44:4782-5.
[108] Nunes A, Amsharov N, Guo C, Van den Bossche J, Santhosh P, Karachalios TK, et al. Hybrid polymer-grafted multiwalled carbon nanotubes for in vitro gene delivery. Small. 2010;6:2281-91.
[109] Pantarotto D, Singh R, McCarthy D, Erhardt M, Briand JP, Prato M, et al. Functionalized carbon nanotubes for plasmid DNA gene delivery. Angew Chem Int Ed Engl. 2004;43:5242-6.
[110] Singh R, Pantarotto D, McCarthy D, Chaloin O, Hoebeke J, Partidos CD, et al. Binding and condensation of plasmid DNA onto functionalized carbon nanotubes: toward the construction of nanotube-based gene delivery vectors. Journal of the American Chemical Society. 2005;127:4388-96.
[111] Liu Z, Winters M, Holodniy M, Dai H. siRNA delivery into human T cells and primary cells with carbon-nanotube transporters. Angew Chem Int Ed Engl. 2007;46:2023-7.
[112] Kam NW, Liu Z, Dai H. Functionalization of carbon nanotubes via cleavable disulfide bonds for efficient intracellular delivery of siRNA and potent gene silencing. Journal of the American Chemical Society. 2005;127:12492-3.
[113] Liu Z, Sun X, Nakayama-Ratchford N, Dai H. Supramolecular chemistry on water-soluble carbon nanotubes for drug loading and delivery. ACS nano. 2007;1:50-6.
[114] Ji Z, Lin G, Lu Q, Meng L, Shen X, Dong L, et al. Targeted therapy of SMMC-7721 liver cancer in vitro and in vivo with carbon nanotubes based drug delivery system. Journal of colloid and interface science. 2012;365:143-9.
[115] Taghdisi SM, Lavaee P, Ramezani M, Abnous K. Reversible targeting and controlled release delivery of daunorubicin to cancer cells by aptamer-wrapped carbon nanotubes. European journal of pharmaceutics and biopharmaceutics : official journal of Arbeitsgemeinschaft fur Pharmazeutisc. 2011;77:200-6.
[116] Lu YJ, Wei KC, Ma CC, Yang SY, Chen JP. Dual targeted delivery of doxorubicin to cancer cells using folate-conjugated magnetic multi-walled carbon nanotubes. Colloids and surfaces B, Biointerfaces. 2012;89:1-9.
[117] Bhirde AA, Patel V, Gavard J, Zhang G, Sousa AA, Masedunskas A, et al. Targeted killing of cancer cells in vivo and in vitro with EGF-directed carbon nanotube-based drug delivery. ACS nano. 2009;3:307-16.
[118] Liu Z, Chen K, Davis C, Sherlock S, Cao Q, Chen X, et al. Drug delivery with carbon nanotubes for in vivo cancer treatment. Cancer research. 2008;68:6652-60.
[119] Hampel S, Kunze D, Haase D, Kramer K, Rauschenbach M, Ritschel M, et al. Carbon nanotubes filled with a chemotherapeutic agent: a nanocarrier mediates inhibition of tumour cell growth. Nanomedicine : nanotechnology, biology, and medicine. 2008;3:175-82.
[120] Zhang X, Meng L, Lu Q, Fei Z, Dyson PJ. Targeted delivery and controlled release of doxorubicin to cancer cells using modified single wall carbon nanotubes. Biomaterials. 2009;30:6041-7.

[121] Yang F, Jin C, Yang D, Jiang Y, Li J, Di Y, et al. Magnetic functionalised carbon nanotubes as drug vehicles for cancer lymph node metastasis treatment. Eur J Cancer. 2011;47:1873-82.
[122] Pastorin G, Wu W, Wieckowski S, Briand JP, Kostarelos K, Prato M, et al. Double functionalisation of carbon nanotubes for multimodal drug delivery. Chem Commun. 2006:1182-4.
[123] Samori C, Ali-Boucetta H, Sainz R, Guo C, Toma FM, Fabbro C, et al. Enhanced anticancer activity of multi-walled carbon nanotube-methotrexate conjugates using cleavable linkers. Chem Commun (Camb). 2010;46:1494-6.
[124] Lay CL, Liu HQ, Tan HR, Liu Y. Delivery of paclitaxel by physically loading onto poly(ethylene glycol) (PEG)-graft-carbon nanotubes for potent cancer therapeutics. Nanotechnology. 2010;21:065101.
[125] Dhar S, Liu Z, Thomale J, Dai H, Lippard SJ. Targeted single-wall carbon nanotube-mediated Pt(IV) prodrug delivery using folate as a homing device. Journal of the American Chemical Society. 2008;130:11467-76.
[126] Liu Z, Yanagi K, Suenaga K, Kataura H, Iijima S. Imaging the dynamic behaviour of individual retinal chromophores confined inside carbon nanotubes. Nature nanotechnology. 2007;2:422-5.
[127] Koshino M, Tanaka T, Solin N, Suenaga K, Isobe H, Nakamura E. Imaging of single organic molecules in motion. Science. 2007;316:853.
[128] Meyer RR, Sloan J, Dunin-Borkowski RE, Kirkland AI, Novotny MC, Bailey SR, et al. Discrete atom imaging of one-dimensional crystals formed within single-walled carbon nanotubes. Science. 2000;289:1324-7.
[129] Hong SY, Tobias G, Al-Jamal KT, Ballesteros B, Ali-Boucetta H, Lozano-Perez S, et al. Filled and glycosylated carbon nanotubes for in vivo radioemitter localization and imaging. Nature materials. 2010;9:485-90.
[130] Moscow JA. Methotrexate transport and resistance. Leukemia & lymphoma. 1998;30:215-24.
[131] Schipper ML, Nakayama-Ratchford N, Davis CR, Kam NW, Chu P, Liu Z, et al. A pilot toxicology study of single-walled carbon nanotubes in a small sample of mice. Nature nanotechnology. 2008;3:216-21.
[132] Zhao X Fau - Liu R, Liu R. Recent progress and perspectives on the toxicity of carbon nanotubes at organism, organ, cell, and biomacromolecule levels.
[133] Folkmann JK, Risom L, Jacobsen NR, Wallin H, Loft S, Moller P. Oxidatively damaged DNA in rats exposed by oral gavage to C60 fullerenes and single-walled carbon nanotubes. Environmental health perspectives. 2009;117:703-8.
[134] Doak SH, Griffiths SM, Manshian B, Singh N, Williams PM, Brown AP, et al. Confounding experimental considerations in nanogenotoxicology. Mutagenesis. 2009;24:285-93.
[135] Poland CA, Duffin R, Kinloch I, Maynard A, Wallace WA, Seaton A, et al. Carbon nanotubes introduced into the abdominal cavity of mice show asbestos-like pathogenicity in a pilot study. Nature nanotechnology. 2008;3:423-8.
[136] Mangum Jb Fau - Turpin EA, Turpin Ea Fau - Antao-Menezes A, Antao-Menezes A Fau - Cesta MF, Cesta Mf Fau - Bermudez E, Bermudez E Fau - Bonner JC, Bonner JC. Single-walled carbon nanotube (SWCNT)-induced interstitial fibrosis in the lungs of

rats is associated with increased levels of PDGF mRNA and the formation of unique intercellular carbon structures that bridge alveolar macrophages in situ.
[137] Madani SY, Mandel A, Seifalian AM. A concise review of carbon nanotube's toxicology. Nano reviews. 2013;4.
[138] Mangum JB, Turpin EA, Antao-Menezes A, Cesta MF, Bermudez E, Bonner JC. Single-walled carbon nanotube (SWCNT)-induced interstitial fibrosis in the lungs of rats is associated with increased levels of PDGF mRNA and the formation of unique intercellular carbon structures that bridge alveolar macrophages in situ. Particle and fibre toxicology. 2006;3:15.
[139] Murray AR, Kisin ER, Tkach AV, Yanamala N, Mercer R, Young SH, et al. Factoring-in agglomeration of carbon nanotubes and nanofibers for better prediction of their toxicity versus asbestos. Particle and fibre toxicology. 2012;9:10.
[140] Shvedova AA, Kisin ER, Mercer R, Murray AR, Johnson VJ, Potapovich AI, et al. Unusual inflammatory and fibrogenic pulmonary responses to single-walled carbon nanotubes in mice. American journal of physiology Lung cellular and molecular physiology. 2005;289:L698-708.
[141] Liu Z, Tabakman S, Welsher K, Dai H. Carbon Nanotubes in Biology and Medicine: In vitro and in vivo Detection, Imaging and Drug Delivery. Nano research. 2009;2:85-120.
[142] Singh R, Pantarotto D, Lacerda L, Pastorin G, Klumpp C, Prato M, et al. Tissue biodistribution and blood clearance rates of intravenously administered carbon nanotube radiotracers. Proceedings of the National Academy of Sciences of the United States of America. 2006;103:3357-62.
[143] Schipper ML, Nakayama-Ratchford N, Davis CR, Kam NW, Chu P, Liu Z, et al. A pilot toxicology study of single-walled carbon nanotubes in a small sample of mice. Nat Nanotechnol. 2008;3:216-21.
[144] Schipper Ml Fau - Nakayama-Ratchford N, Nakayama-Ratchford N Fau - Davis CR, Davis Cr Fau - Kam NWS, Kam Nw Fau - Chu P, Chu P Fau - Liu Z, Liu Z Fau - Sun X, et al. A pilot toxicology study of single-walled carbon nanotubes in a small sample of mice.
[145] Shao W, Paul A, Mai YY, Laetitia R, Prakash S. Carbon Nanotubes for Use in Medicine: Potentials and Limitations. Book : Synthesis and Applications of Carbon Nanotubes and Their Composites. 2013;InTech.
[146] Prakash S, Malhotra M, Shao W, Tomaro-Duchesneau C, Abbasi S. Polymeric nanohybrids and functionalized carbon nanotubes as drug delivery carriers for cancer therapy. Adv Drug Deliv Rev. 2011;63:1340-51.
[147] Lauret JS, Voisin C, Cassabois G, Delalande C, Roussignol P, Jost O, et al. Ultrafast carrier dynamics in single-wall carbon nanotubes. Physical review letters. 2003;90:057404.
[148] Rowinsky EK, Eisenhauer EA, Chaudhry V, Arbuck SG, Donehower RC. Clinical toxicities encountered with paclitaxel (Taxol). Semin Oncol. 1993;20:1-15.
[149] Gardner ER, Dahut WL, Scripture CD, Jones J, Aragon-Ching JB, Desai N, et al. Randomized crossover pharmacokinetic study of solvent-based paclitaxel and nab-paclitaxel. Clinical cancer research : an official journal of the American Association for Cancer Research. 2008;14:4200-5.

[150] Gradishar WJ, Tjulandin S, Davidson N, Shaw H, Desai N, Bhar P, et al. Phase III trial of nanoparticle albumin-bound paclitaxel compared with polyethylated castor oil-based paclitaxel in women with breast cancer. J Clin Oncol. 2005;23:7794-803.
[151] Cheung W, Pontoriero F, Taratula O, Chen AM, He H. DNA and carbon nanotubes as medicine. Adv Drug Deliv Rev. 2010;62:633-49.
[152] Zhang Z, Yang X, Zhang Y, Zeng B, Wang S, Zhu T, et al. Delivery of telomerase reverse transcriptase small interfering RNA in complex with positively charged single-walled carbon nanotubes suppresses tumour growth. Clinical cancer research : an official journal of the American Association for Cancer Research. 2006;12:4933-9.
[153] Varkouhi AK, Foillard S, Lammers T, Schiffelers RM, Doris E, Hennink WE, et al. SiRNA delivery with functionalized carbon nanotubes. International journal of pharmaceutics. 2011;416:419-25.
[154] Zhao D, Alizadeh D, Zhang L, Liu W, Farrukh O, Manuel E, et al. Carbon nanotubes enhance CpG uptake and potentiate antiglioma immunity. Clinical cancer research : an official journal of the American Association for Cancer Research. 2011;17:771-82.
[155] Bertucci C, Cimitan S, Riva A, Morazzoni P. Binding studies of taxanes to human serum albumin by bioaffinity chromatography and circular dichroism. Journal of pharmaceutical and biomedical analysis. 2006;42:81-7.
[156] Horwitz SB. Taxol (paclitaxel): mechanisms of action. Annals of oncology : official journal of the European Society for Medical Oncology / ESMO. 1994;5 Suppl 6:S3-6.
[157] Ansell SM, Johnstone SA, Tardi PG, Lo L, Xie S, Shu Y, et al. Modulating the therapeutic activity of nanoparticle delivered paclitaxel by manipulating the hydrophobicity of prodrug conjugates. Journal of medicinal chemistry. 2008;51:3288-96.
[158] Li C, Yu DF, Newman RA, Cabral F, Stephens LC, Hunter N, et al. Complete regression of well-established tumours using a novel water-soluble poly(L-glutamic acid) paclitaxel conjugate. Cancer research. 1998;58:2404-9.
[159] Bradley MO, Swindell CS, Anthony FH, Witman PA, Devanesan P, Webb NL, et al. Tumour targeting by conjugation of DHA to paclitaxel. Journal of controlled release : official journal of the Controlled Release Society. 2001;74:233-6.
[160] Mellado W, Magri NF, Kingston DG, Garcia-Arenas R, Orr GA, Horwitz SB. Preparation and biological activity of taxol acetates. Biochem Biophys Res Commun. 1984;124:329-36.
[161] Ferrari M. Cancer nanotechnology: opportunities and challenges. Nature reviews Cancer. 2005;5:161-71.
[162] Chen RJ, Zhang Y, Wang D, Dai H. Noncovalent sidewall functionalization of single-walled carbon nanotubes for protein immobilization. Journal of the American Chemical Society. 2001;123:3838-9.
[163] Ostling D, Tomanek D, Rosen A. Electronic structure of single-wall, multiwall, and filled carbon nanotubes. Phys Rev B. 1997;55:13980-8.
[164] Lin MF, Chuu DS, Shung KWK. Thermal conductance and the Peltier coefficient of carbon nanotubes. Phys Rev B. 1996;53:11186-92.
[165] Liu Z Fau - Davis C, Davis C Fau - Cai W, Cai W Fau - He L, He L Fau - Chen X, Chen X Fau - Dai H, Dai H. Circulation and long-term fate of functionalized, biocompatible single-walled carbon nanotubes in mice probed by Raman spectroscopy.

[166] nanowerk. Ensysce Receives Funding for Carbon Nanotube Therapeutics for siRNA Delivery Nano woerk (online) 2012.
[167] Liu Z, Chen K, Davis C, Sherlock S, Cao Q, Chen X, et al. Drug delivery with carbon nanotubes for in vivo cancer treatment. Cancer Res. 2008;68:6652-60.
[168] Gan Y, Wientjes MG, Schuller DE, Au JL. Pharmacodynamics of taxol in human head and neck tumours. Cancer Res. 1996;56:2086-93.
[169] Song S, Yu B, Wei Y, Wientjes MG, Au JL. Low-dose suramin enhanced paclitaxel activity in chemotherapy-naive and paclitaxel-pretreated human breast xenograft tumours. Clin Cancer Res. 2004;10:6058-65.
[170] Worsley KA, Kalinina I, Bekyarova E, Haddon RC. Functionalization and dissolution of nitric acid treated single-walled carbon nanotubes. Journal of the American Chemical Society. 2009;131:18153-8.
[171] Zhao B, Hu H, Yu A, Perea D, Haddon RC. Synthesis and characterization of water soluble single-walled carbon nanotube graft copolymers. Journal of the American Chemical Society. 2005;127:8197-203.
[172] Tagmatarchis N, Maigne A, Yudasaka M, Iijima S. Functionalization of carbon nanohorns with azomethine ylides: towards solubility enhancement and electron-transfer processes. Small. 2006;2:490-4.
[173] Valerie C. Moore MSS, Erik H. Haroz, Robert H. Hauge, and Richard E. Smalley. Individually Suspended Single-Walled Carbon Nanotubes in Various Surfactants. Nano Lett. 2003;3:3.
[174] Kolosnjaj-Tabi J, Hartman KB, Boudjemaa S, Ananta JS, Morgant G, Szwarc H, et al. In vivo behavior of large doses of ultrashort and full-length single-walled carbon nanotubes after oral and intraperitoneal administration to Swiss mice. ACS nano. 2010;4:1481-92.
[175] Elgrabli D, Abella-Gallart S, Robidel F, Rogerieux F, Boczkowski J, Lacroix G. Induction of apoptosis and absence of inflammation in rat lung after intratracheal instillation of multiwalled carbon nanotubes. Toxicology. 2008;253:131-6.
[176] Archana M, Yogesh TL, Kumaraswamy KL. Various methods available for detection of apoptotic cells--a review. Indian journal of cancer. 2013;50:274-83.
[177] Liu Z, Fan AC, Rakhra K, Sherlock S, Goodwin A, Chen X, et al. Supramolecular stacking of doxorubicin on carbon nanotubes for in vivo cancer therapy. Angew Chem Int Ed Engl. 2009;48:7668-72.
[178] Kam NW, Dai H. Carbon nanotubes as intracellular protein transporters: generality and biological functionality. J Am Chem Soc. 2005;127:6021-6.
[179] Ali-Boucetta H, Al-Jamal KT, McCarthy D, Prato M, Bianco A, Kostarelos K. Multiwalled carbon nanotube-doxorubicin supramolecular complexes for cancer therapeutics. Chem Commun (Camb). 2008:459-61.
[180] Li R, Wu R, Zhao L, Wu M, Yang L, Zou H. P-glycoprotein antibody functionalized carbon nanotube overcomes the multidrug resistance of human leukemia cells. ACS nano. 2010;4:1399-408.
[181] Kang B, Li J, Chang S, Dai M, Ren C, Dai Y, et al. Subcellular tracking of drug release from carbon nanotube vehicles in living cells. Small. 2012;8:777-82.
[182] Duncan R, Seymour LC, Scarlett L, Lloyd JB, Rejmanova P, Kopecek J. Fate of N-(2-hydroxypropyl)methacrylamide copolymers with pendent galactosamine residues after intravenous administration to rats. Biochimica et biophysica acta. 1986;880:62-71.

[183] Yang D, Yu L, Van S. Clinically relevant anticancer polymer Paclitaxel therapeutics. Cancers. 2010;3:17-42.
[184] Rooseboom M, Commandeur JN, Vermeulen NP. Enzyme-catalyzed activation of anticancer prodrugs. Pharmacological reviews. 2004;56:53-102.
[185] Senter PD, Beam KS, Mixan B, Wahl AF. Identification and activities of human carboxylesterases for the activation of CPT-11, a clinically approved anticancer drug. Bioconjug Chem. 2001;12:1074-80.
[186] Xu G, Zhang W, Ma MK, McLeod HL. Human carboxylesterase 2 is commonly expressed in tumour tissue and is correlated with activation of irinotecan. Clin Cancer Res. 2002;8:2605-11.
[187] Shao W, Paul A, Zhao B, Lee C, Rodes L, Prakash S. Carbon nanotube lipid drug approach for targeted delivery of a chemotherapy drug in a human breast cancer xenograft animal model. Biomaterials. 2013;34:10109-19.
[188] Pinder MC, Ibrahim NK. Nanoparticle albumin-bound paclitaxel for treatment of metastatic breast cancer. Drugs Today (Barc). 2006;42:599-604.
[189] Ma Y, Nolte RJ, Cornelissen JJ. Virus-based nanocarriers for drug delivery. Adv Drug Deliv Rev. 2012;64:811-25.
[190] Danquah MK, Zhang XA, Mahato RI. Extravasation of polymeric nanomedicines across tumour vasculature. Adv Drug Deliv Rev. 2011;63:623-39.
[191] Duesberg GS, Muster J, Krstic V, Burghard M, Roth S. Chromatographic size separation of single-wall carbon nanotubes. Appl Phys A. 1998;67:117-9.
[192] Doorn SK, Fields RE, Hu H, Hamon MA, Haddon RC, Selegue JP, et al. High Resolution Capillary Electrophoresis of Carbon Nanotubes. Journal of the American Chemical Society. 2002;124:3169-74.
[193] Chen B, Selegue JP. Separation and Characterization of Single-Walled and Multiwalled Carbon Nanotubes by Using Flow Field-Flow Fractionation. Anal Chem. 2002;74:4774-80.
[194] Liu Z, Rimmer S. Synthesis and release of 5-fluorouracil from poly(N-vinylpyrrolidinone) bearing 5-fluorouracil derivatives. Journal of controlled release : official journal of the Controlled Release Society. 2002;81:91-9.
[195] Lee JH, Nan A. Combination Drug Delivery Approaches in Metastatic Breast Cancer. Journal of Drug Delivery. 2012;2012:17.
[196] Holmes FA. Paclitaxel combination therapy in the treatment of metastatic breast cancer: a review. Semin Oncol. 1996;23:46-56.
[197] Aryal S, Hu CM, Zhang L. Polymeric nanoparticles with precise ratiometric control over drug loading for combination therapy. Molecular pharmaceutics. 2011;8:1401-7.